UNIVERSITÀ
DEGLI STUDI
DI PADOVA

Sede Amministrativa: Università degli Studi di Padova

Dipartimento di Tecnica e Gestione dei Sistemi Industriali

CORSO DI DOTTORATO DI RICERCA IN: INGEGNERIA MECCATRONICA E DELL'INNOVAZIONE MECCANICA DEL PRODOTTO
CURRICULUM: MECCANICA DEI MATERIALI
CICLO: XXIX

OTTIMIZZAZIONE DEL PROCESSO DI RAFFINAZIONE DEL ROTTAME D'ALLUMINIO

Coordinatore: Roberto Caracciolo

Supervisore: Giulio Timelli

Dottorando: Stefano Capuzzi

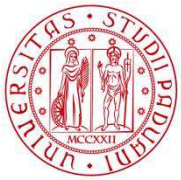

UNIVERSITÀ
DEGLI STUDI
DI PADOVA

Head Office: University of Padua

Department of Management and Engineering

PhD PROGRAM IN MECHATRONICS AND PRODUCT INNOVATION ENGINEERING
CURRICULUM: MECHANICS OF MATERIALS
CYCLE: XXIX

OPTIMIZATION OF THE ALUMINIUM REFINING PROCESS

Coordinator: Roberto Caracciolo
Supervisor: Giulio Timelli

PhD candidate: Stefano Capuzzi

PREFACE

This doctoral thesis concentrates the work and the results of the three years studies at the University of Padua from January 2014 to December 2016. The experimental work was performed both in Industry at Raffineria Metalli Capra, Castel Mella BS (Italy), and in University at the Departement of Management and Engineering, Vicenza (Italy). Part of the work was carried out in collaboration with SINTEF during an exchange period in Trondheim (Norway) from March to June 2016.

Professor Giulio Timelli was the principal supervisor. Senior researcher Anne Kvithyld was my supervisor during the period at SINTEF.

In the first part, PART 1, a background of the aluminium refining process and the industrial technologies and challenges are given. The motivation and contribution of my work are, as well, highlighted.

The second part, PART 2, is a collection of the articles published throughout the three years period related to the thesis subject. The papers are reported in the form they were submitted for publication or printed. The manuscripts included in this section are:

Article 1
Influence of salt quantity on recovery yield of heterogeneous aluminium scrap
S.Capuzzi, G.Timelli, L.Capra and L. Romano. Published in Advanced Materials Research

Article 2
Study of fluxing amount in aluminium refining process by rotary and crucible furnace
S.Capuzzi, G.Timelli, L.Capra and L. Romano. Submitted for pubblication in International Journal of Sustainable Engineering

Article 3
Influence of the cryolite content on the flux properties in Al refining
S.Capuzzi, G.Timelli. Submitted for pubblication in Metallurgical and Materials Transaction A

Article 4
Influence of coating on the coalescence of aluminium drops and effect of the de-coating treatment
S.Capuzzi, A.Kvithyld, G.Timelli, A.Nordmark, T.A. Engh. TMS San Diego, 26th February – 2nd March 2017

Article 5
Coalescence of clean, coated and de-coated aluminium for various salts and salt-scrap ratio
S.Capuzzi, A.Kvithyld, G.Timelli, A.Nordmark, T.A. Engh, E. Gumbmann. Submitted for pubblication in Journal of Sustainable Metallurgy

During the thesis period other topics related to aluminium production have been studied, in particular thermal treatment and casting. The articles published are the following:

1. **Microstructure and mechanical properties of automotive components die cast with secondary aluminium alloys by SEED semi-solid process.** G.Timelli, S.Capuzzi, S.Ferraro, A.Fabrizi, L.Capra. In book: Shape Casting: 5th International Symposium. 2014

2. **Development of thermal treatments for secondary aluminium cast alloy automotive components in semi-solid state**. S.Capuzzi. Published in Metallurgia Italiana, 2014

3. **Development of heat treatments for automotive components die-cast with secondary aluminium alloy at semi-solid state**. S.Capuzzi, S.Ferraro, G.Timelli, L.Capra, G.F. Capra, I. Loizaga. Presented at the 71st World Foundry Congress, Bilbao, Spain, May 2014

4. **The influence of Cr content on the Fe**-rich phase formation and impact toughness of a die-cast AlSi9Cu3(Fe) alloy. G.Timelli, S.Ferraro, A.Fabrizi, S.Capuzzi, F.Bonollo, L.Capra, G.F. Capra. Proceeding of the 71st World Foundry Congress, Bilbao, Spain, May 2014

5. **Evoluzione delle proprietà meccaniche tramite trattamento termico T6 e T7 di leghe di alluminio secondario AlSi9Cu3(Fe) e AlSi7Cu3Mg colate allo stato semisolido**. Presented at 35° convegno nazionale AIM, Rome, Italy, November 2014

6. **Influence of ageing heat treatment on microstructure and mechanical properties of a secondary rheocast $AlSi_9Cu_3$(Fe) alloy**. S.Capuzzi, G.Timelli, A.Fabrizi and F.Bonollo. Published in Materials Science Forum. 2015

7. **Investigation of primary Fe-bearing compounds in secondary aluminium alloys by differential scanning calorimetry.** G.Timelli, S.Capuzzi, A.Fabrizi, D. Caliari. Published in Materials Science Forum. 2015

8. **Precipitation of primary Fe-rich compounds in secondary AlSi9Cu3(Fe) alloy.** G.Timelli, S.Capuzzi, A.Fabrizi Published in Journal of Thermal Analysis and Calorimetry. 2015

9. **Efficiency and yield evaluation of a stack furnace in high –pressure die-casting foundry.** N.Agostini, G.Timelli, S.Capuzzi, M. Furlati. Published in Metallurgia Italiana 2016

SUMMARY

Aluminium recycling offers economic and environmental advantages. The energy consumption is 90% lower compared to primary aluminium production and a reduction of 95% of greenhouse gas is achieved.

Recycling pure aluminium without exogenous materials is simple, i.e. remelt it and cast the liquid metal. However, the aluminium scrap usually contains not only metal; oxides and other non metallic components are present depending on the origin of the scrap.

The higher the homogeneity and the knowledge of the chemical composition of the scrap, the better its quality. High quality scrap is the dream of all the smelters but it is expensive. Therefore low quality scrap has also to be re-melted. Here two strategies have to be taken into account:

- increasing the scrap quality inside the refinery
- removing the non-metal content during the re-melting of the scrap

The aim of this doctoral thesis is to support the aluminium recycling industry in both these aspects highlighting the influence of the pre-melting scrap treatments and the melting practices on the effectiveness of the recycling process in terms of metal recovery.

A review of the literature and several months spent at Raffineria Metalli Capra provided me a wide-ranging view of the whole recycling process and in particular a perspective of the smelters world. Based on this experience, the research has been focused on:

- *thermal de-coating*:
  this process directly impacts on the metal yield of the scrap, i.e. the portion of a scrap consignment that becomes useable metal after proper melting. It is used to remove the organic fraction of the coatings present on the scrap surface allowing an increment in the scrap quality. It is an auto-thermal process, however if not optimized it can oxidise the scrap.

- *fluxing*:
  the scrap is usually remelted under a flux composed of a mixture of salts in order to protect the molten bath from oxidation and to collect the non-metal fraction, mainly oxides. The choice of composition and quantity of salt to be added to the scrap charge is a key aspect in the metal recovery.

In particular the following aspects have been studied:

- the influence of the quantity of flux on the metal recovery of the process
- the effect of cryolite addition on various properties of an industrial flux and its effectiveness in increasing the metal recovery
- the influence of coating and de-coating treatments on the coalescence of metal drops in the flux to allow their recovery
- the influence of the quantity and the composition of the flux on the coalescence of metal to allow their recovery

SOMMARIO

La produzione di alluminio attraverso il riciclo offre vantaggi economici e ambientali, basti pensare che il consumo energetico e la produzione di gas serra sono ridotti del 90% e del 95% rispetto alla produzione primaria.

Riciclare alluminio è idealmente facile partendo da rottame di solo alluminio, è sufficiente rifonderlo e colarlo in nuovi lingotti. Tuttavia, il rottame, oltre alla frazione di alluminio, contiene altri tipi di materiali. In particolare può contenere altri metalli, materiali non metallici e/o ossidi, in base alla tipologia di rottame.

La qualità del rottame viene quindi valutata in relazione alla quantità di materiale non desiderato e alla possibilità di conoscerne la composizione chimica. Rottami di alta qualità sono i più facile da riciclare, ma anche i più costosi. Due vie sono percorribili per rendere possibile il riciclo di rottami con un alto livello di elementi non desiderati:

- aumentarne la qualità attraverso appositi trattamenti pre-fusione
- rimuovere il contenuto non metallico durante la rifusione

Scopo di questa tesi di dottorato è quello di sostenere l'industria del riciclaggio dell'alluminio in entrambi questi aspetti, evidenziando l'influenza dei trattamenti pre-fusione del rottame e delle pratiche di fusione sull'efficacia del processo di riciclaggio in termini di resa metallica del processo stesso.

Una continua revisione della letteratura e diversi mesi trascorsi presso Raffineria Metalli Capra mi hanno permesso di avere una visione ampia di tutto il processo di riciclaggio ed in particolare del mondo delle raffineria. Sulla base di questa esperienza, la ricerca si è focalizzata su:

- *processo di de-coating termico*:
  permette di rimuovere la frazione organica dei rivestimenti presenti sulla superficie dei rottami, ad esempio verniciature. E' un processo auto-termico che impatta direttamente sulla resa metallica del rottame, che è la porzione di una partita di rottami metallici che diventa utilizzabile dopo un'adeguata fusione, aumentandone la qualità. Se tale processo non viene ottimizzato, il rottame rischia una ulteriore ossidazione

- *flussaggio durante la ri-fusione del rottame*:
  il rottame è solitamente rifuso sotto un flusso costituito da una miscela di sali finalizzata a proteggere il bagno dall'ossidazione e a raccogliere la frazione non metallica, soprattutto ossidi, del rottame. Le scelte relative alla composizione e alla quantità di sale da aggiungere alla carica di rottami sono un aspetto chiave per la resa metallica del processo.

In particolare, sono stati affrontati i seguenti aspetti:

- l'influenza della quantità del flussaggio sulla resa metallica del processo
- l'efficacia dell'aggiunta di criolite in un flussaggio industriale per incrementare la resa metallica del processo
- l'influenza di rivestimento e trattamento di de-coating sulla coalescenza delle gocce di metallo nel flusso per consentire il recupero
- l'influenza della quantità e della composizione del flussaggio sulla coalescenza delle gocce di metallo presenti nel flusso al fine di consentirne il recupero

CONTENTS

PART 1

BACKGROUND AND CHALLENGES

INTRODUCTION

Recycling is the cleverest way to save resources and becomes an extremely important and interesting theme in case of non-renewable resources such as aluminium.

Aluminium recycling is important for its economical and environmental advantages and interesting for its fascinating and difficult realisation. In spite of this, a lot of work has to be done to increase the aluminium recycling rate and avoid, in the next future, a scrap surplus. Cooperation in the entire aluminium production chain, politic support and new applications for recycled alloys are necessary.

The optimization or at least the improvement of the melting process is also a critical aspect. Under this point of view, we have to focus on the two main passages for a correct recycling process, which are:

1. Increasing the metal content of the scrap through pre-melting treatments
2. Improving the effectiveness of the melting process

The goals of the main pre-melting treatments applied to the scrap are: increasing the bulk density, removing non-aluminium scrap and reducing the impurity level to raise the fraction of metal in the scrap. Comminution, sorting and de-coating are the applied technologies.

Once the highest metal purity is reached, the scrap is ready for re-melting: a very complex process which is the most important, and also the most difficult, to analyse.

Several parameters affect the process efficiency and in particular the fluxing, which is the addition of chemical compounds into the charge.

This doctoral thesis focuses on the analysis and the improvement of two key-factors in the re-melting processes: effectiveness of de-coating and fluxing.

In the field of pre-melting treatments, comminution and sorting are mainly performed by shredder and sorter factories while de-coating, in particular thermal de-coating, is more likely done by refiners.

Fluxing prevents the metal oxidation and it collects the non-metal content, mainly oxides, coming from the scrap. As side effect, a fraction of the molten metal is entrapped in the flux; this metal is lost if not recovered. The ability of the flux in favouring the metal recovery is a critically property.

Particular attention has been paid to:

- *The quantity of fluxing*: charging the right amount of salt is an underestimated but strategic feature in aluminium recycling. Needless to say, flux composition is basilar in fluxing and has been largely studied. Less attention has been given to fluxing quantity, but charge the right amount of flux is not less important than its composition. It impacts on productive and disposal costs as well as on energy consumption.

- *The effect of cryolite addition in a standard flux*: fluorides are added in a NaCl-KCl flux to improve the recovery of metal entrapped in it. Cryolite is a good candidate in accomplishing this purpose even if CaF_2 is often preferred in European refineries. Moreover the effects of this fluoride on various properties of the flux, like the melting temperature, the viscosity and the ability to dissolve aluminium oxide are not adequately studied.

- *The influence of metal quality and fluxing in the Al coalescence*: the coalescence of the metal drops entrapped in the flux has to be increased to reach a greater level of metal recovery. The amount of impurities, like coatings, can hinder the effectiveness of metal recovery, while the right choice in the composition and in the quantity of the flux aids the metal coalescence and its recovery.

ALUMINIUM RECYLING

Aluminium is the second most plentiful metallic element on earth. It's a light, conductive and corrosion resistant metal; moreover different alloying elements can be added to improve several physical and mechanical properties. This combination of qualities has allowed aluminium alloys to compete for a large number of applications [1].

Aluminium is rarely found in nature as pure element due to its good affinity with oxygen. Therefore, the primary aluminium production starts extracting *alumina,* as properly called the aluminium oxide ($Al_2O_{3)}$, from mineral compounds. Bauxite ore is the major source of alumina and the Bayer process, invented and patented in 1887, is the process by which alumina is obtained from bauxite. Clay minerals, alunite, anorthosite, power plant ash, and oil shale could be used as alternative resources to obtain alumina but at higher costs. Alumina is finally refined in aluminium by means of the Hall-Héroult process which was simultaneously discovered in 1886 by Charles Martin Hall and Paul Héroult.

This is the primary route for the aluminium alloys production, while recycling offers a secondary route starting from aluminium scrap. Aluminium industry is characterized by the widest energy gap between primary and secondary production referring to high volume materials. However, aluminium does not show the highest *recycled fraction* that is the share of secondary production compared to total production.

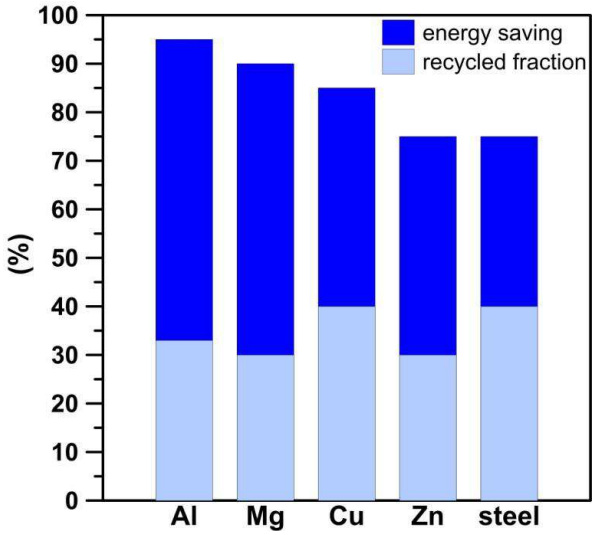

Figure 1. Energy saving from different metals, both non-ferrous alloys and steel, in comparison with primary production route, and relative recycled fraction[2, 3]

Advantages and productivity

In opposition to the primary route, recycling allows a reduction of 95% of the required energy[4] and emits only 5% of greenhouse gas [5]. Furthermore, one ton of recycled aluminium saves up to 8 metric tons of bauxite, 14000 kWh of energy, 6300 litres of oil, 7.6 m^3 of landfill and the average total exhaust emission is about 350 kg of CO_2 [3]. Dust and air emissions from scrap processing are generally at a low level. However, emissions of hazardous air pollutants (e.g. dioxins and furans, metals/metal oxides) may be generated in the secondary production during the melting operations in the furnace.

Based upon USGS data6, the global production of aluminum in 2006 was about 45.9 Mt: 34 Mt was primary aluminum and 11.8 Mt was recycled aluminium. Concerning the secondary aluminium output, the Americas produced 4.46 Mt, Asia 3.57 Mt and

Europe and Eurasia 3.77 Mt; the production in Africa and in the Middle East was negligible.

Figure 2 reports the trends of recycled aluminium production in Europe. A continuous growth is evident since 2008. The European production in 2012 was more than 3000 thousand metric tons.

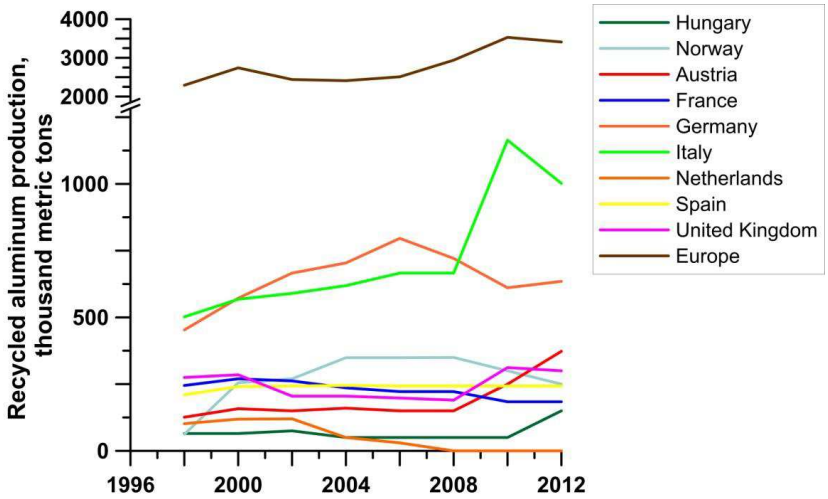

Figure 2. Trend of recycled aluminium production in the main European producing countries from 1998 to 2012[6]

The contribution of individual countries is variable over the years; Figure 3 shows the production levels of the main nations during three different past years (1998, 2006 and 2012).

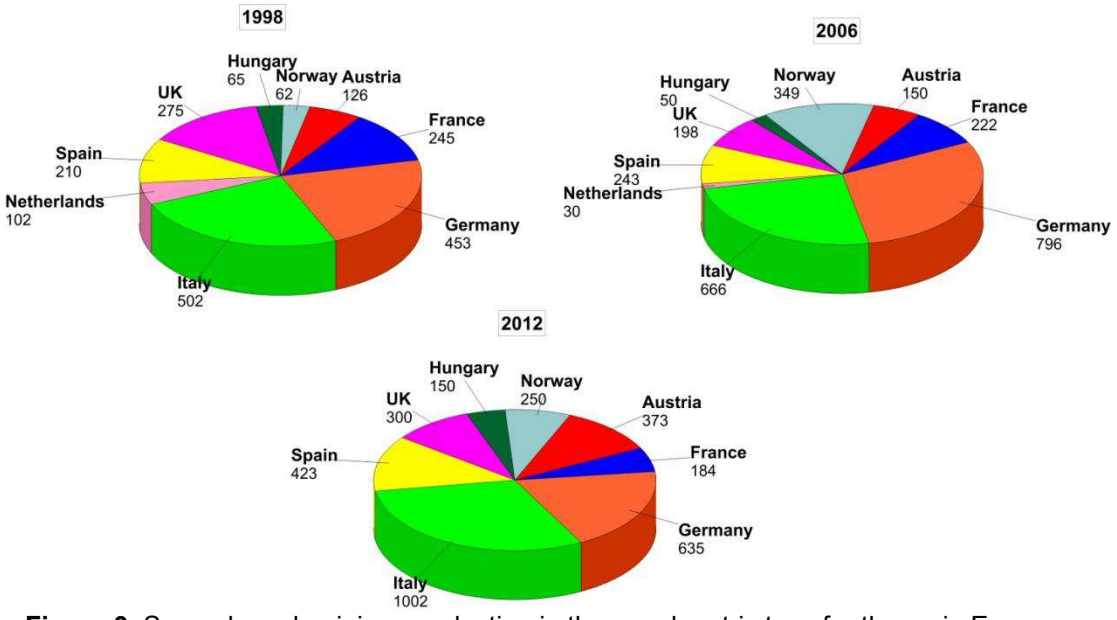

Figure 3. Secondary aluminium production in thousand metric tons for the main European countries[6]

About half of the total production is concentrated in Germany and Italy. Notably, between 1998 and 2012 Italy doubled its production from about 500 to 1000 thousand metric tons, becoming the main producer. Austria, Spain and Hungary have similar trends with a strong increment in the recent years, while France and the Netherlands show an

opposite tendency. Norway in 2012 recorded a quadruple production compared to 1998 but the progress from 2006 to 2012 is toward a decrease in the production.

Recycling strategy

In contrast to many other nonferrous metals, the recycling of postconsumer aluminium scrap is subjected to particular thermo-chemical constraints. It follows that removing un-wanted elements and impurities by refining is complex and not possible for the majority of them.

According to the thermal analysis performed by Nakajima, et al. [7] Mg, Ca, and Be can be transferred to the slag by oxidization and Zn, Cd, and Hg can be removed by evaporation. The other elements, including Cu, Si, Fe, and Mn remain in the metal phase when the scrap is re-melted. These elements can be refined through chemical treatments such as chlorination, filtration and pyro-metallurgical or through electrolytic options. These solutions are costly, they involve the use of hazardous chemicals, and they can lead to metal loss[8].

As a result, the aluminium scrap is usually recycled avoiding the refinement stage. Two possible solutions are currently followed, i.e. downgrading and dilution[9]. By *downgrading*, the low-alloyed scrap is used to obtain alloys with higher alloying contents, while, by *dilution*, molten scrap is diluted with primary aluminium or low-alloyed scrap to reduce the concentration of elements below critical levels[10]. Several authors agree that these strategies will lead to a scrap surplus. Hatayama, et al. [11] applied a regional model to the recycling rate in China, Europe, Japan, and the United States. They concluded that actually a regional scrap surplus in the United States and in Europe may be absorbed in Japan and in China through trade of scrap, whereas in 2050 the four regions together will be a net exporter of scrap. Moreover the introduction of electric and hybrid-electric vehicles can intensify the regional scrap surplus by lowering the demand for recycled cast alloys[12]. According to Løvik, et al. [13], the current practice will result in a scrap surplus from 2025 that will grow to 28% of available scrap in 2050. The expected scrap surplus for Modaresi and Müller [10] implies a loss of energy saving potential of 45-240 TWh/yr, Assuming an electricity demand for smelting of 14 MWh per ton. It is equivalent to the total electricity demand of a medium sized country (e.g., Denmark: 33 TWh/ yr; Iran: 207 TWh/yr, Spain: 268 TWh/yr).

The fraction of recycled aluminium alloys on the whole aluminium alloys production can be increased as a combination of several efforts:

- greater levels of component dismantling before shredding:
- advanced alloy sorting of mixed shredded aluminium;
- closed-loop recycling for automotive components;
- economical refining solution;
- relaxing the composition limits of alloys;
- improved re-melting process;

The improvement of the re-melting process becomes important in the recycling chain to make the recycling attractive for economic returns and not only for environmental concerns.

In the current situation, with a low price difference between primary and recycled alloys, there is a limited economic motivation for promoting investments on a wider use of postconsumer scrap. The target of aluminium refiners is to melt a maximum of metal out of a ton of scrap at the lowest operating cost. Increasing the metal recovery of the re-

melting process can act as the foundation on which the recycling chain improvements are based.

SCRAP CLASSIFICATION AND TREATMENT

Aluminium scrap is often categorized as "*new scrap*" from production processes and "*old scrap*" from post consumer use [14].

New scrap has its origin during the manufacturing process of the material (shavings, off-cuts, moulded parts, etc.) and its quality and composition is usually known. Thus, it can be melted down without any preliminary treatment. Old scrap refers to those products collected after disposal from consumers (cables, pots, radiators, etc.). It is more contaminated than new scrap and preliminary treatments are necessary.

The level of contamination of the scrap is evaluated by means of the metal yield which indicates the portion of a scrap consignment which becomes useable metal after proper melting. In Table 1, a short summary of the different types of aluminium scrap and the main characteristics are reported.

Table 1.
Classification of the aluminium scrap with metal yield (lower limit and main value), mean percentage of undesired materials (oxides and foreign materials) and cost [15].

EN 13920 Part	Scrap	Metal yield limit (%)	Metal yield (%)	Oxides (%)	Foreign material (%)	Cost (€/ton) [16]
2	unalloyed aluminium	0.95	/	/	/	1232-1332
3	wire and cable	≥ 0.95	97.7	1.3	0.5	1182-1282
4	single wrought alloy	≥ 0.95	97.2	1.8	1.8	1272-1377
5	two o more wrought alloy-same family	≥ 0.88	97.2	1.0	2.0	1172-1222
6	two o more wrought alloy	≥ 0.88	94.0	0.8	5.2	
7	casting	≥ 0.9	83.4	6.2	10.4	
8	shredded (not separated)	≥ 0.9	/	/	/	
9	shredded (separated)	≥ 0.9	84.5	5.4	10.1	
10	used beverage can	≥ 0.88	94.0	0.8	5.2	770-820
11	Al-Cu radiators	/	/	/	/	2247-2297
12	turnings single alloy	≥ 0.9	95.3	3.7	1.0	1192-1257
13	mixed turnings	≥ 0.9	84.0	3.3	12.8	1157-1207
14	coated packaging	≥ 0.28	71.5	3.8	24.7	
15	de-coated packaging	≥ 0.8	86.1	12.9	1	
16	dross	≥ 0.3	55.7	44.3	/	158-338

A more exhaustive classification of the aluminium scrap can be found in the standards EN 12258 [14] and EN 13920 [15]. Here the characteristics, the chemical compositions and the metal yield are provided for each category.

Oxidation and presence of foreign materials are the causes of a lower metal yield of scrap. A thin oxide layer always covers the aluminium scrap and the oxidation of the scrap can increase during the charging and melting phases, due to the high temperature involved in the process. The amount of oxides could result higher than the aluminium one in case of *dross,* which is the waste that remains on the surface of molten metal during both primary and secondary aluminium productions. Its metal yield is low and the fraction of oxide cannot be reduced before melting. However, the dross recycling will be a ever more important aspect for economical and environmental reasons.

The aluminium that reacts with the oxygen forming oxides cannot be recovered during the recycling process, while it is possible to reduce the content of foreign materials.

Aluminium alloys are applied in several sectors and they are used together with a lot of different materials. These materials can be metals but also rubber, plastic, glass, paint. The way in which aluminium can be cleared depends on the material and its interaction with the aluminium, i.e. the scrap type.

Packaging and automotive are the main source of old scrap for refiners and both present foreign materials but with different problematic.

Packaging covers less than 20% of the aluminium consumption but it fits desired characteristics for recycling. Aluminium packaging goods present a short product lifetime and a higher recycling rate. However, this kind of scrap is difficult to be submerged in the melt and it cannot be directly re-melted due to the presence of inorganic and organic coatings on the surface. Coatings cannot be separated from the aluminium scrap but they have to be removed.

Today the produced recycled aluminium originates for the 42% from transport and in particular from *automotive*. Some aluminium parts, such as wheels and cylinder heads, are removed during the initial dismantling of the vehicle, while the car body needs comminution and sorting processes.

It has been pointed out how the various types of scrap need different pre-melting treatments; these preliminary treatments can be divided into three steps: comminution, sorting and de-coating.

Comminution

Remove unwanted materials as rubber, magnesium and zinc from the aluminium alloy is the main advantage coming from the scrap comminution[17]. However its objectives are various: obtaining adequate size distribution steps, increasing the bulk density and liberating the components of assemblies. The scrap size can influence directly the melting rate [18] while the bulk density is important to favour the submersion of the scrap in the molten metal.

Comminution knowledge and modelling are usually referred to brittle materials while there is poor understanding about the comminution of non-brittle materials. This gap is due to the intensive use of comminution in mineral industry.

Scrap streams have other properties than natural minerals, in particular larger particle size, higher ductility and greater heterogeneity in size and shape[19]. The fragments' size and the mass distribution as well as their median values are the characteristics usually considered to evaluate the results of comminution. Each fragment can be described by three main dimensions a, b and c, whereby the rule $a > b > c$ has to

be fulfilled. The *b* dimension has been established to be indicative for the fragment size. The evaluation of the deformation process can be carried out by the *degree of bending B* and the *degree of compaction K*, as defined by Schubert et al.[20]

A variety of machines are present on the market as rotary shears [21], rotary cutters [22], translator shears (guillotine, alligator) and rotary shredders[23]. *Swing-hammer shredders* (Figure 4) are the most widespread as they achieve both the production of specific particle size distribution and liberation of assemblies of parts.

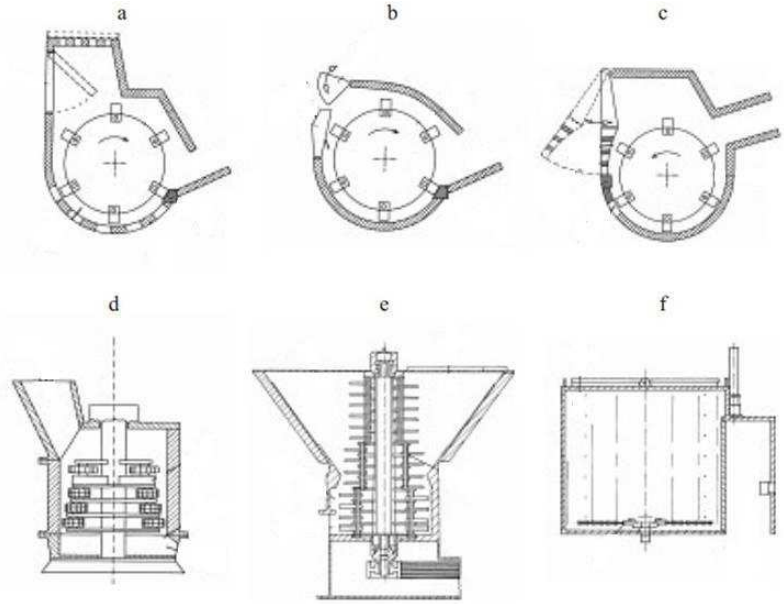

Figure 4. Types of swing-hammer shredders: a-c horizontal shaft shredders; d-f vertical shaft shredders[24]

The innovation in comminution aims at achieving a lower energy consumption and a longer life of the comminution machines[24].

To this day, mechanical comminution cannot be substituted by other processes since it achieves the wanted results with the highest rate. On the other hand, the alternative processes can be used to separate aluminium from other materials in specific goods. For example, high-pressure water-jets, already used with other materials [25], can be applied to obtain best liberation in assembly products as washing machines [26].

The optimization of the comminution process is not merely linked to the process effectiveness. The design development of the products is the starting point. It is showed that the efficiency of the comminution process increases avoiding chemical joints between materials not compatible for recycling and minimizing the number of physical joints [27].

Sorting

As said earlier, the removal of unwanted elements from the molten bath by refining technologies[28] is challenging due to thermodynamic barriers. The best way to obtain a cleaner melt bath is the physical separation of solid scrap streams.

The technical benefits of a preliminary sorting are not completely evident. Different types of scrap require indeed different sorting methodologies and different results can be obtained; thus, it is necessary to understand when the benefits outweigh the required investment [29]. The separation between cast and wrought alloys, for example, allows the

production of high quality wrought alloys, which is not possible with mixed scrap. On the other side sorting technologies for this issue have high initial and running costs.

Table 2 summarizes the main consolidate and innovative sorting technologies.

Table 2.
Classification of sorting methods divided in consolidate and innovative with physical parameter and desired separation; the main technologies developed are also reported, for each method.

	Separator type	Physical parameter	Desired separation	Technology
consolidate	magnetic separator	magnetic susceptibility	ferrous fraction, nickel-based alloy	magnetic drum, overhead belt magnet[30]
	air separator	mass	low density material as paper, foam and plastic	vertical zig-zag, air table, eluatrior, air knives[31]
	eddy current	conductivity	non metal, and metal types	eddy current system[32], electromagnetic system[33]
	dense media	density	non metal and metal types	soak float[34], wet jig[35]
	hand sorting	aspect	metal types and wrought-cast alloys	manual operation[36]
	thermal	melting point	wrought-cast alloys	hot crush[36]
innovative	elemental composition	vapor phase plasma x-ray energy, γ-ray energy	alloys family	LIBS[37], XRF[38], PGNAA*[39]
	image analysis	colour and shape		colour, etch[40], 3D shape[41]
	transmission	atomic number		XRT*[42, 43]

* XRF: X-ray fluorescence, LIBS: Laser-Induced Breakdown Spectroscopy, PGNAA: Prompt Gamma Neutron Activation Analysis, XRT: X-ray trasmission

The practice of *manual sorting* is still considerably widespread as it is still economically attractive in developing countries with low labour costs, such as China, India, and Brazil. It is estimated that workers in China can achieve accuracies up to 99% when sorting non-ferrous automotive shred. They are capable of separating cast and wrought alloys based on their differing visual appearance [36].

Manual sorting is a barrier to the development of new technologies. For America Pacific Coast industry, trading sorted scrap with Asian country is cheaper than investing in mechanical sorting technologies. As proof of that, the value of scrap exported from the United States to Taiwan, Korea, Hong Kong and China has grown fivefold in the last five years.

Magnetic and air separators are the oldest sorting technologies used to remove ferrous components and light-weight materials, such as plastics, rubbers and foams, respectively. Magnetic separators are extensively used in the secondary aluminium industry while the use of air separator is expected to increase in the next future. Sorting technologies based on *eddy current* and *dense media* have been developed but they are mainly used by sorting factories than refineries.

All these consolidated sorting technologies are aimed at sorting aluminium scrap from other materials. The research is now oriented to the separation of aluminium scrap,

free from foreign materials, in the different aluminium families and specific aluminium alloys.

De-coating

Coatings are responsible for increasing the amount of metal lost, the gaseous emissions, and the salt flux disposal once aluminium is recycled [44, 45]. All coatings should contain either organic and inorganic compounds and very often both [46].

The organic fraction comes from paint, oil or cellulose compounds; it represents a significant carbon input into the process route of the aluminium recycling. The carbon input has effect on the quality and quantity of the recycled aluminium [47]. Moreover, carbon partially reacts with aluminium to form aluminium carbide (Al_4C_3).

The inorganic compounds contain different unwanted elements depending on the on the used colour [46]. Titanium dioxide (TiO_2) is the most widely used white pigment because of its brightness and very high refractive index; it is outclassed only by few other materials, and during the melting phase it reacts with molten aluminium:

$$3TiO_2 + 4Al_{(l)} = 3Ti(\textit{dissolved in metal}) + 2Al_2O_3(\textit{dross}) \qquad \text{Equation 1}$$

From the metallurgical point of view, this reaction has two consequences: Ti, that over certain levels has negative effects [48, 49] , is added to the metal bath and part of the Al content is lost due to the reaction with oxygen that increases also the dross amount.

De-coating is the process by which paint, ink, paper, plastic and oil are removed from the surface of a material to make the scrap more suitable for recycle[50].

The process has important advantages on both economical and environmental points of view. Firstly, the possible water content present in the scrap is suppressed avoiding the risk of explosion. Moreover, the melting process effectiveness increases due to the greater scrap quality. This leads to lower salt flux usage during melting, lower dross formation and minimization of chemical impurities. Burn-off of oil and organic fraction of coatings are reduced, weakening the oxidation of the metal bath. From the environmental point of view, emissions are reduced since evolved gases produced by the process may be collected and cleaned before release.

Conventional de-coating is based on thermal or chemical processes [51]; both of them present merits and defects. *Reagent method*s are complex solutions that allow obtaining a complete de-coating and low impurity content in the bath. *Thermal method* is less complicated and auto-thermal even if it cannot eliminate inorganic compounds like TiO_2 [52]. The organic component can be volatilized while the inorganic compounds do not respond to thermal processing; they remain on the surface of the pyrolyzed scrap as exogenous inclusions. According to Meskers, et al. [53] a mechanical force applied by rubbing is necessary to completely de-coat the aluminium substrates.

The aim of the thermal de-coating process is to combust all the carbonized material without oxidizing the metal. As shown in Figure 5, firstly the scission occurs and here the coating decomposes, releasing hydrocarbons and leaving pigment/fillers/carbon residues. Subsequently, the residual carbon reacts with the oxygen in the combustion phase, generating CO, CO_2 and heat, leaving a surface with inorganic pigments and filler particles[54].

During the coating combustion, the organic fraction generates large amounts of gaseous emissions; the fuel value of the gases can be used to make the process auto-thermal, capable of supplying its own energy need [55].

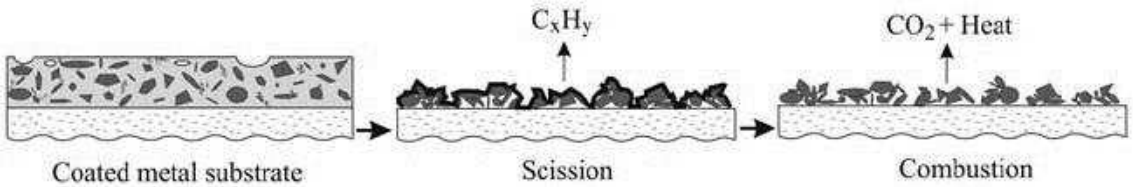

Figure 5. Evolution of the coating during the scission and combustion reaction in a thermal de-coating process[54]

SCRAP MELTING

The aluminum scrap recycled today is nearly all re-melted in furnaces fired with fossil fuels, usually natural gas. Melting capacity, flexibility and energy cost have established reverberatory and rotary furnaces as reference processes for re-melting aluminum scrap.

Electric furnaces offer several benefits thanks to the lack of gas combustion: the metal bath is cleaner, the dross generation decreases and the environmental harmful emissions are reduced. In addition, electric furnaces are more efficient than fossil fuel ones. One the other hand, there are significant disadvantages: electricity is often more expensive than fossil fuels and electric furnaces have higher capital. Last and most important aspect: electric furnaces have difficulties in matching the melting capacity of a large-scale production.

For the same reason, in industry the use of crucible furnaces for high-volume scrap recycling is avoided. More in detail, this kind of fossil fuel furnace offers lower capital costs at expense of the energy efficiency and it is suitable for on-off operations, rather than steady-state operations used for larger melting operations.

Melting technologies

Reverberatory furnaces are brick-lined and constructed with a curved roof. The term reverberatory is used because the heat rising from ignited fuel is reverberated back down to the charge from the curved furnace roof. The molten metal is held inside the furnace at the required temperature before it is tapped out for pouring or transferred to a holding furnace. The rectangular furnace design with its front door across the full furnace width allows the maximum access during charging and skimming.

The main advantages provided by reverberatory aluminium smelters are the high volume processing rate and the low operating and maintenance costs. Their disadvantages are the high metal oxidation rates, the large space requirements and the low energy efficiencies. Typical reverberatory furnaces present a ratio between the amount of heat absorbed by the raw material and the amount of heat generated from the total fuel consumed ranging from 15 to 39%.

Rotary furnaces are more expensive to install and more difficult to maintain efficient than ordinary reverberatory furnaces. However, higher melting rates, reduced emissions, consistent metal composition and lower fuel consumption are achieved because the hot refractory rotates and transfers more heat to the charge via direct contact. As a result, rotary furnaces are generally best suited in countries with high energy costs, as European countries, for melting dross and other oxidized scrap as suggest by Velasco and Nino [56]

The first mention in the patent literature of a *rotary furnace* for processing aluminum scrap is the Schmidt patent (GB 520,533) going back to 1940 in which a fixed-

axis wet-salt flux rotary furnace system was described. A rotary furnace consists of a cylindrical steel drum with refractory. The scrap feed is charged into the rotary furnace that is heated by a burner of natural gas with air that generates high temperatures inside the refractory lined drum.

Technological evolution

The earliest and simplest type of reverberatory furnace design is the wet-heart single chamber furnace; here scrap is simply loaded into the furnace, the door is closed and the melting begins. Usually, a heel of molten metal is left inside the chamber bottom after tapping to easier melt the new charge.

Dry-heart furnace is the successive step in the evolution of this kind of melting furnaces. The innovation consists of a sloping hearth present before the melting zone onto which solid scrap is placed for initial heating. Metal remains on the dry hearth until the bath temperature has recovered the set point. Subsequently the preheated and semi-molten charge is pushed into the bath and cold metal is placed onto the dry hearth. The advantages are various: the average melting rate is improved, the energy consumption is reduced and the furnace utilization increases[57].

The *stack furnace* can be considered as a modified reverberatory ones; their efficiency is improved by a better sealing of the furnace and by using the fuel gases to preheat the charge materials. Here the scrap is introduced directly into the exhaust stack, forcing the exhaust gas to go through the scrap as it leaves the furnace. Additional burners melt the heated scrap and let it flow into the molten bath. This in turn allows more scrap to descend to the hearth, creating a semi-continuous melting operation. The energy efficiency of the stack furnace is improved by 40 to 50%. The stack furnace must be higher than 20 feet (6 meters) due to the charging mechanism and this is clearly a constructive disadvantage. Moreover, the refractories at the bottom of the charging door are subjected to repeated impact and wear[58].

An important design evolution is represented by the *multi-chamber furnace* that is generally based on a integrated scrap preheating/delaquering and a submerged melting process. In the preheat compartment the scrap load is exposed to an intense hot gas flow and organic compounds are transformed into combustible gases. Combustion and post combustion takes place in all the furnace chambers. The melting occurs for the heat that comes from the molten metal and not for direct flame impingement thus the metal loss is drastically reduced without using any flux [59].

A lot of innovations on this furnace were implemented to increase energy efficiency without affecting the metal recovery. In particular, we have to mention exhaust gas recirculation, regenerative burners and molten metal pump and continuous advancements still are being implemented [60-62]

The most important innovation for rotary furnaces is the transition from stationary to *tilting drums*. The ability of the furnace to tilt minimizes the amount of time spent on non-melting operations such as charging, tapping, drossing-off and cleaning. Tilting rotary furnaces allow the melting of high quality scrap without the use of flux avoiding all the salt slag treatments

Custom-scrap strategies

Dross, turnings and *usage beverage can* (UBC) attracted a lot of attention in the recent years Specific recycling strategies have been developed for these particular types of scrap.

The recycling of UBCs is oriented to a closed loop system. This solution can avoid the main problem during the remelting process: the removal of impurities. This aim is pursued creating an efficient supply chain from the manufacturer to the final users through the recycling process. Collection and transportation are the starting point to reduce the needs for expensive sorting processes. UBCs perform a global recycling rate higher than the 70% even if the percentage strongly varies by countries. De-coating process is performed before re-melting with traditional melting techniques. New de-coating processes are continuously proposed and also specific crusher system have been developed [63].

The conventional melting processes lose part of their effectiveness when they are performed with *turnings* deriving from the machining of semi-finished aluminium products; the elongated spiral shape, the small size and the surface contaminations lead to the loss of a lot of metal as a result of oxidation. As a response to this issues, some technologies to avoid the melting phase have been considered: in particular hot extrusion[64], hot forging[65] and high pressure torsion[66]. All these processes are characterised by low energy consumption, large metal saving and very low air pollution. They can be successfully used to achieve fully dense recycled bulk samples from the machined chips, but to this day the optimization of all processes is required [67].

As regards the recycle of *dross* several R&D activities, aim at developing a salt-free process, have been conducted by the main aluminium producers. Table 3 reports all the processes according to the Unlu and Drouet [68] review.

Table 3.
Comparison of several technologies proposed for recycling the aluminium dross[68, 69]

Name(owner)	process	dross	energy source	in industry
(Alcan)	plasma	cold	electric	yes
DROSCAR (Hydro)	graphite electrodes	cold	electric	no
Alurec (AGA)	tilting rotary furnace	cold	oil	yes
ECOCENT (Focon)	centrifuge	hot	dross	-
DROSRITE (PyroGenesis)	rotation in Ar atmosphere	hot	dross	-

Fluxing

The term *fluxing* is used to represent all the additions and treatments applied to the molten aluminum in which chemical compounds are used. These compounds are usually inorganic and may perform several functions, such as degassing, demagging, cleaning, and alloying.

During scrap melting, the main purpose of the flux is to protect the bath from oxidation and salt mixtures are used. Peterson [70] conducted tests to compare the processing results obtained from a no-flux option and a conventional option with salt flux.

A 8.35% drop in the metal recovery was observed by melting dross with no flux due to an higher oxidation.

The metal oxidation is reduced but not completely avoided by the flux. Oxidation that is favoured by the process temperature, the melting of fines and chips or by the high Mg content. The metal loss due to oxidation is usually evaluated as burn-off rate which is defined as the percentage of the metal content of the scrap converted inside a furnace into oxide. The *burn-off rates* for various scrap categories were deduced through a combined mass and energy balance based on 26 smelters results by Boin, et al. [71].

Fluxes take part also in the metal cleanness. Oxides tend to accumulate at or near the melt surface due to surface tension effects, even if they are denser than liquid aluminium. Salt flux accelerates the inclusion separation process because it wets the oxides that are touched, increasing the effect of aluminium's surface tension that acts to repulse oxide inclusions from the melt [72].

The non metallic components from the scrap are completely absorbed by the liquid flux and they form, with the flux, a waste so-called *salt slag* or *salt cake*. Worldwide, the aluminum industry produces annually nearly 5 million tons of waste and this number continues to grow with the increase in the use of aluminium and its recycling [73]. Salt slag is classified as toxic and hazardous waste according to the European Catalogue for Hazardous Wastes [74]. Table 4 shows the main properties of the salt slag that make it as hazardous material.

There are two possibilities for the management of the salt cake: the separation of its components for possible recovery and application[75], or the storage in controlled landfills [76, 77]. Today, the treatment of the salt slag is generally done in the US, Canada and Europe. Economic and environmental reasons justify, for large refining companies, the investment of a salt cake recycling facility on site. Aluminium metal, salt and compounds containing alumina are recoverable as high quality products for the recycling process, or sold, since residuals so generated are non-toxic.

Table 4.
Comparison of several technologies proposed for recycling the aluminium dross[74]

Code	Title	Meaning
H3-A	Highly flammable	Substances and preparations which, in contact with water or damp air, evolve highly flammable gases in dangerous quantities
H4	Irritant	Non-corrosive substances or preparations which through immediate prolonged or repeated contact with the skin or muccus membrane can cause inflammation
H5	Harm-full	Substances and preparations which, if they are inhaled or ingested or if they penetrate the skin, involve limited health risk
H13	Leachable	Substances and preparations capable by any means, after disposal, of yielding another substance

Industrial practice

Most of the fluxes are composed of *sodium and potassium chlorides*. This salts are usually preferred due to the low cost and the low melting point[78]. Sodium chloride is cheaper, while the addition of potassium chloride decreases the viscosity and the surface tension, increasing the fluidity. American recyclers typically use the equimolar mixture due to its low melting point at 645°C (Figure 6) while European recyclers mostly use 70:30 ratios because of historical experience.

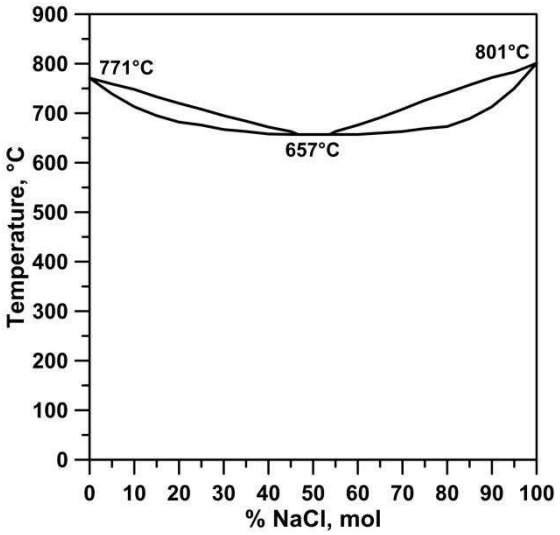

Figure 6 The phase equilibrium diagram for the NaCl-KCl system[78]

In response to the increment in the prize of the KCL, Bolivar and Friedrich [79] tested the metal recovery melting aluminium with a NaCl:KCl ratio ranging from 70 wt.% to 100 wt.%. A non-statistical influence on the metal recovery at different NaCl:KCl ratios was found.

A mixture of $BaCl_2$-NaCl is proposed by Ueda, et al. [80] as alternative flux while Utigard, et al. [81] investigated the effectiveness of a KCl-Mg_2Cl salt. Encouraging results were achieved with both of them however the NaCl-KCl is still the world-wide standard thanks to its lower cost.

Figure 7 shows the equilibrium constant of the reaction between aluminium and several chlorides. Equilibrium constants much greater than unit, i.e. logarithm of the constant greater than 0, imply that the aluminium reacts with the chlorine forming $AlCl_3$. Consequently, the metal element of the chloride (e.g. Zn in case of $ZnCl_2$) is added in the bath.

A value lower than one indicates that the reaction goes in reverse. Therefore, sodium and potassium chlorides are suitable as cover flux as they have no tendency to react with aluminium.

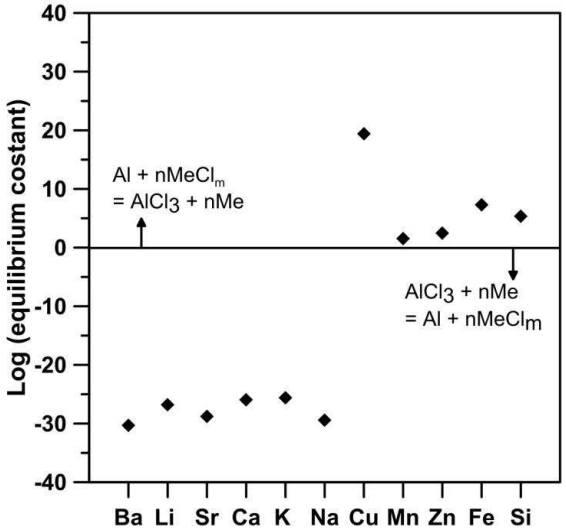

Figure 7 Exchange equilibrium between aluminium and various metal chlorides at 723°C[82]

On the other side, NaCl-KCl does not offer good *refining properties*. Ideally, the metal impurities can be removed by the flux through the formation of metal chlorides. This reactions can take place only if the metal chlorides are more stable than $AlCl_3$, i.e. with a value of the standard Gibbs energy of formation more negative than that for $AlCl_3$ (Figure 8) [83]. The removal of impurities such as Zn, Si, Fe and Cu by chlorine treatment is basically impossible and if fluxes contain these metals, they will contaminate the aluminum. Li, Na, K, Ca, Mg and Ba all form chlorides more stable than aluminum and that therefore can be removed by the addition of Cl_2 [84]. However, the reduction of the amount of Mg cannot be performed by exchange reactions with a flux containing only NaCl and KCl salts due to the very low equilibrium constants for these exchange reactions as explained in Equation 2.

$$2NaCl + Mg = 2Na + MgCl_2, \; K_{eq} = 1.1 * 10^{-18} \qquad \text{Equation 2}$$

In general there are three types of *demagging* processes to reduce the Mg content: i) chlorination, ii) use of solid chlorine-containing fluxes (C_2Cl_6), and iii) injection of AlF_3 or $NaAlF_4$.

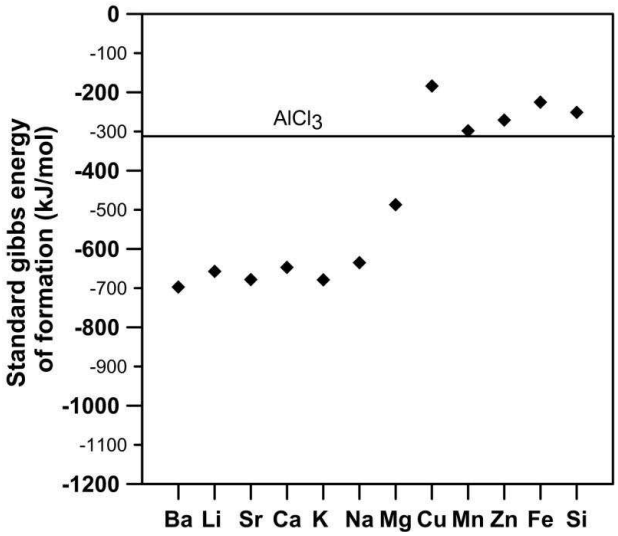

Figure 8 Standard Gibbs energy formation for several chlorides at 723°C per mole of Cl_2 [82]

The addition of fluorides like NaF and KF to the chloride flux aids the removal of magnesium from aluminum scrap causing the contamination of the molten bath with sodium and/or potassium as shown in Figure 9. *Fluorides* are normally added to the flux but the Mg removal is not the reason. They are used with the aim of enhancing the coalescence of the metal entrapped in the flux leading to its recovery, as discussed in the next chapter.

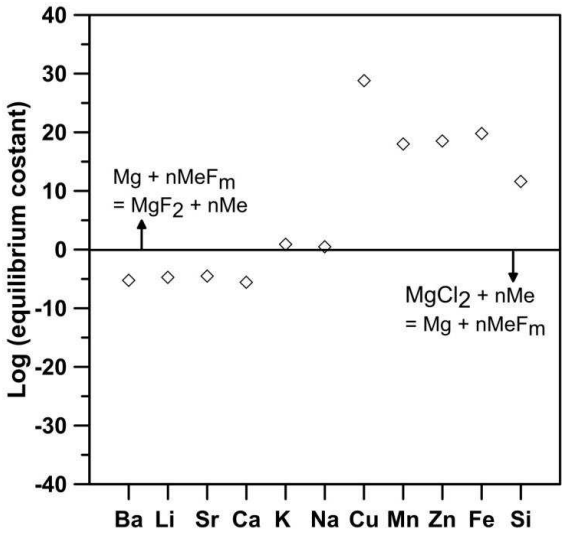

Figure 9 Exchange equilibrium between magnesium and various metal chlorides at 723°C[82]

In view of the results described above, great deal of attention has been paid to the flux composition. On the other side, a market study carried out by Foseco[85] revealed that a negligible effort has been done to characterize the necessary amount of salt.

The amount of salt has to be correlated to the quality of the scrap, i.e. the amount of non metallic content present in the scrap. The amount of salt to be charged increases for a greater fraction of impurities in the scrap, thus the introduction of a *salt factor* (SF), as reported in Equation 3, is necessary.

$$SF = \frac{m_{salt}}{m_{scrap} \times (1 - \mu_{metal})} \qquad \text{Equation 3}$$

here m_{salt} and m_{scrap} are the weights of salt and scrap charged in the furnace, respectively, and μ_{metal} is the metal yield of the scrap.

Tilting furnaces allow a greater reduction in the salt consumption than fixed rotary furnaces but as regards the latter the values of salt factor proposed vary over a wide range. Boin and Bertram [86] assumed a salt factor equal to 1.3 in a mass balance model for refiners in Europe, while according to Moloodi, et al. [87] salt factors ranging from 1.5 to almost 2 are used, and a value equal to 1.8 is an often published value, while in the Aluminium recycling roadmap[88] it ranges from 1 to 2.

This amount of salt used during the scrap re-melting involves different aspect in the refining process as:

- energy consumption
- slag disposal
- metal recovery

The theoretical *energy consumption* of a rotary drum furnace was investigated as function of the oxide content in the scrap for various salt factor values by Friedrich, et al. [89]. The energy consumption decreases of approximately 900 MJ/t_{Al} if the salt factor is reduced from 1.6 to 0.8. The slag disposal cost and recovery were studied by several authors considering economic and environmental aspects.

A lack of results can be observed regarding the influence of the salt factor on the metal recovery both on laboratory (***Article 1, pp. 37-43***) and industrial scale (**Article 2, pp. 45-64**).

Recovery of molten metal from the cover flux

The flux entraps a portion of molten metal as side effect. The non-metallic residues generated from scarp/dross smelting contain 5–7% residual metallic aluminium according to Tsakiridis [90]. The amount of aluminium lost in the dross depends on different factors, including flux properties. The ability of the flux in realising the molten metal from the slag is fundamental in increasing the metal recovery of the process. This capability is linked with the capacity of the metal to coalesce inside the flux.

The coagulation of metal drops leads to a growth in the droplets diameter, resulting in a higher probability of their separation from the salt flux and in the metal settling in the molten. Therefore, the greater the metal coalescence, the higher the metal recovery. Different properties have an impact on the metal coalescence:

- *Density*: a lower density of the salt allows a better metal/salt settling.
- *Viscosity*: a decrease in the salt viscosity allows a better mobility of the metal droplets in the flux and induces better conditions for the coalescence.
- *Interfacial tension*: decreasing the interfacial tension between salt and metal allows a better coalescence.
- *Dissolution of the oxides*: the removal of oxide film from the aluminium surface is necessary to favour the coalescence between aluminium droplets.

Several authors conducted coalescence experiments in the salt flux in order to determine the best salt flux composition for an optimized coalescence, i.e. the largest metal droplets. Fluorides are suggested as the most effective additives, while addition of other chlorides, like $MgCl_2$ or $CaCl_2$, seems not to encourage the coalescence[91].

Flux density and viscosity

The addition of fluorides increases the salt density according to Roy, et al. [92], who proved this effect for various fluorides, i.e. NaF, LiF, KF and Na_3AlF_6. A higher density does not help the metal coalescence since the metal settling is hinder.

On the other side , Tenorio, et al. [93] found a decrease in the viscosity of the flux when NaF or KF is added to an equimolar mixture of NaCl and KCl, that favours the metal coalescence. More in detail, the viscosity of the NaCl-KCl mixture decreases from 0.012 P to 0.004 P adding 20 wt.% of these two fluorides. This positive effect is inhibited by the increment of viscosity due to the presence of the oxides collected in the flux. Xiao, et al. [94] assessed the influence of the oxides adding non metallic components with a size ranging between 10 and 30 µm. The viscosity increases dramatically when the volume percentage of *non metallic content* (NMC) is about 10%, but it is higher than 0.1 P for a content of about 2%.

In conclusion, the effects of the fluorides addition on the density and the viscosity of the flux do not seem to justify an increment of the metal drops coalescence

Flux-salt interfacial tension and oxide dissolution

It is generally believed that the real advantage of the fluorides addition is their ability in removing the oxide layer. However, the mechanism of the oxide removal is still unclear.

Jordan and Milner [95] and Storchai and Baranov [96] suggested an *electrochemical* nature where the anions F^- penetrate through pores and defects present in the oxide film

and enter into electrochemical reaction with the aluminium. According to this theory, the rupture of the oxide film is related to the formation of the aluminium fluoride

The variation of the *interfacial tension* between the molten metal and the salt is an alternative taken into account. Martin-Garin, et al. [97] measured the interfacial tension with the addition of NaF, KF, LiF and cryolite (Na_3AlF_6) from melting pure aluminium in an equimolar NaCl-KCl mixture. Interfacial tension decreases for all the additions in the following order: Na_3AlF_6 < LiF < NaF < KF. Similar results were achieved melting UBC scrap under the same fluxes[98]. It is accepted that a low interfacial tension between the molten metal and the salt is responsible for the removal of the oxide film.

The decrease in interfacial tension is explained by the adsorption of sodium and potassium at the metallic side of the interface. The activity of sodium and potassium is very low when aluminium is in equilibrium with pure equimolar NaCl-KCl melt, and therefore no significant adsorption of surface active elements takes place[83]. The fluorides act increasing the activity of sodium and potassium as highlighted in Table 5. A lower equilibrium constant means a greater element activity and therefore absorption.

Table 5.
Equilibrium constant for the reactions between aluminium and different chlorides and fluorides[83]

reaction	equilibrium constant
$Al + 3NaCl = 5AlCl_3 + 3Na$	$6.08*10^{-24}$
$Al + 3KCl = 5AlCl_3 + 3K$	$2.29*10^{-27}$
$Al + 3LiCl = 5AlCl_3 + 3Li$	$1.31*10^{-25}$
$2Al + 3CaCl_2 = 2AlCl_3 + 3Ca$	$7.85*10^{-48}$
$Al + 3NaF = 5AlF_3 + 3Na$	$6.95*10^{-9}$
$Al + 3KF = 5AlF_3 + 3K$	$2.50*10^{-8}$
$Al + 3LiF = 5AlF_3 + 3Li$	$9.88*10^{-17}$
$2Al + 3\ MgF_2 = AlF_3 + 3Mg$	$1.05*10^{-18}$
$2Al + 3\ CaF_2 = AlF_3 + 3Ca$	$1.05*10^{-34}$
$2Al + 3\ BaF_2 = AlF_3 + 3Ba$	$3.16*10^{-33}$
$2Al + 3\ SrF_2 = AlF_3 + 3Sr$	$6.35*10^{-36}$

Tenorio and Espinosa [99] assessed that the oxide removal behavior is similar to the *hot corrosion process* where a metal that develops a protective oxide layer is submitted to an atmosphere containing chlorides (Figure 10). Under these conditions chlorine or chloride penetrates the oxide and an increase of the chlorine concentration occurs near or at the interface between the oxide and the metal. This accumulation of chlorides causes a weakness in the mechanical stability of the oxide layer, which becomes susceptible to blistering, cracking or spalling.

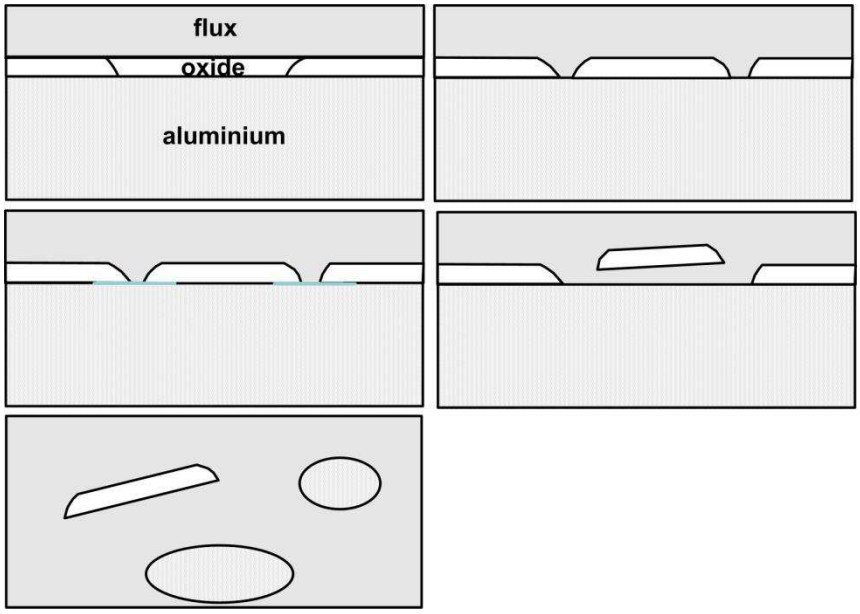

Figure 10 Evolution of the oxide removal caused by the flux: (a) flux-salt interaction, (b) corrosion of the oxide at the boundaries, (c) diffusion of Cl at the oxide/aluminium interface, (d) oxide removal and (e) aluminum drops formation in the salt. [99]

Features affecting the metal drops coalescence in the flux

The way in which the oxide is removed and the coalescence favoured is still a topic of debate, while all the results in literature agree on the fact that fluorides are the best salts to achieve this goal[100-102]. In particular NaF, KF and cryolite (Na_3AlF_6) offer excellent results according to Friesen, et al. [103].

Roy and Sahai [104] classified various salts in four categories depending on their *coalescence ability* when added to a NaCl-KCl mixture:

- Excellent NaF; KF; Na_3AlF_6
- Good CaF_2; MgF_2
- Moderate AlF_3
- Poor NaCl-KCl with no addition

Cryolite is accredited as one of the most effective fluorides in favouring the drop formation. However, the influence of cryolite on several flux properties is not completely investigated ***(Article 3, pp. 65-81)***

The effectiveness of a flux in increasing the metal recovery does not depend only on its composition. Majidi, et al. [105] assessed the importance of proper fluxing temperature in aluminum recycling by means of tensile tests, metallographic and SEM analyses, RPT test and K-mould. Based on the results obtained in this research, the optimum fluxing temperature is about 740 °C for a 45NaCl-45KCl-8Na_2SiF_6-2CaF_2 salt.

The scrap melted also plays a major role. Ye and Sahai [106] compared the removal of the oxide using a mixture of NaCl-KC-NaF salts melting scrap with a content of Mg ranging from 0 to about 4.5%. Cylindrical shape samples were melted and the removal of the oxide was assessed observing if they became spherical drops. The presence of Mg slowed down the oxide removal and in the case of pre-oxidised samples with the higher Mg content, i.e. more than 2%, they did not change morphology.

The presence of Mg accelerates the oxidation of the alloy promoting the formation of a thicker oxide layer. Melting Al-Mg alloy, Masson and Taghiei [107] observed the formation

of an interfacial layer consisting of either $KMgF_3$ or K_2NaAlF_6. Both compounds have a high melting temperature and therefore can avoid the metal coalescence as for the oxides.

The same compounds were found by Besson, et al. [100] melting Al-Mg alloy chips under a NaCl:KCl flux with the addition of cryolite in several amounts. Melting pure aluminium, the drop coalescence always increased with the content of cryolite, while melting the Al-Mg chips the best result was achieved with a concentration of 2%. The coalescence effectiveness of the drops decreased for greater amount of cryolite and the formation of K, Na-Mg-F species was detected.

The coalescence can be affected not only by its composition but also by the presence of *coatings* ***(Article 4, pp. 83-93)***. The residues from the coatings, as for oxides, worsen the salt slag properties by increasing its density and viscosity and making the settling of the metal droplets and the separation of the metal from the slag difficult. Thoraval and Friedrich [108] assessed that the salt slag density and viscosity are predominant over the fluorides addition for an amount of oxide above the 40 wt.%. In conclusion, optimizing the flux in terms of quantity and composition and considering pre-melting scrap treatments is necessary to obtain the greatest drop coalescence ***(Article 5, pp. 95-118)***

OBJECTIVIES AND SURVEY OF THE ARTICLES

► Investigate the influence of the quantity of salt charged with the scrap on the metal recovery melting heterogeneous scrap.

Article 1

The influence of the salt quantity on the metal recovery was studied melting a heterogeneous scrap charge in a crucible furnace. The metal content of the various types of scrap, i.e. shredded, turning and dross, was evaluated according to the standard and a melting procedure was defined to replicate a rotary furnace cycle. The amount of salt was related to the scrap quality using the salt factor, which is defined as the ratio between the non-aluminium content in the scrap and the quantity of salt required. Two levels of salt factor were considered, 1.2 and 1.8. The influence of the salt quantity on the metal recovery was verified by means of the analysis of variance.

Article 2

The results obtained on a laboratory scale using a crucible furnace were compared with those obtained on industrial level by means of a rotary furnace. The metal recovery was studied as function of the salt factor. Two salt factor levels were tested with a discrepancy of 0.1 point.
The procedure used in Article 1 was performed for melting the scrap in the crucible furnace while the experiments with the rotary furnace were conducted during the normal production and more than 50 casts were considered.
A charge composed of the same kind of scrap was melted under a NaCl-KCl-Na_3AlF_6 flux in both furnaces but a greater amount of scrap was processed in the rotary furnace, i.e. about 90 ton instead of 5 Kg

► Study the influence of the addition of cryolite in a standard NaCl-KCl salt on several properties that can affect the coalescence ability of the flux

Article 3

The influence of the cryolite (Na_3AlF_6), a widely used fluoride, on several properties of a typical industrial flux composed by a mixture of 95NaCl-5KCl was investigated. The properties chosen are those that can affect the coalescence of metal drops inside the flux: the melting temperature and the viscosity of the flux and its ability in dissolving the aluminium oxide. Moreover, the dissolving time of the flux in water was studied.
Thermal analysis (TA) was performed to measure the melting temperature and a body falling method was set to evaluate the viscosity. The oxide dissolution was assessed as the reduction in weight of alumina balls immersed in the molten flux while the weight reduction of a representative sample of the solidified salt was used to appraise the leachability.

► Study the coalescence of molten aluminum melting coated and de-coated scrap

Article 4

The effectiveness of the de-coating treatment was assessed comparing the results achieved melting coated scrap and the same ones after de-coating treatments at various temperatures.
One hundred discs were stamped from aluminium alloy sheets with and without coating. They were melted, covered in NaCl-KCl-Na_3AlF_6 molten salt, in an induction furnace at 790°C for 8 minutes. The solidified aluminum droplets were extracted by leaching the salt with water. The same tests were repeated for various holding time, i.e. 8, 16, 60 minutes, melting the coated discs.
The fraction of coalesced drops and their average diameters were determined to evaluate the coalescence efficiency by means of custom Matlab software (Appendix A).

Article 5

This work investigates the aluminium coalescence behaviour melting the scrap with different impurity contents under fluxes with various compositions, namely 1) Cryolite salt 2) Industrial salt and 3) Recycled salt.
All the salts were a mixture of NaCl and KCl while different fluorides were used. CaF_2 was added in the Industrial and in the Recycled salts ranging from 2 to 6 wt. %, while Na_3AlF_6 in 2wt.% was present in the Cryolite salt. The scrap was stamped out from AA3000 foil with and without coating in the form of discs.
The study of the influence of the coating on the metal coalescence present in the Article 4 was extended testing the same surface conditions under various quantity of salt. Four different salt-scrap ratios were investigated, i.e. 0.5, 2 and 4.

CONCLUSIONS

► Influence of salt quantity on metal recovery from remelting heterogeneous scrap.

The metal content in the scrap has to be assessed to evaluate the metal recovery of the melting process and the use of the standard is suggested. The salt factor is suitable for defining the quantity of salt to charge with the scrap. A positive relation was found between the salt factor and the metal recovery. This result was verified both on laboratory and industrial scale by means of crucible and rotary furnaces respectively.

Crucible furnace achieved better results due to a better control of the charge and a lower amount of scrap melted. The low capacity of crucible furnaces avoids their use on industrial scale. More interesting was that the yield difference between the two salt factors is similar for the two melting furnaces; thus it allows the use of a crucible furnace for preliminary tests in order to optimize the fluxing in a rotary furnace.

The increment of the metal recovery due to the higher levels of salt factor leads to a greater amount of metal tapped only melting scrap with a metal yield higher than 0.85. Indeed the amount of tapped metal depends on the metal recovery and the amount of scrap processed. For a fixed salt factor level, the higher the non-metal content in the scrap the higher the quantity of salt at the expense of the amount of scrap that can be melted.

► Effect of cryolite addition on the properties of a NaCl-KCl mixture

The cryolite addition produces an increment in the viscosity of the molten salt according to a polynomial trend, while increasing the temperature the viscosity weakly decreases. A higher viscosity makes less favourable the coalescence of the metal drops in the flux badly affecting the metal recovery. This negative effect is opposite to the consequence of the addition of other fluorides like NaF and KF, but it is overshadowed by the greater increment of the viscosity due to the presence of non metallic components.

The metal coalescence is strongly favoured by the cryolite addition because it allows the release of aluminium from the oxide layer, while a flux composed by NaCl and KCl is not able to dissolve the alumina. The dissolution rate of the alumina rises from 0.004 to 0.038 wt.%/min if the cryolite content is increased from 5 to 20 wt%..

The melting temperature of the 95NaCl-5KCl flux is 795°C and it decreases adding cryolite, reaching 755°C for a cryolite content equal to 20 wt.%. A lower melting temperature means a reduction in energy and time consumptions.

Finally, the dissolution of the flux in water is slowed down by the addition of cryolite that is in agreement with the different solubility in water between NaCl and Na_3AlF_6.

► Interaction between coating and metal coalescence and effectiveness of the de-coating treatment.

The coat that covers the scrap surface can hinder the coalescence of the aluminium drops in the molten salt, preventing their recovery. A temperature of de-coating equal to 400°C is too low and does not help the drops coalescence. The drop coalescence increases if the combustion reaction temperature is reached during the de-coating treatment.

The results obtained with a complete combustion reaction, i.e. de-coating at 600°C, are equal to those achieved with a clean scrap.

► Aluminium drop coalescence in fluxes with various compositions and quantities

The addition of cryolite promotes a better coalescence of clean aluminium scrap of AA300 alloy than the addition of CaF_2. The effect of CaF_2 does not change increasing its amount from 2wt.% to 6wt.%. Moreover, the presence of S in the salt seems to hinder the positive effect of the fluorides addition.

The coalescence of the coated scrap is not achieved with the tested salts, therefore de-coating is necessary.

The influence of the salt scrap ratio is perceptible only for lower amounts of coating. Clean scrap coalesces also for low amounts of salt, i.e. salt scrap ratio equal to 0.5, while the coalescence of coated discs is not achieved for amounts of salt four times higher than the amount of scrap.

REFERENCES

1. G.E. Totten, D.S. MacKenzie, Handbook of Aluminum: Vol. 1: Physical Metallurgy and Processes, Marcel Dekker, Inc., 270 Madison Avenue, New York, NY 10016, 2003.
2. H. Antrekowitsch, G. Hanko, P.Ebner, Magnesium Technology 2002, TMS: The Mineral, Metal, and Materials Society, USA, 2002, pp. 43-48.
3. Information on www.bir.org
4. G. Rombach, Integrated assesment of primary and secondary aluminium production, Material for the future: Aluminium production and process, DMG Business Media Limited, Surrey UK, 1998.
5. S.K. Das, J.A.S. Green, J.G. Kaufman, The development of Recycle-friendly automotive aluminum alloys, JOM 59 (2007) 47-51.
6. Information on http://minerals.usgs.gov/minerals/pubs/country/
7. K. Nakajima, O. Takeda, T. Miki, K. Matsubae, S. Nakamura, T. Nagasaka, Thermodynamic Analysis of Contamination by Alloying Elements in Aluminum Recycling, Environ. Sci. Technol. 44 (2010) 5594-5600.
8. A. Gesing, R. Wolanski, Recycling Light Metals from End-of-Life Vehicles, JOM (2001) 21-23.
9. J.M. Cullen, J.M. Allwood, Mapping the Global Flow of Aluminum: From Liquid Aluminum to End-Use Goods, Environ. Sci. Technol. 47 (2013) 3057-3064.
10. R. Modaresi, D.B. Müller, The Role of Automobiles for the Future of Aluminum Recycling, Environ. Sci. Technol. 46 (2012) 8587-8594.
11. H. Hatayama, I. Daigo, Y. Matsuno, Y. Adachi, Assessment of Recycling Potential of Aluminum in Japan, the United States, Europe and China, Mater. Trans. 50 (2009) 650-656.
12. H. Hatayama, I. Daigo, Y. Matsuno, Y. Adachi, Evolution of aluminum recycling initiated by the introduction of next-generation vehicles and scrap sorting technology, Resour. Conserv. Recycl. 66 (2012) 8-14.
13. A.N. Løvik, R. Modaresi, D.B. Müller, Long-Term Strategies for Increased Recycling of Automotive Aluminum and Its Alloying Elements, Environ. Sci. Technol. 48 (2014) 4257-4265.
14. E.C.f. Standardization, European Committee for Standardization, 2012.
15. E.C.f. Standardization, Bruxelles, 2003.
16. Information on www.metalonmarket.com
17. M.B.G. Castro, J.A.M. Remmerswaal, M.A. Reuter, U.J.M. Boin, A thermodynamic approach to the compatibility of materials combinations for recycling, Resour. Conserv. Recycl. 43 (2004) 1-19.
18. B. Zhou, Y. Yang, M.A. Reuter, U.M.J. Boin, Modelling of aluminium scrap melting in a rotary furnace, Mineral. Eng. 19 (2006) 299-308.
19. G. Schubert, S. Bernotat, Comminution of non-brittle materials, Int. J. Mineral Process. 74S (2004) S19-S30.
20. G. Schubert, S. Sander, G. Timmel, Characterisation of fragments produced by the comminution of metals especially considering the fragment shape, Powder Technol. 122 (2002) 177-187.
21. D. Woldt, G. Schubert, H.-G. Jackel, Size reduction by means of low-speed rotary shears, Int. J. Mineral Process. 74S (2004) S405-S415.

22. D. Wustenberg, J. Kasper, Required energy and structural breakdown at the process of dynamic cutting—comminution of polypropylene and aluminium, Int. J. Mineral Process. 74S (2004) S417-S424.
23. G. Schubert, S. Sander, H.G. Jackel, The fundamentals of the comminution of metals in shredders of the swing-hammer type, Int. J. Mineral Process. 74S (2004) S385-S393.
24. S. Sander, G. Schubert, Size reduction of metals by means of swing-hammer shredders, Chem. Eng. Technol. 4 (2003) 409-415.
25. L. Cui, L. An, W. Gong, Effects of process parameters on the comminution capability of high pressure water jet mill, Int. J. Mineral Process. 81 (2006) 113-121.
26. H.Z. Kuyumcu, L. Rolf, Application of high-pressure waterjets for comminution, Int. J. Mineral Process. 74S (2004) S191-S198.
27. M.B. Castro, J.A.M. Remmerswaal, J.C. Brezet, A.v. Schaik, M.A. Reuter, A simulation model of the comminution–liberation of recycling streams: relationships between product design and the liberation of materials during recycling Int. J. Mineral Process. 75 (2005) 255-281.
28. G. Gaustad, E. Olivetti, R. Kirchain, Improving aluminum recycling: A survey of sorting and impurity removal technologies, Resour. Conserv. Recycl. 58 (2012) 79-87.
29. P. Li, J. Dahmus, S. Guldberg, H.O. Riddervold, R. Kirchain, How Much Sorting Is Enough Identifying Economic and Scrap-Reuse Benefits of Sorting Technologies, J. Ind. Ecol. 15 (2011) 743-753.
30. S. Bell, B. Davis, A. Javaid, E. Essadiqi, Government of Canada, 2003.
31. A. Veasey, The physical separation and recovery of metal from waste, Gordon and Breach Science, 1993.
32. S. Zhang, E. Forssberg, B. Arvidson, W. Moss, Separation mechanisms and criteria of a rotating eddy-current separator operation, Resour. Conserv. Recycl. 25 (1999) 215-232.
33. M.B. Mesina, T.P.R.d. Jong, W.L. Dalmijn, Improvements in separation of non-ferrous scrap metals using an electromagnetic sensor, Phys. Sep. Scie. Eng. 12 (2003) 87-101.
34. G. Coates, S. Rahimifard, Modelling of post-fragmentation waste stream processing within UK shredder facilities, Waste Manag. 29 (2009) 44-53.
35. T.P.R.d. Jong, W.L. Dalmijn, Improving jigging results of non-ferrous car scrap by application of an intermediate layer, Int. J. Mineral Process. 49 (1997) 59-72.
36. D.B. Spencer, The High-Speed Identification and Sorting of Nonferrous Scrap, JOM (2005) 46-51.
37. P. Werheit, R. Noll, C. Fricke-Begemann, T. Erdmann, M. Gesing, A. Pichat, J. Makowe, Sensor based sorting 2012, Aachen, 2012.
38. R. Comtois, T. Jansen, Sensor-Based Sorting & Control 2008, 2008, pp. 53-54.
39. A. Gesing, TMS (The Minerals, Metals & Materials Society), Annual Meeting and Exhibition, 2007.
40. P.B. Schultz, R.K. Wyss, color sorting aluminum alloys for recycling-Part II, Plat. Surf. Finish. 87 (2000) 62-65.
41. S. Koyanaka, K. Kobayashi, Y. Yamamoto, M. Kimurab, K. Rokucho, Elemental analysis of lightweight metal scraps recovered by an automatic sorting technique combining a weight meter and a laser 3D shape-detection system, Resour. Conserv. Recycl. 75 (2013) 63-69.

42. K. Tsuchiya, Y. Goto, T.-a. Hatano, S. Owad, A. Takasugi, Y. Kato, T. Funakoshi, H. Tannno, H. Yamazaki, 11th international conference on mining, materials and petroleum engineering, Chiang Mai, Thailandia, 2013, pp. 21-24.
43. T. Takezawa, M. Uemoto, K. Itoh, Combination of X-ray transmission and eddy-current testing for the closed-loop recycling of aluminum alloys, J. Mater. Cycles Waste Manag. 17 (2015) 84-90.
44. E. David, J. Kopac, Use of Separation and Impurity Removal Methods to Improve Aluminium Waste Recycling Process, Mater. Today: P. 2 (2015) 5071-5079.
45. A. Kvithyld, A. Nordmark, D. Dispinar, S. Ghaderi, H. Lapointe, Quality comparison between molten metal from remelted sheets, mill finish and coated, in: C.E. Suarez (Ed.) Light Metals 2012, TMS: The Minerals, Metals & Materials Society, 2012, pp. 1031-1035.
46. A.A. Tracton, Coatings technology handbook, third ed., CRC Press Taylor & Francis Group, 6000 Broken Sound Parkway NW, Suite 300 Boca Raton, FL 33487-2742, 2006.
47. B. Jaroni, A. Lucht, B. Friedrich, European Metallurgical Conference, Dusseldorf, 2011, pp. 1-12.
48. X.-G. Chen, M. Fortier, TiAlSi intermetallic formation and its impact on the casting processing in Al–Si alloys, J. Mater. Process. Tech. 210 (2010) 1780-1786.
49. R. Ghomashchi, The evolution of AlTiSi intermetallic phases in Ti-added A356 Al–Si alloy, J. Alloy Comp. 537 (2012) 255-260.
50. R. Evans, G. Guest, Aluminum decoating handbook, 2005.
51. M.A. Rabah, Preparation of aluminium–magnesium alloys and some valuable salts from used beverage cans, Waste Manag. 23 (2003) 173-182.
52. M. Wang, K.-D. Woo, D.-K. Kim, L. Ma, Study on de-coating used beverage cans with thick sulfuric acid for recycle, Ener. Convers. Manage. 48 (2007) 819-825.
53. C.E.M. Meskers, M.A. Reuter, U. Boin, A. Kvithyld, A Fundamental Metric for Metal Recycling Applied to Coated Magnesium, Metallurgical and materials transaction B 39B (2008) 500-517.
54. A. Kvithyld, C.E.M. Meskers, S. Gaal, M. Reuter, T.A. Engh, Recycling light metals: optimal thermal de-coating, JOM 60 (2008) 47-51.
55. A. Kvithyld, J. Kaczorowski, T.A. Engh, Microscope studies of thermal decoating of aluminium scrap, in: A.T. Taberaux (Ed.) Light Metals 2004, TMS: The Minerals, Metals & Materials Society, 2004.
56. E. Velasco, J. Nino, Recycling of aluminium scrap for secondary Al–Si alloys, Waste Manage. Res, 29 (2011) 686-693.
57. P. Newman, Dry heath melting furnace, Mater. Sci. Forum 630 (2010) 103-110.
58. J.F. Schifo, J.T. Radia, U.S. Department of Energy, 2004.
59. J.d. Groot, J. Migchielsen, Multi chamber melting furnaces for recycling of aluminium scrap, in: P. Whiteley (Ed.) Aluminium Cast House Technology 2003, (Eighth Australasian Conference), TMS: The Minerals, Metals & Materials Society, 2003, pp. 50-70.
60. Hertwich, in: Hertwich (Ed.), 2012.
61. A.M. Peel, J. Herbert, D. Roth, M.J. Collins, Furnace Operations to Reduce Dross Generation, Mater. Sci. Forum 630 (2010) 45-52.
62. P. Campbell, The Benefits of Forced Circulation for Aluminium Reverberatory Furnaces, Mater. Sci. Forum 630 (2010) 111-117.

63. A. Elfasakhany, J. Marquez, E.Y. Rezola, J. Benitez, Design and development of an economic autonomous beverage cans crusher, International Journal of Mechenical Engineering and Technology 3 (2012) 107-122.
64. M. Samuel, A new technique for recycling aluminium scrap, J. Mater. Process. Tech. 135 (2003) 117-124.
65. S.S. Khamis, M.A. Lajis, R.A.O. Albert, A sustanaible direct recycling of aluminum chip (AA6061) in hot press forging emplying response surface methodology, Procedia CIRP 26 (2015) 477-481.
66. M.I.A.E. Aal, E.Y. Yoon, H.S. Kim, Recycling of AlSi8Cu3 alloy chips via high pressure torsion, Mater. Sci. Eng. A 560 (2013) 121-128.
67. S.N.A. Rahim, M.A. Lajis, S. Ariffin, A review on recycling aluminum chips by hot extrusion process, Procedia CIRP 26 (2015) 761-766.
68. N. Unlu, M.G. Drouet, Comparison of salt-free aluminum dross treatment processes, Resour. Conserv. Recycl. 36 (2002) 61-72.
69. H.T. Ingason, T.I. Sigfusson, Processing of Aluminum Dross: The Birth of a Closed Industrial Process, JOM 66 (2014) 2235-2242.
70. R.D. Peterson, A historical perspective on dross processing, Mater. Sci. Forum 693 (2011) 13-23.
71. U. Boin, M.A. Reuter, T. Probst, Measuring – Modelling: Understanding the Al Scrap Melting Processes Inside a Rotary Furnace, World of Metallurgy 57 (2004) 264-269.
72. P.N. Crepeau, M.L. Fenyes, L.J. Jeanneret, Solid fluxing practices for aluminum melting (part 1), Mod. Cast. 82 (1992) 28-30.
73. X.-L. Huang, A.E. Badawy, M. Arambewela, R. Ford, M. Barlaz, T. Tolaymat, Characterization of salt cake from secondary aluminum production, J. Hazard. Mater. 273 (2014) 192-199.
74. E.P. Agency, 2002.
75. A. Gil, S.A. Korili, Management and valorization of aluminum saline slags: Current status and future trends, Chem. Eng. J. 289 (2016) 74-84.
76. A. Gil, S.A. Korili, Management of the Salt Cake Generated at Secondary Aluminium Melting Plants, in: S. Sarkar (Ed.) Environmental Management, InTech, Rijeka, Croatia, 2010.
77. K.E. Lorber, H. Antrekowitsch, 2nd International Conference on Hazardous and Waste materials, 2010.
78. D.S. Coleman, P.D.A. Lacy, The phase equilibrium diagram for the KCl-NaCl system, Mat. Res. Bull. 2 (1967) 935-938.
79. R. Bolivar, B. Friedrich, The influence of increased NaCl:KCl ratios on Metal Yield in salt bath smelting processes for aluminium recycling, World of Metallurgy 62 (2009) 1-10.
80. M. Ueda, M. Amemiya, T. Ishikawa, T. Ohtsuka, Recovery of aluminium alloy from aluminium dross by treatment of cholride-fluoride mixture melt, J. Jpn. Inst. Met. 63 (1999) 279-283.
81. T.A. Utigard, R.R. Roy, K. Friesen, The roles of molten salts in te treatment of aluminum, Canadian Metallurgical Quarterly 40 (2001) 327-334.
82. T.A. Utigard, K. Friesen, R.R. Roy, J. Lim, A. Silny, C. Dupuis, The Properties and Uses of Fluxes in Molten Aluminum Processing, JOM 50 (1998) 38-43.
83. R.R. Roy, T.A. Utigard, Interfacial Tension between Aluminum and NaCl-KCl–Based Salt Systems, Metallurgical and materials transaction B 29B (1998) 821-827.

84. T. Hiraki, T. Miki, K. Nakajima, K. Matsubae, S. Nakamura, T. Nagasaka, Thermodynamic Analysis for the Refining Ability of Salt Flux for Aluminum Recycling, Metals 7 (2014) 5543-5553.
85. R. Gallo, Development, evaluation and application of granular and powder fluxes in trasfer ladles, crucible and reverberatory furnace, Foundry Practice 237 (2002) 8-16.
86. U. Boin, M. Bertram, Melting Standardized Aluminum Scrap: A Mass Balance Model for Europe, JOM 57 (2005) 26-33.
87. A. Moloodi, H. Amini, E.Z.V. Karimi, M. Golestanipour, On the Role of Both Salt Flux and Cold Pressing on Physical and Mechanical Properties of Aluminum Alloy Scraps, Mater. Manuf. Process. 26 (2011) 1206-1012.
88. SINTEF/NTNU, Workshop on aluminium recycling, Trondheim, 2010.
89. B. Friedrich, M. Gerke, J. Kruger, A. Arnold, European Metallurgical Conference, 2001.
90. P.E. Tsakiridis, Aluminium salt slag characterization and utilization – A review, J. Hazard. Mater. 217-218 (2012) 1-10.
91. R.D. Peterson, Effect of salt flux additives on aluminum droplets coalescence, in: J.H.L.v. Linden, J. Donald L. Stewart, Y. Sahai (Eds.) Second International symposium-Recycling of Metals and Engineered Materials, TMS: The Minerals, Metals & Materials Society, 1990, pp. 69-84.
92. R.R. Roy, J. Ye, Y. Sahai, Viscosity and density of molten salts based on equimolar NaCl-KCl, Mater. Trans. 38 (1997) 566-570.
93. J.A.S. Tenorio, D.C.R. Espinosa, M.C. Carboni, Recycling of aluminum-effect of fluoride additions on the salt viscosity and on the alumina dissolution, J. Light Met. 1 (2001) 195-198.
94. Y. Xiao, M.A. Reuter, U. Boin, Aluminium Recycling and Environmental Issues of Salt Slag Treatment, J. Environ. Sci. Heal. A 40 (2005) 1861-1875.
95. M.F. Jordan, D.R. Milner, The removal of Oxide from. Aluminium by Brazing Fluxes, J. Inst. Metals 85 (1956) 33-40.
96. E.I. Storchai, N.S. Baranov, Optimization of the flux bath brazing process for aluminium parts, Chem. Petrol. Eng+ 12 (1976) 252-255.
97. L. Martin-Garin, A. Dinet, J.M. Hicter, Liquid-liquid interfacial tension measurements applied to molten AI-halide systems, J. Mater. Sci. 14 (1979) 2366-2372.
98. R.R. Roy, Y. Sahai, Interfacial tension between aluminum alloy and molten salt flux, Mater. Trans. 38 (1997) 546-552.
99. J.A.S. Tenorio, D.C.R. Espinosa, Effect of salt/oxide interaction on the process of aluminum recycling, J. Light Met. 2 (2002) 89-93.
100. S. Besson, A. Pichat, E. Xolin, P. Chartrand, B. Friedrich, European metallurgical conference 2011, Dusseldorf, 2011, pp. 1-16.
101. J.H.L.V. Linden, D.L. Stewart, Molten salt flux composition effects in aluminum scrap remelting, in: P.G. Campell (Ed.) Light Metals 1988, TMS: The Minerals, Metals & Materials Society, 1988, pp. 173-181.
102. Y.-S. Kim, E.-P. Yoon, K.-T. Kim, W.-J. Jung, D.-H. Jo, Effects of Salt Flux and Alloying Elements on the Coalescence Behaviour of Aluminum Droplets, J. Korea Foundry Soc. 20 (2000) 39-45.
103. K.J. Friesen, T.A. Utigard, C. Dupuis, L.P. Martin, Coalescence behaviour of aluminum droplets under a molten salt flux cover, in: R. Huglen (Ed.) Lights Metals 1997, TMS: The Minerals, Metals & Materials Society, 1997.

104. R.R. Roy, Y. Sahai, Coalescence behaviour of aluminum alloy drops in molten salts, Mater. Trans. 38 (1997) 995-1003.
105. O. Majidi, S.G. Shabestari, M.R. Aboutalebi, Study of fluxing temperature in molten aluminum refining process, J. Mater. Process. Tech. 182 (2007) 450-455.
106. J. Ye, Y. Sahai, Interfacial Behaviour and Coalescence of Aluminum Drops in Molten Salts, Mater. Trans. 37 (1996) 175-180.
107. D.B. Masson, M.M. Taghiei, Interfacial reaction between aluminum alloys and salt flux during melting, Mater. Trans. 30 (1989) 411-422.
108. M. Thoraval, B. Friedrich, European Metallurgical Conference 2015, Dusseldorf, 2015, pp. 359-367.

PART 2

ARTICLES

ARTICLE 1

INFLUENCE OF SALT QUANTITY ON RECOVERY YIELD OF HETEROGENEOUS ALUMINIUM SCRAP

Stefano Capuzzi[1], Giulio Timelli[1], Leonardo Capra[2], Luca Romano[2]

[1]Department. of Management and Engineering-DTG
University of Padua
36100 Vicenza
ITALY

[2]Raffineria Metalli Capra-RMC
25030 Castel Mella (BS)
ITALY

Published in: Advanced Materials Research

Abstract

The influence of the salt quantity on the recovery yield of aluminium scrap was studied considering a heterogeneous charge. The analysed heterogeneous charge was composed by different types of scrap such as turning, shredded materials and dross. The amount of salt was related to the scrap quality using the *salt factor*, which is defined as the ratio between the non-aluminium content in the scrap and the quantity of salt required. Two levels of salt factor were considered, 1.2 and 1.8. The analysis of variance was then implemented to verify the influence of the salt quantity on the recovery yield. The results were statistically confirmed using the Anderson-Darling test, the Dixon's outliers test and the coefficient of variance. An increment of the recovery yield from 95% to 97% was revealed by increasing the salt factor from 1.2 to 1.8.

Keywords: aluminium recycling, salt factor, heterogeneous scrap, ANOVA

Introduction

Aluminium has grown to be a great competitor for engineering applications from the end of 19th century when it became economically viable. Recyclability plays an important role in increasing the Al production. Secondary Al production starts from Al scrap and it offers economical and environmental advantages [1,2].

Scrap is the raw material and its quality is a key feature for secondary Al alloy properties. Remelters produce wrought alloys, usually in the form of extrusion billets and rolling ingots, from mainly clean and sorted wrought alloy scraps; on the other hand, refiners are able to add alloying elements and to remove some undesired elements after the melting process, so producing foundry alloys from lower quality scrap. The scrap quality is evaluated through the metal yield that is the portion of scrap which, after proper melting, can become useable metal. This scrap presents oxides, undesired materials, as other metals and coats, and it is usually heterogeneous.

Fluxing has to be considered in case of low quality scrap; this consists on the addition of chemical compounds to cover the molten bath avoiding new oxidation, separating the oxide layer from the melt and growing metallic Al droplets in the oxide layer and taking them into the liquid metal.

The flux composition and the effects of different compounds are largely studied. The flux is usually composed by an equimolar mass of NaCl-KCl because these salts form an eutectic with low melting temperature (~657°C).

Fluorides are frequently added to the flux as they promote the stripping of the Al oxide layer and the metal coalescence.

On the other side, the amount of salt is less considered even if it plays a key role in the efficiency of the whole melting process. For instance, it impacts on the productive cost, energy consumption and disposal costs.

In this work, the salt quantity has been related to the theoretical scrap quality by the *salt factor* (*SF*), which is the ratio between the non-aluminium content in the scrap and the quantity of the salt required. A mass balance model defined for European refiners establishes the salt factor level at 1.3, but no studies investigated the optimized level.

The main features of Al refiners are the ability to melt any type of scrap with high production volume. Therefore, the study of the melting process is difficult due to the amount and the heterogeneity of the scrap. The aim of this work is to define a procedure able to obtain reliable results on the recovery yield by considering a heterogeneous scrap and to study the influence of the salt content on the recovery yield.

Experimental procedure

Flux was composed by a mixture of 95% NaCl and 5% KCL, and the addition of cryolite in 3.3% of the salt quantity. Two different levels of salt factor were tested, i.e. 1.8 and 1.2. Each condition was replicated at least seven times.

A heterogeneous charge was defined using different types of scrap, such as turning, shredded materials and dross, as shown in Figure 1. The charge weight was 5 kg and the mixture was maintained constant for all testing.

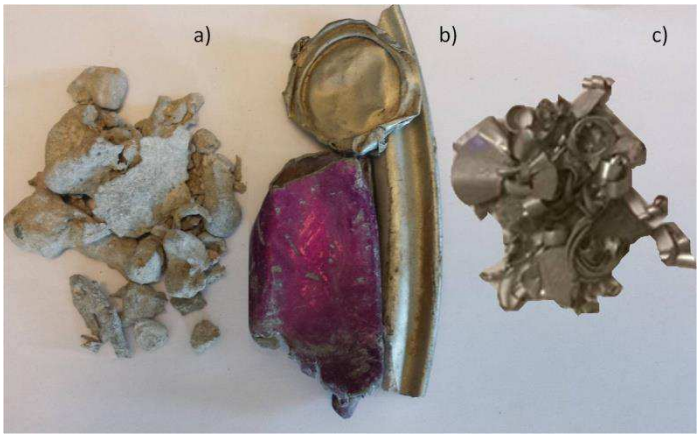

Fig. 1. Representative samples of the scraps used during testing: (a) dross, (b) shredded and (c) turning

The metal yield was evaluated according to the EN 13920-01 standard and calculated for each condition. Table 1 resumes the charge mixture and the measured metal yield for each level of salt factor studied. The metal yield was used to calculate the metal content present in the scrap as follows:

$$Metal\ content = \sum_{i=1}^{n} (scrap\ weight_i \cdot metal\ yield_i) \qquad \text{Equation 1}$$

where n is the number of the different scrap types.
The melting process was carried out in a 10 kg capacity graphite crucible inside a fossil fuel furnace. Natural gas was used as fuel with the same crucible for all tests.

Table 1: Weight of different scraps used for the charge and metal yield for each *SF* level

Type of scrap	weight (kg)	metal yield	
		SF=1.2	*SF*=1.8
turnings	2.4	0.96	0.96
shredded	2.3	0.90	0.90
dross	0.3	0.73	0.73

The scrap was charged in three different steps. Firstly, the flux was added in the first phase within the scrap. During the last step, the cryolite was added. Each step included 7 minutes of melting. This time was used to melt the scrap, and in the case of the cryolite to give time to react with the dross. The total melting time was 27 minutes and the molten aluminium was manually rotated for 30 seconds after each charge.
The aluminium and the dross were separately poured into different steel moulds. The recovery yield was calculated as the ratio between the cast aluminium and the metal content in the scrap.
The highest *SF* level (1.8) was used to statistically verify the repeatability of the test and to define the number of tests required. A significant level equal to 0.05 was used for all the statistical tests.
The Dixon's test was selected for outlier test and a coefficient of variance of 0.01 for the recovery yield was defined to accept the repeatability of the results. The normal distribution was verified by Anderson-Darling testing.
The same control was performed for the lower *SF* level and an analysis of variance (ANOVA) was implemented to verify the influence of the salt content on the recovery

yield. The Bonett's test was used to verify the homoscedaticity of the samples. The analysis of residuals was used to support the results of ANOVA.

Results and discussion

Scrap melted by refiners are usually heterogeneous and with low quality. The metal yield is strongly related to the scrap type so it has to be verified for every charge. This uncertainty is reduced with scrap as turnings and UBCs where only few and known alloys are present. Results obtained with heterogeneous scrap otherwise can produce valid information regarding the recovery yield. Outlier values can be related to undesired materials present in the scrap. Figure 2 reports the boxplot for the tests made with a salt factor equal to 1.8. An outlier is evident, with a recovery yield equal to 90.4 in spite of a mean of 97.2. Dixon's text confirms that this value is not representative of the sample. This result can be addressed to the presence of magnesium scrap. Magnesium at high temperatures, as those reached in the Al melting, reacts with oxygen and dissolves. The typical glares generated by this reaction were seen during the test.

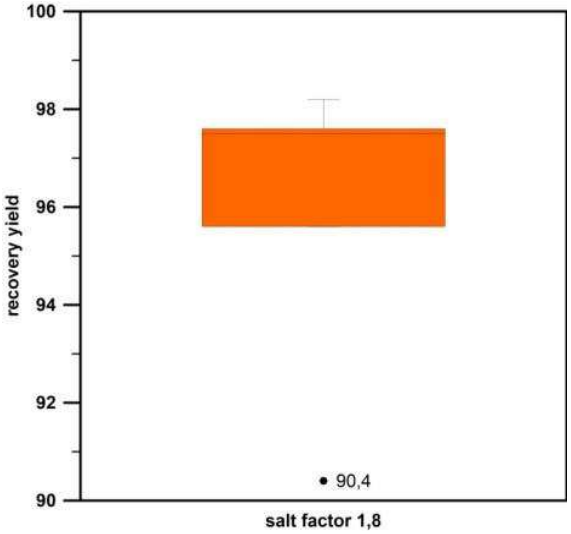

Fig. 2. Box plot for the tests with a salt factor equal to 1.8 with indicated an outlier value

Mean values and standard deviations were calculated and the coefficient of variance, that is the ratio between these two parameters, was equal to 0.87 %. The normal distribution was also verified and confirmed from the *p*-value (0.073) for the normality test. This procedure was also used to validate the results for the lowest *SF* level. Table 3 reports all the statistical results obtained. ANOVA was performed to statistically confirm the influence of the salt quantity on the recovery yield. Firstly, the ANOVA assumptions were verified. The results of normal distribution test are reported in Table 2, the independence of the samples was assured with the sampling method and the homoscedaticity was confirmed by Bonett's test with a *p*-value equal to 0.681.

Table 2: Recovery yield obtained for the analyzed salt factor levels and results of the Dixon's test for outliers and Anderson-Darling's test for normal distribution

Salt factor	Mean	Standard deviation	Coefficient of variance	*p*-value Dixon	*p*-value Anderson
1.8	97.2	0.849	0.85	0.229	0.073
1.2	94.8	0.905	0.9	0.850	0.429

The ANOVA exhibits a *p*-value equal to 0.001 that is lower than 0.05; this means a statistically difference of recovery yield with the two levels of salt factor considered. Therefore, the influence of the salt content on the recovery yield was confirmed. The residual analysis supports this conclusion.

Residuals present a normal distribution and no trends versus both the estimated response and the order were detected.

The increase in the salt factor from 1.2 to 1.8, and by using the selected charge, produces an increase of the salt content equal to 300 gr. On industrial scale where a rotary furnace can contain for instance a scrap volume over 100 tons, the 0.1 increase in the salt factor can deeply impact on the salt content related to the metal yield of the scrap.

Otherwise, increasing the salt factor from 1.2 to 1.8 allows an increment of the recovery yield of more than 2%. This means an increase of metal poured during the experiments of more than 100 gr. Two more tons of refined liquid metal can be obtained from a single casting in a rotary furnace with a charge volume of 100 tons and a metal yield of the scrap equal to 90%.

Conclusions

Heterogeneous scrap can be used to evaluate the influence of the amount of salt on the recovery yield. Undesired elements, as magnesium, strongly influence the results. Thus the control of the charge is necessary. Metal yield varies among different scraps and it is necessary to calculate it for each charge with a rigorous method. Charging method has also to be defined and it must be equal for all tests. A variation of salt factor from 1.2 to 1.8 increases the recovery yield of more than 2 %. This result highlights the importance of defining the optimum salt level, not only its composition. On industrial scale, this leads to an increase of refined liquid metal. Energy and disposal costs related to the amount of new salt have to be considered.

Reference

[1] J. Blomberg, P. Söderholm, The economics of secondary aluminium supply: An econometric analysis based on European data, Resour. Conserv. Recycl. 53 (2009) 455-463.
[2] E. Sevigné-Itoiza, C.M. Gasola, J. Rieradevalla, X. Gabarrella, Environmental consequences of recycling aluminum old scrap in a global market, Resour. Conserv. Recycl. 89 (2014) 94-103.
[3] T.A. Utigard, K. Friesen, R.R. Roy, J. Lim, A. Silny, C. Dupuis, The Properties and Uses of Fluxes in Molten Aluminum Processing, JOM 50 (1998) 38-43.
[4] J.A.S. Tenorio, D.C.R. Espinosa, Effect of salt/oxide interaction on the process of aluminum recycling, J. Light Met. 2 (2002) 89-93.
[5] J.A.S. Tenorio, D.C.R. Espinosa, M.C. Carboni, Recycling of aluminum-effect of fluoride additions on the salt viscosity and on the alumina dissolution, J. Light Met. 1 (2001) 195-198.
[6] B. Friedrich, M. Gerke, J. Kruger, A. Arnold, European Metallurgical Conference, Dusseldorf, 2011.
[7] U.M.J. Boin, M. Bertram, Melting Standardized Aluminum Scrap: A Mass Balance Model for Europe, JOM 57 (2005) 26-33.
[8] E.C.f.S. CEN, Bruxelles, 2003.

ARTICLE 2

STUDY OF FLUXING IN AL REFINING PROCESS BY ROTARY AND CRUCIBLE FURNACES

Stefano Capuzzi[1], Giulio Timelli[1], Leonardo Capra[2], Luca Romano[2]

[1]Department. of Management and Engineering-DTG
University of Padua
36100 Vicenza
ITALY

[2]Raffineria Metalli Capra-RMC
25030 Castel Mella (BS)
ITALY

Submitted for pubblication in: International Journal of Sustainable Engineering

Abstract

The process used to obtain recycled Al alloys depends on the scrap quality. Rotary furnaces are normally used in Europe as they allow a high productivity and they can process low quality scrap using a salt flux to protect the molten metal from oxidation.

In this article, the effect of the quantity of salt on the metal recovery has been experimentally investigated melting different types of scrap under a mixture of NaCl-KCl-Na_3AlF_6 salts. The quantity of salt has been related to the *salt factor* (SF), which is the ratio between the non-metallic content in the scrap and the quantity of salt required. The same levels of salt factor have been tested by melting the scrap in rotary and crucible furnaces.

The metal recovery increases with the salt content for both furnaces. The results obtained with the different melting processes are comparable because the yield difference is similar considering different salt factors. Crucible furnace gives greater metal recovery but it cannot replace rotary furnace in Al refining industry due to the lower melting capacity. However, the results highlight that the optimization of the Al refining process can be supported by preliminary tests through crucible furnaces reducing the time and material consumptions.

Keywords: aluminum recycling; rotary furnace; salt factor; heterogeneous scrap; ANOVA

List of symbols

m_{scrap} weight of the scrap, Kg

μ_{metal} metal yield of the scrap

SF salt factor

m_{salt} weight of salt, Kg

m_{Al} weight of molten aluminium, Kg

p perimeter of the projection of the Al drop, mm

A area of the projection of the Al drop, mm^2

V_f capacity of the melting furnace, ton

$\dot{m}_{scrap}$ amount of scrap that can be charged in the rotary furnace for fixed metal yield and salt factor, ton

Al_{tap} amount of tapped aluminium for fixed metal yield and salt factor, ton

v falling velocity of the Al drop in the salt, m/s

μ viscosity of the salt, P

r_s radius of the Al drop, m

g the gravity acceleration, m/s^2

ρ_s aluminium density, Kg/m^3

ρ_l salt density, Kg/m^3

1. Introduction

Aluminium is the most widely used nonferrous metal in the world being present in sectors as diverse as transportation, packaging, construction, electricity and medicine. It has grown to be a great competitor for engineering applications from the end of 19th century when it became economically viable. The capacity of being recycled plays an important role in increasing the aluminium spread.

Recycled Al alloys offer economical and environmental advantages compared to primary production: Rombach (1998) estimated an energy reduction from 174 GJ/ton to 20 GJ/ton while a reduction equal to the 95% of the CO_2 emission is achieved according to Das, Green, and Kaufman (2007).

Their production starts from Al scrap, which is the core of the whole process. A closed-loop recycling could be the best way to increase the effectiveness of the process, as occurred for cans (Baeyens, Brems, and Dewil 2010), but it is not possible for all types of scrap.

Heterogeneity is an important aspect of scrap. It is clear that various categories of scrap differ not only in their origin and composition, but also in the fraction of oxides and other foreign materials. The quality of the charged scrap affects both the metal yield and the metal recovery. The *metal yield* is the portion of a scrap consignment which becomes useable metal after proper melting and can be used to estimate the metal content of the scrap, while the *metal recovery* is defined as the percentage of metal gained from the metal content of the scrap.

An exhaustive classification of the Al scrap can be found in the EN 1676 (2010) and EN 13920 (2003) standards where characteristics, chemical composition and metal yield are provided for each category. The scrap quality is a key factor for the metal recovery, thus different technologies have been developed to increase the obtainable metal content. Comminution, sorting and de-coating are the main preliminary treatments applied to the scrap. Schubert, Sander, and Jackel (2004) highlighted that the aim of comminution is to increase the scrap bulk density to favour handling and melting and they also explained the fundamentals of this process. Several processes have been developed to remove the non aluminium content of the scrap depending on the not wanted material, as well summarized by Gaustad, Olivetti, and Kirchain (2012). The advantages of de-coating is the reduction of the impurity coming from the scrap surface, in particular from the organic fraction of the scrap coat as found out by Kvithyld et al. (2008) through thermal analysis on coated scrap.

The final quality of the scrap influences the choice of the melting process. Rotary and reverberatory furnaces are the main melting technologies as they allow high productive rate, while crucible and electric furnaces are most suitable for lower productive volumes. Traditional reverberatory furnace is less expensive to install and less difficult to maintain, but rotary furnace is faster and more efficient, and it can treat scrap of poorer quality. Higher melting rates, reduced emissions, consistent metal composition and lower fuel consumption are achieved with the latter because the hot refractory rotates to transfer more heat to the charge via direct contact. As a result, rotary furnaces are generally best suited in countries with high energy cost, as European countries, for melting dross and other oxidized scrap as suggest by Velasco and Nino (2011).

The furnace design is not sufficient to melt low quality scrap, but fluxing is also needed. *Fluxing* indicates the addition of chemical compounds in the scrap feed in order to improve the recovery of aluminium and the quality too. The basic function of fluxes is to protect the molten bath from oxidation that increases by increasing the furnace temperature. However, fluxes are applied for several specific purposes depending on their

composition, and are usually classified depending on their application. Utigard et al. (1998) individuated and explained five different categories of flux: cover, cleaning, drossing, refining and furnace wall cleaning.

In rotary furnace, the salt flux is used to protect the bath from oxidation and to collect the oxides present in the scrap. According to Crepeau, Fenyes, and Jeanneret (1992) the flux is usually composed by an equimolar mass mixture of sodium and potassium chlorides (NaCl-KCl) due to the low cost and the low melting point. Sodium chloride is cheaper, while the addition of potassium chloride decreases the melting temperature because these two salts form, at 44% and 56% respectively, an eutectic that melts at about 665°C.

Different parameters affect the fluxing treatment such as the morphology of the salt, i.e. powder or granular and the temperature. Gallo (2002) compared powder and granular flux highlighting that the latter reduces pollution and smoke emissions and offers more homogeneity in the composition. Majidi, Shabestari, and Aboutalebi (2007) studied the influence of the flux temperature on the refining efficiency with chips and turnings and they found out that a low temperature, i.e. 700°C, compromise the refining process while if the temperature is too high, i.e. 790°C, the hydrogen absorption in the molten bath increases. Among all the flux properties, the chemical composition has been the most studied. Fluorides are frequently added to the flux as they promote the stripping of the Al oxide layer, as explained by Tenorio and Espinosa (2002), and the metal coalescence. Besson et al. (2011) investigated the influence of the cryolite content on the Al drop coalescence starting from two different alloys and in both cases a positive relation was found.

The salt amount has been less studied even if it plays a crucial role in the efficiency of the whole melting process. It impacts on productive and disposal costs as well as energy consumption. The required salt amount is generally related to the quality of the scrap by the *salt factor* (SF), which is the ratio between the non-aluminium content in the scrap and the quantity of salt. In the Al recycling processes, large salt factors ranging from 1.5 to almost 2 are used with rotary furnaces; Moloodi et al. (2011) indicates a value of 1.8 as often published while a salt factor equal to 1.3 was used in a mass balance model for refiners in Europe by Boin and Bertram (2005).

Investigating the effect of the process parameters on the industrial scale is difficult because it is expensive and time consuming. The charge of industrial rotary furnaces is heterogeneous and high volumes of scrap have to be processed. Furthermore, the melting process is difficult to be controlled and the real industrial production is based on a three-shift system.

This work investigates the effect of the amount of salt on the metal recovery in Al refining process using rotary and crucible furnaces. A comparison between the two melting furnace is proposed and the use of the salt factor is discussed.

2. Materials and Method

2.1 Charged materials

The charge was composed by heterogeneous scrap and salt. Scrap, coming from several suppliers, was used in an industrial rotary furnace and the fraction of the different types of scrap varied depending on the experimental conditions.

A heterogeneous charge composed of the same types of scrap was used to perform the tests with a crucible furnace. The charge was a mix of turning, shredded materials and

dross (Figure 1). The scrap used during the entire experimental campaign was taken from the same lot for each kind of scrap.

The metal yield for each lot was evaluated in agreement with the procedure described in the EN 13920 (2003) standard. Briefly, a representative sample of 2 to 5 kg was collected from each batch and transferred to a graphite crucible where it was melted in a fossil fuel furnace with salt addition equal to 50% of the scrap mass. After melting, the molten metal and the slag were poured into different ingot moulds and solidified. Metal entrapped in the salt was recovered by grounding the salt slag. The metal yield was then calculated as the weight ratio of the tapped aluminium to the scrap.

The metal yield was used to estimate the metal content in the charge as sum of the amounts of the different types of scrap weighted by their metal yield (Equation 1)

$$metal\ content = \sum_{i=1}^{n} \left(m_{scrap\_i} \times \mu_{metal\_i} \right) \qquad \text{Equation 1}$$

here i indicates the type of scrap, m_{scrap} is the weight of the scrap and μ_{metal} is the metal yield of the scrap.

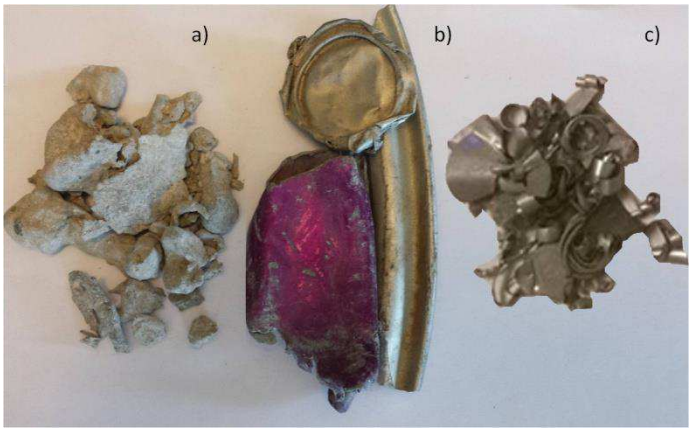

Fig. 1 Scrap used for the tests: (a) dross, (b) shredded materials and (c) turning.

The salt used as flux was a mixture of NaCl and KCl with addition of cryolite (Na_3AlF_6). A constant ratio (k) of the amount of cryolite to the amount of NaCl-KCl was used. The salt amount was calculated as the product between the tested level of salt factor (SF) and the metal content in the charge, where SF is defined as

$$SF = \frac{m_{salt}}{m_{scrap} \times (1 - \mu_{metal})} \qquad \text{Equation 2}$$

here m_{salt} and m_{scrap} are the weights of salt and scrap charged in the furnace, respectively, and μ_{metal} is the metal yield of the scrap.

Due to the sensitive nature of the process being monitored, the SF levels cannot be reported in this work since they are related to standard operating conditions. The analysed SF levels will be indicated hereafter as A and B, with B as the highest one.

2.2 Testing with the rotary furnace

A series of experiments were performed during normal production to calculate the metal recovery for the rotary furnace (Figure 2) with the two SF levels.

Fig. 2 Charging door of the rotary furnace used in the present work.

At least 50 consecutive experiments were considered to obtain an average value of the metal recovery for each SF level. During the considered period, the bath temperature, the charged volume, as well as the metal yield of the charge, varied according to the production demands. These variables have been monitored and their ranges are reported in Table 1.

The molten metal was tapped before the slag in a holding furnace equipped with a weighing system. The metal recovery was calculated as

$$\text{metal recovery} = \frac{m_{Al}}{\text{metal content}} \qquad \text{Equation 3}$$

here m_{Al} is the weight of molten aluminium tapped from the rotary furnace.

Table 1.
Ranges of bath temperature, volume of the charge and metal yield of the scrap during the experimental campaign with the rotary furnace.

	min	average	max
Temperature (°C)	790	834	890
Scrap volume (tons)	84.9	85.8	88.5
Metal yield	0.88	0.90	0.93

2.3 Testing with the crucible furnace

The scrap was melted in a 10 kg capacity graphite crucible through a fossil fuel furnace. Natural gas was used as fuel and the same crucible was used for all the tests. Figure 3 shows the furnace used for the experiments. The charge sequence was divided in four different steps as reported in Table 2. The amount of scrap was equal for all the experiments, while the amount of flux and cryolite varied depending on the salt factor. The mixture of NaCl-KCl was added in the first step together with the scrap, while the cryolite was added during the last step. The duration of each step was 7 minutes, necessary for melting the scrap and to give to the cryolite the time to react with the dross, in the last step. The total melting time was 28 minutes and the molten bath was manually stirred for 30 s after each charge. The liquid metal was poured prior to the dross in a permanent ingot mould, while the dross was separately poured. The metal recovery was measured in accordance with Eq. 3.

Table 2.
Charging process of the scrap in the fossil fuel crucible furnace; the weight of the different scrap and the melting time are indicated.

Charge step	Holding time (min)	Scrap weight (Kg)		
		turning	shredded	dross
first	7	0.8	0.8	
second	7	0.8	0.8	
third	7	0.8	0.7	0.3
fourth	7			
total	28	2.4	2.3	0.3

The flux composition and the SF levels were equal to those used during fluxing in the rotary furnace. Each experimental condition was repeated at least 8 times.

One representative sample for both the SF levels was used to investigate the coalescence of the Al drops in the salt. The solidified dross was collected and it was mechanically crushed to release the Al drops entrapped inside. The size and morphology of the Al drops were evaluated by means of optical microscopy and image analysis. The aspect ratio, the roundness and the equivalent diameter of the projection of the drops were measured. The aspect ratio is the ratio of the maximum to the minimum Feret diameters, while the roundness is defined as

$$\text{roundness}=\frac{p^2}{4*\pi*A} \qquad \text{Equation 4}$$

here p and A are the perimeter and the area of the projection of the Al drop.

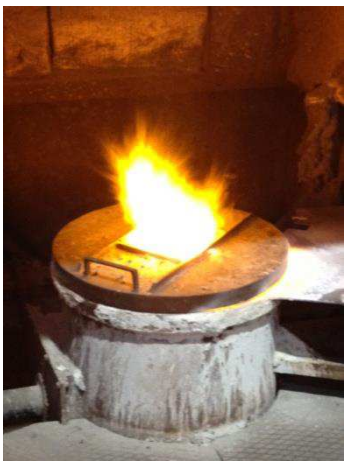

Fig. 3 Fossil fuel crucible furnace used.

2.4 Statistical analysis

The data were processed using commercial statistical software. All the results coming from the rotary and crucible furnaces were analysed with the same statistical data processing. Average values and standard deviations were firstly estimated and then the coefficient of variance, i.e. the ratio between the standard deviation and the average, was calculated. A coefficient of variance lower than 2 was selected as rate of acceptance for the repeatability. The outliers were identified by Dixon test according to Dixon and Dean

(1951). If an outlier was found, a new experiment was performed and the Dixon test repeated with the new data.

Box plots were used as representation of the data showing the full range of variation (from min to max), the likely range of variation (the interquartile range, IQR) and a typical value (the median): "whiskers" above and below the box indicate the location of minimum and maximum values; the central box ranges from the first quartile to the third quartile (IQR); the band inside the box shows the median.

The influence of the salt quantity on the metal recovery was verified using the one-way analysis of variance (one-way ANOVA) defined by Fisher (1921). Definition and specific assumption for this work are here reported, while a detailed description of the ANOVA procedure is given elsewhere by Montgomery (2013). A hypothesis test is generally used to determine which of two statements is better supported by the data. These two statements are called the null hypothesis (and the alternative hypothesis. The null hypothesis was assumed to be that the data obtained with the experimental SF levels are simply random samples of the same population; this means that the SF would not affect the metal recovery. The hypothesis test calculates the probability to obtain the observed sample data under the assumption that the null hypothesis is true. If this probability (the *p*-value) is below a user-defined cut-off point (*α-level*), then this assumption is probably incorrect. Therefore, the null hypothesis is rejected and the alternative hypothesis is selected. The α-level was selected equal to 0.05.

Since only two averages were compared, the t-test for independent samples is a valid alternative test. All the ANOVA assumptions were previously verified: the Anderson-Darling's test was firstly applied to test the assumption of normality developed by Anderson and Darling (1952), while Levene's test was used for the assumption of homoscedaticity as defined by H.Levene (1960). The independence of observations was obtained with a random sequence of the experiments.

3. Results and discussion

3.1 Scrap metal yield

The metal content in the scrap is a key factor when the efficiency of a rotary furnace is studied; indeed the charge is usually composed by several types of scrap, coming from different supplied lots.

Figure 4 shows the metal yields referred to the different scrap used in this work; further, the experimental results are compared with the average EU values reported by Boin and Bertram (2005) and with the range suggested by the EN 13920 (2003) standards.

Various metal yields were reached depending on the scrap type. The dross shows a metal content lower than 20% if compared to that of turning and shredder materials, which have a yield greater than 90%.

Different considerations can be drawn comparing the experimental data and the average EU values. The metal yield for turning from this work is comparable to the average EU data, while the EN 13920 standard indicates a lower value. Shredder scrap shows here lower metal yield than turning and a greater difference with the average EU values. The metal yield decreases significantly in the dross; further, the present data and the average EU values strongly differ.

Turnings are new scrap whose origin is known and the main contamination, that is cutting oils, can be removed by de-coating. Therefore, the metal yield is high and

constant. For greater amount of contaminants, the metal yield decreases and the variance between different lots increase.

Xiao and Reuter (2002) evidenced how the metal yield can vary in turning, depending on size, morphology and amount of contaminates. According to these results, the Al content in the scrap depends on its cleanliness and on the ratio between its surface and volume. Xiao et al. (2000) stated that a greater amount of non-metallic contaminates and a higher ratio of surface area to body volume of the scrap usually leads to lower metal yield

Important remarks can be also drawn about the correlation between metal yield and metal recovery. Firstly, measuring the metal yield of each scrap charged in the furnace is fundamental when the metal recovery of a melting process is studied. Otherwise, it is not possible to understand if a variation in the metal recovery may be associated with a change in the process parameters or with a lower metal yield of the charge. The variance in the measurement of the metal yield increases the spread in the results of the metal recovery, thus increasing the number of the experimental tests is required to obtain good repeatability. Furthermore, the efficiency of the flux in increasing the metal recovery is affected by the amount of oxides and other foreign materials in the scrap and therefore the salt amount has to be correlated to the metal yield when heterogeneous scrap are melted. The salt factor is a good solution to solve this need.

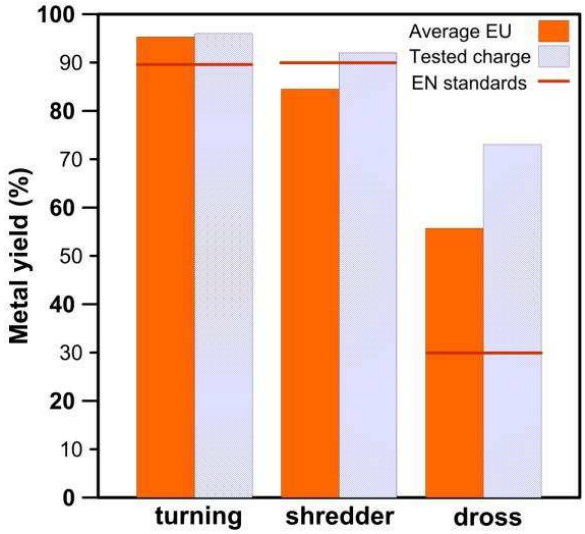

Fig. 4 Metal yield measured for the different experimental types of scrap; the average EU values (Boin and Bertman, 2005) and the data from the standard EN 13920 (2003) are also indicated.

3.2 Validation of the statistical hypothesis

A coefficient of variance lower than 2% (see Table 3) was achieved for the various levels of salt factor used with both the melting furnaces. The crucible furnace shows a greater repeatability compared with rotary furnaces as a greater number of experiments was needed for the latter

Table 3 shows the results for the tests used to verify the presence of outliers as explained in §2.4. No outliers are present in the results.

Table 3.
Coefficient of variance and *p*-value from the Dixon's tests for all the experimental conditions.

furnace	salt factor level	number of samples	coefficient of variance (%)	*p*-value Dixon's test
crucible	A	8	0.73	0.229
	B	8	1.12	0.850
rotary	A	50	1.77	0.345
	B	50	1.14	0.453

The results of the statistical tests performed to verify the assumption of ANOVA are summarized in Table 4. The normality was verified by the Anderson-Darling's test and all the conditions achieved a *p*-value higher than the α-level (0.05). The homoscedaticity was verified by the Levene's test and the null hypothesis was accepted for the results obtained with rotary and crucible furnaces.

Table 4.
Results of the Anderson-Darling's and Levene's tests used to verify the assumption of ANOVA.

furnace	salt factor level	Anderson-Darling's test		Levene's test	
		p-value	null hypothesis: normality	*p*-value	null hypothesis: homoscedaticity
crucible	A	0.179	accepted	0.443	accepted
	B	0.293	accepted		
rotary	A	0.907	accepted	0.119	accepted
	B	0.101	accepted		

3.3 Metal recovery from rotary furnace

The metal recovery in the rotary furnace increases with the salt content within the considered SF levels. Table 5 summarizes the results of the one-way ANOVA for the experimental conditions. The *p*-value lowers than 0.05 indicates that null hypothesis has to be rejected and so the metal recovery is significantly affected by the salt factor.

Table 5.
One-way ANOVA for the metal recovery from the rotary furnace.

Source	Degrees of freedom	Sum of squares	Mean squares	F-test	*p*-value
Salt factor	1	27.35	27.35	12.29	0.001
Error	98	218.03	2.22		
Total	99	245.38			

Figure 5 reports the results in the form of box plot. The distribution for both the SF levels are symmetrical and the interquartile ranges are comparable, which means similar data distributions. The average metal recovery at the lowest salt factor (level A) is 92.4%, while it increases to 93.5% with the highest one (level B); the standard deviations are 1.3% and 1.6%, respectively.

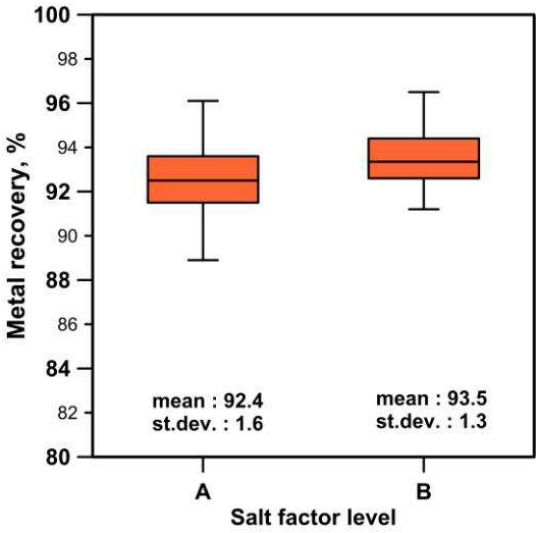

Fig. 5 Box plot relative to the metal recovery obtained with two different SF levels in the rotary furnace.

3.4 Metal recovery from crucible furnace

The results of the one-way ANOVA for experimental conditions used with the crucible furnace are listened in Table 6. The influence of the SF was statistically confirmed also in the case of crucible furnace (p-value<0.05).

Table 6.
One-way ANOVA for the metal recovery from the crucible furnace.

Factor	Degrees of freedom	Sum of squares	Mean square	F-test	p-value
Salt factor	1	5.28	5.28	4.98	0.045
Error	12	12.72	1.06		
Total	13	18.00			

The box plots in Figure 6 show an asymmetrical distribution for both samples, positive in the case of the higher SF level (level B), negative in the other case (level A). The normality can be however assumed through the results of the Anderson Darling test. The level B presents a wider interquartile range which corresponds to higher dispersion of the data.

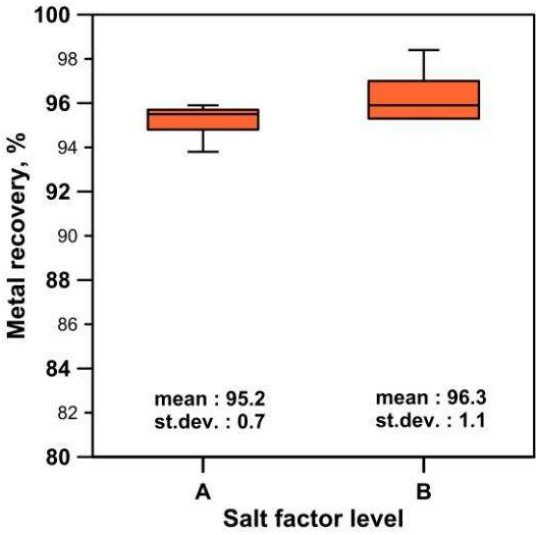

Fig. 6 Box plots relative to the metal recovery obtained with two different SF levels in the crucible furnace.

The metal recovery increases if the salt factor increases in the considered SF range. The average value for the lowest SF level is equal to 95.2 while it increases to 96.3 for the highest SF level; the standard deviations are 0.7% and 1.1%, respectively.

3.5 Metal recovery comparison between the two melting process

The effect of the salt factor on the metal recovery is evident using both rotary and crucible furnaces as clearly shown in Figure 7. In literature, the amount of flux to be added in the furnace during melting is generally estimated as the percentage of flux with respect to the total amount of scrap, independently from the scrap quality. Verran and Kurzawa (2008) found an increase in the metal recovery by adding a flux percentage up to 10%; Ozer et al. (2013) fixed this limit at 5%. The percentage of flux cannot be converted in terms of salt factor as the metal yield of the scrap is not known.

The results obtained by means of the rotary furnace shows a greater variance than those achieved using the crucible furnace thus more experimental tests were needed to obtain reliable data. This behaviour can be addressed to greater volume and heterogeneity in the metal yield of the scrap charged inside the furnace.

Crucible furnace gives better results in terms of greater repeatability and greater metal recovery in all the experimental conditions. The metal recovery is 0.9% and 0.8% greater using crucible furnace than rotary furnace, considering the SF levels A and B, respectively. According to these results, the salt amount alone cannot explain the greater efficiency of the crucible furnace respect to the rotary furnace, because the yield difference is similar considering different salt factors. The charge volume, the melting process and the charging system are the main differences between the two melting systems.

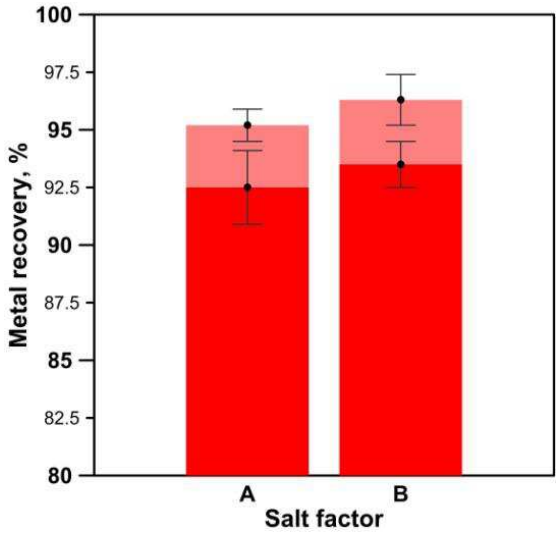

Fig. 7 Bar plots comparing the metal recovery with rotary and crucible furnaces for the two SF

In the melting process, rotation and heating system differ between the two furnaces. Rotary furnace rotates to better heat the refractory, reducing the energy consumption. This movement also promotes the interaction between the bath and the salt. More oxides are collected and the coalescence of Al droplets is supported. However, the rotation rate does not seem to influence the efficiency of the process as proved by Khoei, Masters, and Gethin (2002) who tested three different rates in a rotary furnace and by Sydykov, Friedrich, and Arnold (2002) who studied the rotation rate ranging from 1 to 4 rpm. The results in both the studies show a similar metal recovery changing the rotation rate.

Moreover even if the crucible furnace is static during the present experiments, the molten bath has been manually stirred to favour the metal-salt content as in the rotary furnace.

The difference in the metal recovery between the investigated melting furnaces can be related to the charging system and to the way in which the heat is transferred to the scrap. In a rotary furnace a flame directly heats the salt flux and the refractory, then the heat is transferred to the scrap; in a crucible furnace, the heat source heats the crucible and the scrap mainly melts through the contact with the crucible. If the scrap charged inside a rotary furnace doesn't directly fall down under the salt, it comes into contact with the flame and this strongly increases the oxidation rate. In a crucible furnace, the heat source never affects directly the scrap, thus reducing the fraction of *burn-off*, i.e. the scrap that intensively oxidizes and decreases the final metal content.

Crucible furnace is more efficient, in terms of metal recovery, than rotary furnace, but it is not an alternative on industrial scale due to lower melting capacity. However, it is highlighted that the spread in terms of metal recovery between the two melting process is constant changing the salt factor. According to this finding, the use of a crucible furnace on laboratory scale gives useful information in the optimization of the industrial process where rotary furnaces are used.

3.6 Salt factor in Al refining industry

The volume of the charge in the rotary furnace can range from 10 to 100 tons depending on the operating conditions. Therefore, if the metal recovery increases of 1%, the increment in the total amount of poured Al metal ranges between 0.1 and 1 ton. The salt factor is useful for evaluating the metal recovery with heterogeneous charge because

it correlates the salt content to the amount of non-metallic fraction in the scrap. The main limit of the salt factor is that the real amount of salt to be added varies with the metal yield of the scrap, and this influences the amount of scrap that can be charged inside the furnace. From an industrial point of view, higher metal recovery does not mean greater amount of aluminium tapped from the furnace, if the salt amount and, consequently, the amount of charged scrap change too. Higher the salt factor, higher the amount of salt and lower the amount of scrap in the charge.

Figure 8 shows the variation in the amount of liquid metal poured after melting as a function of the metal yield of the scrap for the SF levels A and B. The total capacity of the charge was assumed equal to 100 ton while the amount of scrap that can be charged and the amount of tapped Al were calculated according to Equations 5 and 6, respectively:

$$\dot{m}_{scrap} = \frac{V_f}{1+SF-SF*\mu_{metal}} \qquad \text{Equation 5}$$

$$Al_{tap} = \dot{m}_{scrap} * metal\ recovery \qquad \text{Equation 6}$$

here V_f is the capacity of the melting furnace and the other variables have been previously described. The highest salt factor (level B) achieves the highest metal recovery, but the amount of metal tapped is greater using the lowest salt factor (level A) when the metal yield is lower than 0.85. On increasing the salt factor, the amount of scrap that can be charged decreases negatively affecting the amount of Al metal that can be poured. If the metal yield of the scrap is too low, the decrease in the amount of scrap charged in the furnace is more important than the increment of the metal recovery; consequently the poured metal decreases by increasing the salt factor. The opposite result is obtained if the metal yield is higher than 0.85 in the present experimental conditions.

On increasing the salt content, the energy consumption during melting process increases too. This is due to the fact that the salt mixture has to be heated and the heat transfer from the heat source to the molten metal is hindered by the salt layer floating over the liquid metal. Higher the salt factor higher the amount of salt to be heated and greater the thermal barrier.

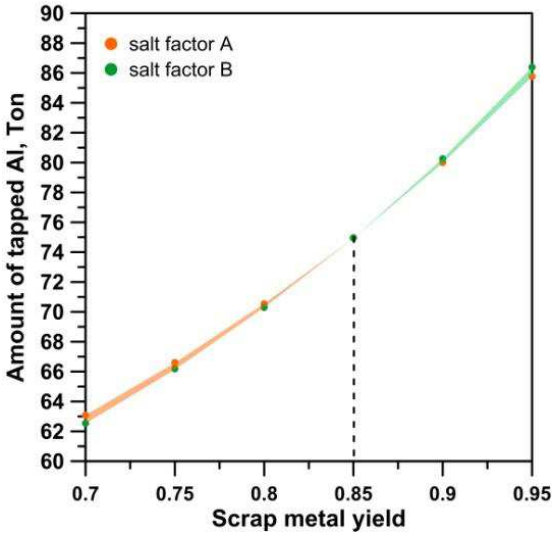

Fig. 8 Amount of poured liquid metal as function of the metal yield of the scrap for the two SF level for the rotary furnace. The experimental metal recovery was considered.

3.7 Effect of the salt amount

In order to support the results obtained in the present study, several works concerning the properties of the salt flux that influences the metal recovery have been reviewed.

The flux entraps a considerable amount of aluminium as suspended drops in a wide size range. The loss of this metal strongly influences the final metal recovery. Promoting the coalescence of Al drops is a key factor: if the size of the drops increases, they can easily return to the molten aluminium bath trough the salt slag. The addition of various fluorides to increase the coalescence behaviour of the Al drops is a well known solution. It is opinion of the author that the Al drops coalescence is favoured increasing the SF too. The physical properties of flux affecting the coalescence are viscosity, alumina dissolution and wettability. These features are not directly influenced by the different amount of flux; however if the salt content increases the fraction of non-metal components (NMC) inside the slag decreases. The level of NMC increases the density of the slag making more difficult the recovery of Al drops in the bath. As reported by Xiao, Reuter, and Boin (2005), the viscosity of the slag increases with greater amount of NMC. A greater slag viscosity negatively affects the metal recovery because the velocity of the Al drop, which is falling down into the bath, is reduced according to the Stoke law

$$v=\frac{2*r_s*g(\rho_s-\rho_l)}{9*\mu} \qquad \text{Equation 7}$$

here μ is the viscosity, r_s is the radius of the falling body, g is the gravity force, ρ_s the body density, ρ_l the fluid density and v the falling velocity.

The influence of NMC on the coalescence efficiency was studied by Thoraval and Friedrich (2015), and they found that oxides worsen the salt slag properties making the settling of the metal droplets and the separation of the metal from the slag difficult.

The metal drops entrapped in the slag after testing in the crucible furnace with the SF levels A and B were analysed in terms of size and morphology (Figure 9). The drops concerning the highest salt factor are fewer and appear smaller and rounded.

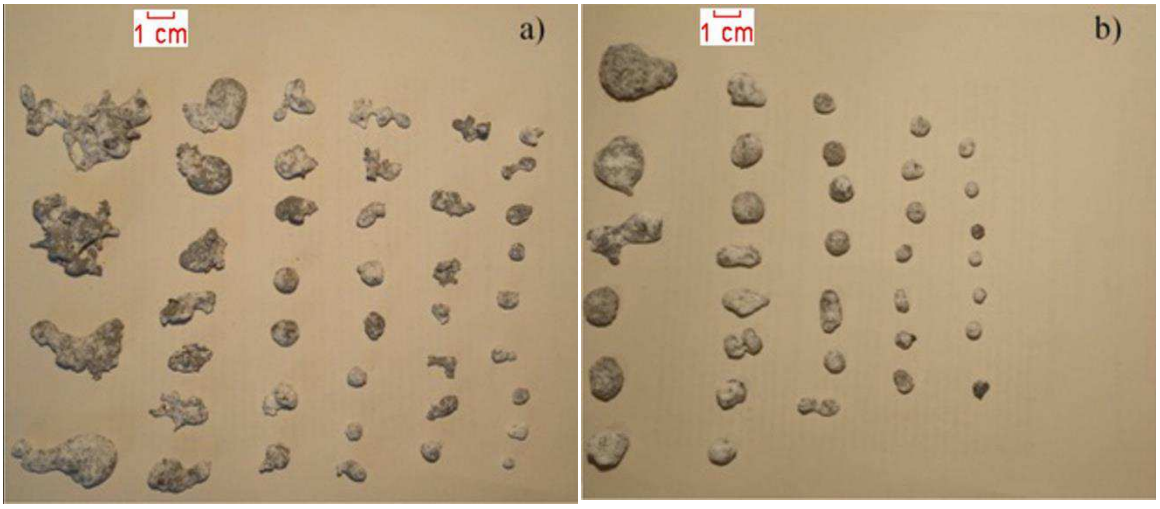

Fig. 9 Al drops extract from the slag of the scrap melted in the crucible furnace using the SF (a) levels A and (b) B

Perimeter, roundness and equivalent diameter are reported in Table 7, the results obtained confirm what stated before, observing Figures 9a-b. The size, here evaluated as

the equivalent diameter, little varies between the two samples while more evident is the difference in terms of morphology.

The perimeter and the roundness of drops extracted from the dross obtained with the lowest salt factor are higher compared to those obtained with the highest one. This means that the capacity of the drops to become spherical and to coalesce was more prevented with the lowest SF level.

Only an indication can be drawn by these results and new tests are needed to define the relation between the salt factor and the coalescence efficiency.

Table 7.
Size and morphology of Al drops extracted from the dross obtained melting the scrap with the experimental salt factor levels.

salt factor	perimeter, mm	roundness	equivalent diameter, mm
A	5.06 ± 2.37	1.77 ± 0.54	1.02 ± 0.58
B	3.56 ± 2.31	1.36 ± 0.32	1.16 ± 0.43

4. Conclusions

The effect of the salt factor on the metal recovery during Al recycling was investigated using rotary and crucible furnaces. The following conclusions can be drawn.

- The metal yield of scrap decreases by increasing the fraction of impurities, while the variance between different lots of the same kind of scrap increases.
- The metal recovery increases progressively with the salt factor independently from the melting system.
- The salt factor is a useful parameter to investigate the influence of the salt amount on the refining process performance such as the metal recovery.
- The crucible furnace allows better results in terms of metal recovery, and it shows lower variance for results due to the better charge control and the lower quantity of scrap melted.
- Laboratory experiments with a crucible furnace can be used to support the optimization of an industrial process where rotary furnaces are used.

Acknowledgements

The authors gratefully acknowledge the support of Raffineria Metalli Capra. We would particularly like to thank Angelo Volpe, Gualtiero Boni, Angelo Agliardi, Michela Tiraboschi, Leonardo Deste and Mauro Amadio for their helpful technical assistance and insights.

This research did not receive any specific grant from funding agencies in the public, commercial, or not-for-profit sectors.

References

Anderson, T.W., and D.A. Darling. 1952. "Asymptotic Theory of Certain "Goodness of Fit" Criteria Based on Stochastic Processes." *The Annals of Mathematical Statistics* no. 23 (2):193-212.

Baeyens, Jan, Anke Brems, and Raf Dewil. 2010. "Recovery and recycling of post-consumer waste materials. Part 1. Generalities and target wastes (paper, cardboard and aluminium cans)." *International Journal of Sustainable Engineering* no. 3 (3):148-158.

Besson, Sandra, Anne Pichat, Elodie Xolin, Patrice Chartrand, and Bernd Friedrich. 2011. Improving coalescence in Al-Recycling by salt optimization. In *European metallurgical conference 2011*. Dusseldorf.

Boin, U.M.J., and M. Bertram. 2005. "Melting Standardized Aluminum Scrap: A Mass Balance Model for Europe." *JOM* no. 57 (8):26-33.

CEN, (European Committee for Standardization) 2003. EN 13920 Aluminium and Aluminium Alloys-Scrap.

CEN, (European Committee for Standardization) 2010. EN 1676 Aluminium and aluminium alloys — Alloyed ingots for remelting — Specifications.

Crepeau, P.N., M.L. Fenyes, and L.J. Jeanneret. 1992. "Solid fluxing practices for aluminum melting (part 1)." *Modern casting* no. 82 (7):28-30.

Das, Subodh K., J. A. S. Green, and J. Gilbert Kaufman. 2007. "The development of Recycle-friendly automotive aluminum alloys." *JOM* no. 59 (11):47-51.

Dixon, W.J., and R.B. Dean. 1951. "Simplified statistics for small numbers of observation." *Analytical Chemistry* no. 23 (4):636-638.

Fisher, Ronald Aylmer. 1921. "On the "Probable Error" of a Coefficient of Correlation Deduced from a Small Sample." *Metron* no. 1:3-32.

Gallo, R. 2002. "Development, evaluation and application of granular and powder fluxes in trasfer ladles, crucible and reverberatory furnace." *Foundry Practice* no. 237:8-16.

Gaustad, Gabrielle, Elsa Olivetti, and Randolph Kirchain. 2012. "Improving aluminum recycling: A survey of sorting and impurity removal technologies." *Resources, Conservation and Recycling* no. 58:79-87.

H.Levene. 1960. "Robust tests for the equality of variances." In *Contributions to Probability and Statistics*, edited by Ingram Olkin, Sudhish G. Ghurye, Wassily Hoeffding, William G. Madow and Henry B. Mann, 278–292. Stanford: Stanford University Pres.

Khoei, Amir R., I. Masters, and D.T. Gethin. 2002. "Design optimisation of aluminium recycling processes using Taguchi technique." *Journal of Materials Processing Technology* no. 127:96-106.

Kvithyld, A., C.E.M. Meskers, S. Gaal, M. Reuter, and T. A. Engh. 2008. "Recycling light metals: optimal thermal de-coating." *JOM* no. 60 (8):47-51.

Majidi, Omid, Saeed G. Shabestari, and M.R. Aboutalebi. 2007. "Study of fluxing temperature in molten aluminum refining process." *Journal of Materials Processing Technology* no. 182:450-455.

Moloodi, A., H. Amini, E. Z. V. Karimi, and M. Golestanipour. 2011. "On the Role of Both Salt Flux and Cold Pressing on Physical and Mechanical Properties of Aluminum Alloy Scraps." *Materials and Manufacturing Processes* no. 26:1206-1012.

Montgomery, Douglas C. 2013. "Experiments with a single factor: The Analysis of Variance." In *Design and analysis of experiment*, edited by Douglas C. Montgomery, 65-130. New Jersey: John Wiley&Sons, Inc.

Ozer, Gokhan, Caglat Yuksel, Zekeriya Yasar Comert, and Kemer Altug Guler. 2013. "The effects of process parameters on the recycling efficiency of Used Aluminum Beverage Cans (UBCs)." *Materials Testing for recycling technologies* no. 55 (5):396-400.

Rombach, G. 1998. "Integrated assesment of primary and secondary aluminium production." In *Material for the future: Aluminium production and process*. Surrey UK: DMG Business Media Limited.

Schubert, Gert, Steffen Sander, and H.G. Jackel. 2004. "The fundamentals of the comminution of metals in shredders of the swing-hammer type." *International Journal of Mineral Processing* no. 74S:S385-S393.

Sydykov, A., B. Friedrich, and A. Arnold. 2002. "Impact of parameter changes on the aluminum recovery in a rotary kiln." In *Light Metals 2002*, edited by Wolfgang Schneider, 1045-1052. TMS: The Minerals, Metals & Materials Society.

Tenorio, J. A. S., and D. C. R. Espinosa. 2002. "Effect of salt/oxide interaction on the process of aluminum recycling." *Journal of Light Metals* no. 2:89-93.

Thoraval, Marion, and B. Friedrich. 2015. Metal entrapment in slag during the aluminium recycling process in tilting rotary furnace. In *European Metallurgical Conference 2015*. Dusseldorf.

Utigard, T.A., K. Friesen, R.R. Roy, J. Lim, A. Silny, and C. Dupuis. 1998. "The Properties and Uses of Fluxes in Molten Aluminum Processing." *JOM* no. 50 (11):38-43.

Velasco, Eulogio, and Jose Nino. 2011. "Recycling of aluminium scrap for secondary Al–Si alloys." *Waste managment and research* no. 29 (7):686-693.

Verran, G.O., and U. Kurzawa. 2008. "An experimental study of aluminum can recycling using fusion in induction furnace." *Resources, Conservation and Recycling* no. 52:731-736.

Xiao, Y., M. Reuter, P. Vonk, and J. Vonken. 2000. Experimental study on aluminum scrap recycling. In *Fourth International Symposium on Recycling of Metals and Engineered Materials*. St. Louis.

Xiao, Y., and M.A. Reuter. 2002. "Recycling of distributed aluminium turning scrap." *Minerals Engineering* no. 15:963-970.

Xiao, Yanping, Markus A. Reuter, and Udo. Boin. 2005. "Aluminium Recycling and Environmental Issues of Salt Slag Treatment." *Journal of Environmental Science and Health, Part A: toxic/hazardous substances and enviromental engineering* no. 40:1861-1875.

ARTICLE 3

INFLUENCE OF CRYOLITE CONTENT ON FLUX PROPERTIES IN AL REFINING

Stefano Capuzzi, Giulio Timelli

[1]Department. of Management and Engineering-DTG
University of Padua
36100 Vicenza
ITALY

Submitted for pubblication in : Metallurgical and Materials Transaction A

Abstract

In order to maximize the efficiency of fluxing during scrap melting, the addition of fluorides is necessary. This study investigates the influence of the cryolite (Na_3AlF_6), a widely used fluoride, on several properties of a typical industrial flux. The flux was composed by a mixture of 95NaCl-5KCl salts and the cryolite addition ranged from 0 to 20% in weight.

The melting temperature, the viscosity and the ability in dissolving the aluminium oxide were considered as well the dissolving time of the salt in water.

Thermal analysis (TA) was performed to measure the melting temperature and a body falling method was set to evaluate the viscosity. The oxide dissolution was assessed as the reduction in weight of alumina balls immersed in the molten flux while the weight reduction of a representative sample of the solidified salt was used to appraise the leachability.

The melting temperature of the flux decreases while the viscosity increases for greater fraction of cryolite in the flux. The oxide dissolution ability is favoured by this fluoride addition, also for low quantities and low holding times. Oxide dissolution allows aluminium entrapped in the scrap to be freed and return in the molten bath increasing the metal recovery of the process.

Keywords: fluxing, cryolite, aluminum recycling, viscosity, oxide dissolution

List of symbols

cr’	point of the first derivate of the cooling curve, K/s
T	temperature, K
t	time, t
η	viscosity of the fluid, cP
r_s	radius of the falling sphere, m
g	the gravity acceleration, m/s^2
ρ_s	falling sphere density, Kg/m^3
ρ_l	fluid density, Kg/m^3
v	falling velocity of the falling sphere in the flux, m/s
ds	diameter of the falling sphere, m
D	diameter of the tube, m
w_{is}	initial weight of alumina sphere, g
w_{fs}	weight of alumina sphere after the experiment, g
w_{ic}	initial weight of the crucible and salt inside it, g
w_{fc}	weight of the crucible and salt inside it after the experiment, g
R^2	goodness coefficient
xi	discrete variable
f(xi)	experimental value associated to xi
g(xi)	value associated to xi calculated with the regression function
F(xi)	mean value of the experimental values
A	frequency factor, cP
E	activation energy, J/mol
R	gas constant, 8.134 J/(mol*K)

I. Introduction

Recycling will be among the most important activities of aluminium industry in the next future. It offers great advantages if compared to primary aluminium production thanks to lower production cost [1], energy consumption [2] and gas emission [3]. Moreover, depletion of the primary raw materials is reduced, and this is a key factor considering how the aluminium competes for a large number of applications and its consumption is still increasing.

Rotary and reverberatory furnaces are the mainly used technologies to remelt the aluminium alloy scrap especially if it presents a high non-metallic content. They allow a high productive rate [4], while crucible and electric furnaces are best suitable with a lower productive volume and a higher quality level of the scrap [5].

The choice of a suitable furnace design is not sufficient to melt low-quality scrap. The addition of chemical compounds in the scrap charge, called *flux*, is necessary. These compounds are usually sodium and potassium chlorides. Different mixtures of these salts can be used. However, an equimolar mass mixture of NaCl-KCl allows lower melting point because an eutectic reaction develops with a concentration of 44% Na and 56% KCl at about 938 K (665 °C) [6]. The aim of the flux is to protect the bath from oxidation because the molten Al bath rapidly forms an oxide layer over the surface exposed to an oxygen-containing atmosphere [7]; thus, the flux has to be at the liquid state during melting of the scrap. Further, a decrease on the melting temperature means a reduction in energy and time consumptions.

Although a NaCl-KCl mixture prevents oxidation, the addition of other salts leads to increase the metal recovery. The flux collects these oxides, which originate from the scrap, thus forming a slag where metal Al drops are entrapped [8]. The ability of the salt to favour the coalescence of these drops becomes an important feature for determining the Al recovery. A drop with a greater diameter results from the coalescence of smaller droplets thus increasing the probability to settle down from the slag into the molten metal.

Firstly, the salt flux has to remove the oxide layer covering the Al drops to allow the coalescence among them. Wang and Brochu [9] stated that the metal inside the oxide layer tends to assume a spherical shape when it melts. The difference in volume expansion between the molten metal and the oxide creates small cracks in the oxide layer but this is not sufficient to release the liquid aluminium.

Various salts added to the NaCl-KCl mixture have been considered to increase the oxide stripping and consequently the drops' coalescence. All the results available in literature agree on the fact that fluorides can lead to this specific aim [10]; in particular, sodium fluoride (NaF), potassium fluoride (KF) and cryolite (Na_3AlF_6) offer excellent results according to Roy and Sahai [11] and Friesen, et al. [12].

The way in which fluorides act is not completely understood and various mechanisms are proposed. Peterson [13] considered the solubility of the alumina in the molten salt; an electrochemical behaviour is proposed by Jordan and Milner [14] and by Storchai and Baranov [15] who stated the aluminium acts as an anode, the oxide provides a cathode and the salt flux is the electrolyte. The interfacial tension between the metal and the salt flux is often proposed as the main affecting factor. Minimizing the interfacial tension increases the affinity between the metal and the salt and facilitates the removal of the oxide layer [16]. Tenorio and Espinosa [17] suggested that the stripping of the Al oxide layer by means of the salt flux take places according to a mechanism similar to a hot corrosion process.

Once the molten metal is released from the oxide layer the Al drops have to be able to move for coalescing. Viscosity is the property of the slag that effects the drops

movements. Upon increasing the viscosity of the slag, the movement of the drops becomes more difficult. Both the salt and the oxide affect the final properties of the slag. Tenorio, et al. [18] proved that the addition of NaF and KF decreases the viscosity of the equimolar mixture of NaCl and KCl from $1.2 \cdot 10^{-3}$ Pa•s (1.2 cP) to $0.4 \cdot 10^{-3}$ Pa•s (0.4 cP). On the contrary, Xiao, et al. [19] highlighted an increase of the slag viscosity by adding non-metallic components (NMCs) in the salt. The viscosity is greater than 1 Pa•s (1000 cP) if the content of the NMC exceeds 10%.

The solidified slag is a hazardous waste that is called "*salt cake*". There are two possibilities of managing the salt cake: the separation of its components for possible recovery or the storage in controlled landfills. Because of increasing local environmental and institutional barriers to the development of new landfills, the disposal of salt cake residue is expected to be forbidden or become scarce and costly in the next future [20]. Recovery of the salt cake allows the separation between the salt fraction and the non metal content by dissolving the salt. The ability of the flux to be dissolved is a key factor in lowering the water consumption and the time.

In this work, several properties of a mixture of NaCl-KCl-Na_3AlF_6 have been investigated as function of different quantities of cryolite. In particular, the melting temperature, the viscosity, the ability in dissolving the Al oxides and the leachability have been investigated.

The effects of the temperature and the holding time on the viscosity and the oxide dissolution have been also considered, respectively. The analysis of variance (ANOVA) has been performed to validate the results and a statistical approach based on the linear regression method has been implemented in order to calculate the dissolution rate of the oxide with different amounts of cryolite.

II. Experimental procedure

The experimental salt fluxes were composed by a mixture of 95%NaCl-5%KCl with the addition of cryolite ranging from 0 to 20 wt. %. Several techniques have been used to investigate various salt properties. More in detail, thermal analysis have been performed to investigate the solidification behaviour of the salts while the body falling method was chosen to measure their viscosity. The dissolution of alumina in the salts and the salts in water has been also studied.

A. Thermal analysis

Thermal analysis (TA) was performed to assess the melting temperatures for the various fluxes. The levels of cryolite added to the baseline NaCl-KCl mixture were 0, 5, 10 and 20 wt. %, respectively.

The salt was melted in a muffle furnace at 1173 ± 3 K (900 ± 3 °C) and poured in a cylindrical steel cup, whose diameter and height were 30 and 50 mm, respectively. Prior to cast the salt, the cup was preheated at 1073 ± 3 K (800 ± 3 °C) in order to attain a cooling rate lower than 1 K/s which, in turn, results in well-defined cooling curves suitable for further thermal analysis.

During solidification, the cooling curves were measured by means of a K-type (Chromel–Alumel) thermocouple located at the centre of the cup, and the data were collected using a data acquisition system, with a sampling rate of 0.5 s, connected to a PC. During the experiments, the thermocouple was protected by tightly fitted steel tube so as to allow it to be used throughout the experimental plan.

The first derivate was calculated for each adjacency pair of temperature and time values as follows:

$$cr' = \frac{\Delta T}{\Delta t} = \frac{T_i - T_{i+1}}{t_i - t_{i+1}}$$ Equation 1,

where cr' is a point of the first derivate of the cooling curve, T is the temperature, t is the time and the subscriptions i and i+1 indicate two adjacent data.

The cooling curve and the first derivate were smoothed by means of the moving average algorithm. The smoothed point was calculated as the average of ten consecutive points of the raw data. The number of consecutive points was chosen in order to reduce the signal-to-noise ratio without missing sensitive information.

For each set of temperature/time relations in the centre of the sample, the cooling curves and the corresponding derivate curve were plotted to determine the nucleation T_{nuc}, minium T_{min}, and growth T_{growth} temperatures for the NaCl. The eutectic nucleation temperature T_{eut} and the solidus temperature T_{sol} of the salts were also calculated.

Figure 1 shows the way in which the temperatures have been obtained in the case of the cryolite addition equal to 10 wt%. The nucleation temperature can be detected as a flex in the first derivate of the cooling curve while the solidus temperature was measured when the cooling rate curve drops back to the baseline curve.

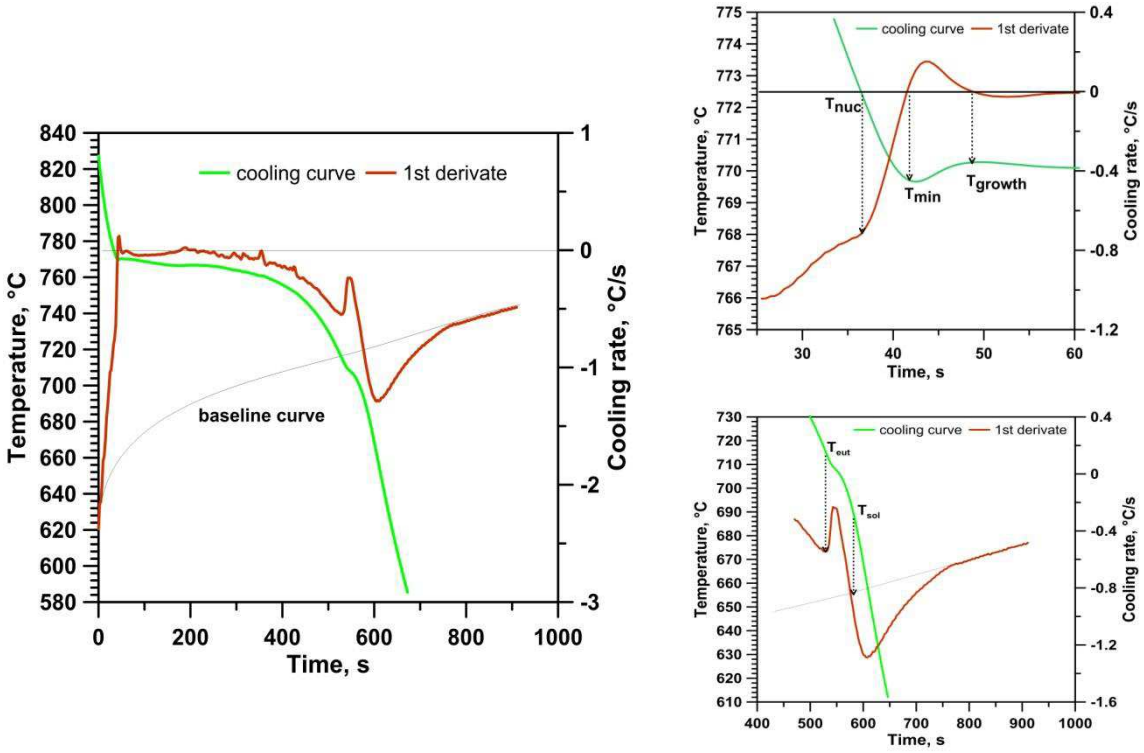

Fig. 1 - (a) Colling curve and first derivate of the NaCl-KCl flux with the addition of 10% of ryolite, (b) magnification plots showing the method used to determine the characteristic points, such as T_{nuc}, T_{min}, T_{growth}, T_{eut} and T_{sol}

B. Body falling testing

The viscosity tests were performed by means of the body falling method [21] which is based on the Stokes' law. The viscosity of a fluid is correlated to the falling velocity of a sphere inside it, as expressed in Equation 2:

$$\eta = \frac{2 * r_s^2 * g * (\rho_s - \rho_f)}{9 * v_s}$$ Equation 2

where η is the viscosity, r_s and ρ_s are the radius and density of the sphere respectively, ρ_f is the density of the fluid, g is the gravity acceleration and v_s is the falling velocity.

The premise in this method is that only the gravity force acts, while the thermal volumetric expansion of the salt was taken into consideration using Equation 3 [22]

$$\eta = \frac{2*r_s^2*g*(\rho_s-\rho_f)}{9*(1+2.1\frac{d_s}{D})v_s} \quad \text{Equation 3}$$

where d_s is the sphere radius and D is the tube diameter. The radii ratio has to be lower or equal to 0.1.

In the experiments, the salt flux acted as fluid, while silicon nitride spheres with a diameter equal to 3 mm were used as falling body. A quartz tube with an inner diameter of 30 mm was filled with the salt and placed inside a muffle furnace.

The tests were carried out at 1063 ± 3 K (790 ± 3 °C) and 1083 ± 3 K (810 ± 3 °C) and at least three tests were performed for each condition. Therefore, the viscosity of the different salts was measured. The apparatus was calibrated against to the data in literature of the salt 95NaCl–5KCl at 1083 K (810 °C) [23] and a correction factor equal to 0.102 was found.

C. Dissolution of Alumina

An alumina sphere with a 6 mm diameter was placed inside a ceramic crucible together with 30 g mixture of NaCl-KCl and cryolite, which was varied according to the experimental conditions. The experiments were performed in a muffle furnace set up at 1083 ± 3 K (810 ± 3 °C). Various holding times were considered for each flux, such as 10, 30, 40 and 60 minutes. The alumina ball was extracted from the salt when it was cooled down, by dissolving the salt in water. Each sphere was weighed before and after the experiment, and the oxide dissolution was estimated as the weight reduction of the alumina sphere according to:

$$\%dissolution_{oxide} = \frac{w_{is}-w_{fs}}{w_{is}}\ \% \quad \text{Equation 4}$$

where w_{is} and w_{fs} are the initial and the final weight of the alumina sphere. Each experimental condition was repeated at least 5 times with new alumina balls.

D. Investigation of salt dissolution

The salt dissolution was studied as function of the holding time in water at room temperature.

A porcelain crucible filled with 10 g of salt mixture was hold inside a muffle furnace set up at 1083 ± 3 K (810 ± 3 °C) for 10 minutes and then removed to cool in air. The solidified salt was submerged into a tank with 0.9 dm^3 of water and hold for various times, 10, 30, 60 and 120 minutes. The material was then heated at 373 ± 1 °C K (100 ± 1 °C) to remove the excess water.

The salt dissolution was evaluated as the weight reduction according to:

$$\%dissolution_{oxide} = \frac{w_{ic}-w_{fc}}{w_{ic}} \quad \text{Equation 5}$$

where w_{ic} and w_{fc} are the initial and final weights of the experimental salt.

E. Statistical analysis

The results obtained from the flux viscosity and the oxide dissolution tests were statistically verified by the ANOVA. Definitions and specific assumptions for this work are here reported, while a detailed description of the ANOVA procedure is given elsewhere [24]. A hypothesis test is used to determine which statement is best supported by the data. These two statements are called the null hypothesis and the alternative hypothesis, respectively. In this work, the null hypothesis is that the data obtained with the different levels of cryolite are simply random samples of the same population; this means that the addition of cryolite doesn't affect the viscosity and the oxide dissolution, respectively. The test calculates the probability to obtain the observed sample data under the assumption that the null hypothesis is true. If this probability (the *p*-value) is below a user-defined cut-off point (the α-level), then this assumption is probably wrong. Therefore, the null hypothesis is rejected and the alternative hypothesis is selected. In this study, the α-level was selected equal to 0.05; this means that if the null hypothesis is rejected then the probability of reject a true null hypothesis is equal to 5%.

A regression model can be developed describing the relationship between the response and the predictor variables. The reliability of the model is based on the goodness coefficient R^2. It measures the quality of the least-squares fitting to the original data; hen when R^2 =1, the fit is perfect.

III. Results and Discussion

A. Thermal analysis

Figure 2 shows the solidified samples with different salts after thermal analysis. The visual aspect sensibly changes when the cryolite is added. The sample corresponding to baseline salt flux (95NaCl-5KCl) presents a uniform crystalline structure (Figure 2a), while adding cryolite the central zone changes in a porous structure (Figure 2b). The porous zone is bigger for greater content of cryolite and it is always placed in the middle. (Figure 2c-d). Consequently, it is the last zone which solidified and it can be related to the formation of the eutectic between NaCl and Na_3AlF_6 [25]

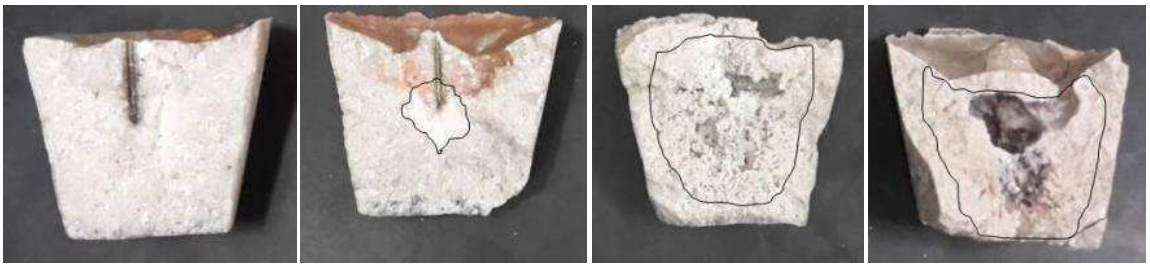

(a) (b) (c) (d)

Fig. 2 - TA samples with different fraction of cryolite in the flux: a) 0 b) 5, c) 10 and 20 wt%. The black line defined the porous region x

The addition of cryolite affects the crystallization path of the salt flux as clearly shown in Figure 3. In particular, the time needed to cool the sample from 1103 K (830 °C) to 933 K (660 °C) increase from 470 s for the baseline salt flux up to 700 s if the 20% in weight of cryolite is added to the mixture.

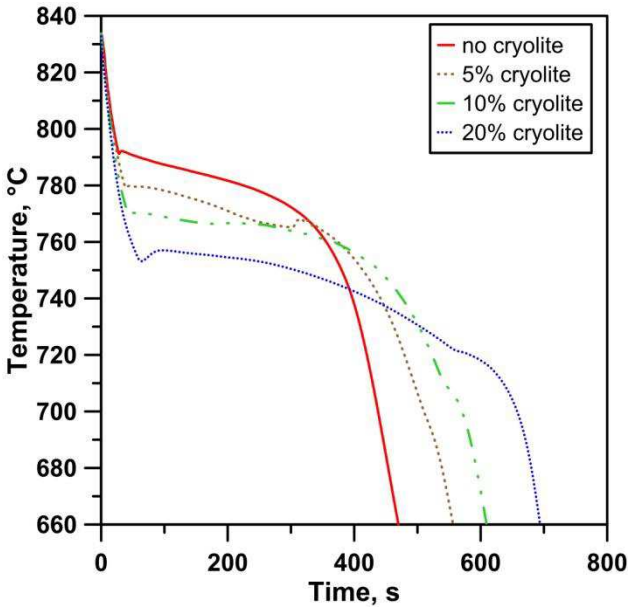

Fig. 3 - Effect of the cryolite addition on the solidification behavior of the 95NaCl-5KCl flux

Table I summarized the solidification characteristic temperatures for the different salts. The nucleation temperature is in agreement with the published melting temperature of a 95NaCl-5KCl mixture [26]. The characteristic temperature measured with the addition of cryolite of the ternary system NaCl-Na3AlF6-KCl strongly differs from the phase diagram of the binary system NaCl-Na_3AlF_6 phase [25].

Table I. The solidification characteristic temperatures for the different salts

wt% Na_3AlF_6	Tnuc	Tmin	Tgrowth	Teut	Tsolidus
0	795	792	793	-	728
5	783	780	781	714	692
10	772	769	770	716	694
20	760	754	756	720	692

The liquidus temperature is a key factor on industrial point of view; a reduction in the melting temperature means a reduction in the energy consumption and in the related costs.

B. Viscosity

In literature, theoretical determination of viscosity has been performed using molecular dynamics calculation for some binary salts [27]. The application of the same method to ternary salts is challenging due to the complexity of calculations. Therefore the experimental measurements of viscosity of ternary salts are very useful.

The tests performed with the molten 86NaCl-4KCl-10Na_3AlF_6 salt are shown in Figure 4. The falling velocity of the sphere decreases when the cryolite is added; consequently the time needed to go from the upper limit to the lower limit, increases from 34cs to 38cs. A variation of 1cs in the falling time within the experimental conditions means a discrepancy of the viscosity equal to $0.176 \cdot 10^{-3}$ Pa•s (0.176 cP).

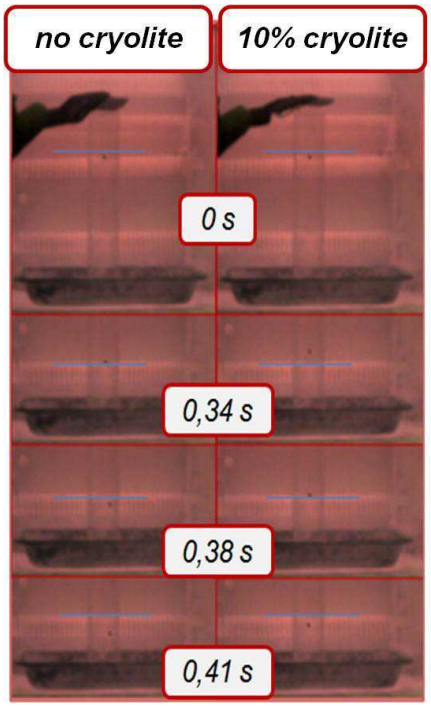

Fig. 4 - Falling time of a silicon nitride sphere inside a (left) 95NaCl-5KCl with no cryolite and inside (right) the same flux with the addition of 10wt% of cryolite

Figure 5 shows the variation in the viscosity of the 95NaCl-5KCl flux as function of the cryolite content at 1063 K (790 °C) and 1083 K (810 °C). It is possible to conclude that the cryolite addition increases the viscosity of the molten salt according to a polynomial trend. The increase of the temperature seems to decrease the viscosity.

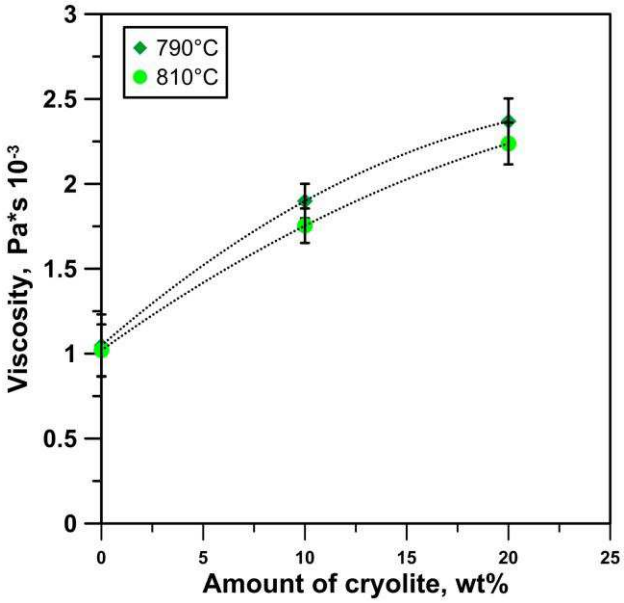

Fig. 5 - Variation in the viscosity of the molten salt as function of the percentage of cryolite added to the mixture of NaCl-KCl

The viscosity of the ternary system NaCl-KCl-Na_3AlF_6 was not studied before. Nevertheless, experiments on the influence of the Na_3AlF_6 on the viscosity of the NaCl salt are reported in literature and trends similar to those presented in this work were found. Janz and Tomkins [28] studied a mixture of NaCl-Na_3AlF_6 with the cryolite ranging from 6% to 71% at 1273 K (1000 °C). The viscosity of the salt rises from

$0.74 \cdot 10^{-3}$ Pa•s (0.74 cP) to $0.74 \cdot 10^{-3}$ Pa•s (2.12 cP) if the cryolite fraction is increased from the lowest to the highest level. The same binary salt was investigated by Votava and Matiasovsky [29] using the torsion pendulum method within the temperature interval 1123 K (850 °C) to 1223 K (1050 °C). A positive relation between viscosity and the quantity of cryolite is reported in the temperature range studied, while an inverse relation is highlighted between viscosity and temperature.

Roy, et al. [30] performed experiments on the density and the kinematic viscosity of an equimolar mixture of NaCl with the addition of cryolite ranging from 0 to 2%.The density increases while the kinematic viscosity decreases. The viscosity, which is the product of these two properties, increases. This is at odds with previous findings, but a lower quantity of cryolite was considered

From the experimental results of this work, in the worst case, i.e. 20% of cryolite at 1063 K (790 °C), an increment of viscosity is lower than $1.5 \cdot 10^{-3}$ Pa•s (1.5 cP). According to Xiao, et al. [19] with an amount of NMC smaller than 10wt% a increment ten times higher is achieved. The negative effect of the cryolite is, therefore, covered by the greater impact of the non metallic particles, always present in the salt during the re-melting of the scrap.

Figure 6 shows the falling time of an aluminium drop considering the experimental viscosity for the various salts as function of the drop radius. The time was calculated using Equation 1 with a height of 100 mm and both temperatures were considered. A sensible difference can be noted only with small radii, lower than 2 mm, but the falling time is in both cases lower than 3 seconds.

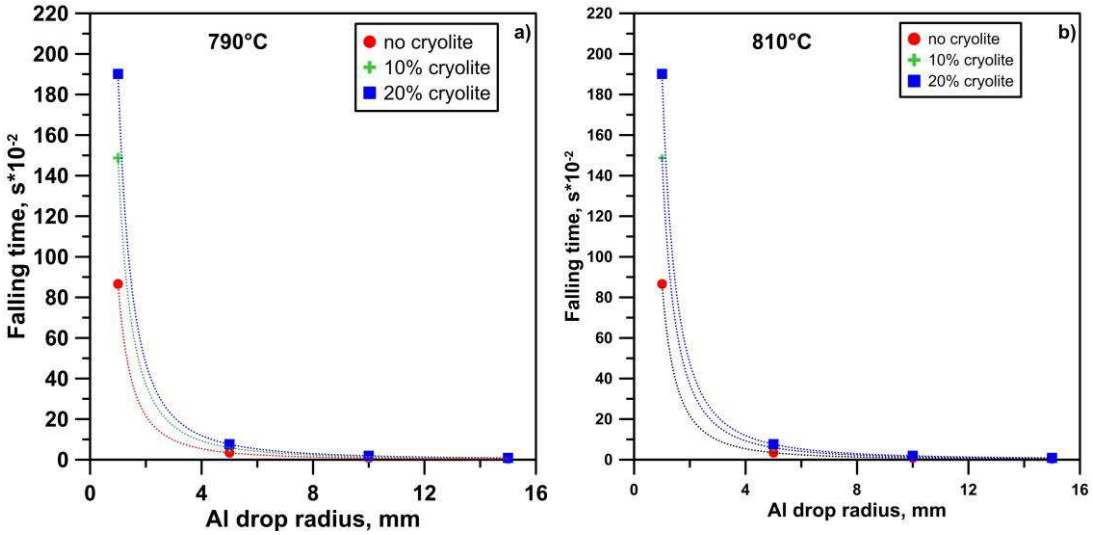

Fig. 6 - Evolution of the time needed by an Al drop to fall for 100 mm in the tested salts as function on its radius at a)1063 K (790 °C) and b) 1083 K (810 °C)

The results of the ANOVA analyses are reported in Table II and the p-values confirm the influence of the quantity of cryolite on the flux viscosity, while the temperature does not statistically affect this property of the salt. Indeed, in the first case the p-value is lower than the α-level (0.05) while the p-value for the temperature exceeds this level. The non-statistical significance of the temperature in the experimental conditions is probably due to the little difference between the temperatures (20 K) and the dispersion of the results.

Table II. Results of ANOVA for the influence of the fraction of cryolite in the flux and temperature on the viscosity of the flux

Factor	Degrees of freedom	Sum of squares	Mean square	F-test	p-value
wt% cryolite	2	0.000493	0.000246	169.7	0.000
temperature	1	0.000004	0.000004	3.18	0.096
Error	14	0.000020	0.000001		
Total	35	0.000518			

The influence of temperature on the viscosity of various salts is widely studied and an Arrhenius equation is generally proposed [31]:

$$\eta = A * e^{\frac{E}{R*T}} \qquad \text{Equation 6}$$

Where η is the viscosity, A is a constant called frequency factor, E is the activation energy for viscous flow at constant pressure, R is the gas constant and T the absolute temperature. In Table III, the coefficients of the Arrhenius equation obtained with the experimental data are listed.

Table III. Coefficients of the Arrhenius equation for the relation viscosity-temperature for the various experimental salts

	fraction of cryolite, wt%		
	0	10	20
A, cP	0,002416	0,000254	0,001093
E, J/mol	12693	37330	26607

C. Oxide dissolution

Figure 7 shows the oxide dissolution curve for various additions of cryolite to the mixture of NaCl-KCl. No effects were detected if the flux was only composed by chlorides, while increasing the fluoride content in the salt, the alumina dissolution increases at each experimental time. The magnitude of this effect appears greater in the first 30 minutes while the slope of the curves decreases in the last 30 minutes.

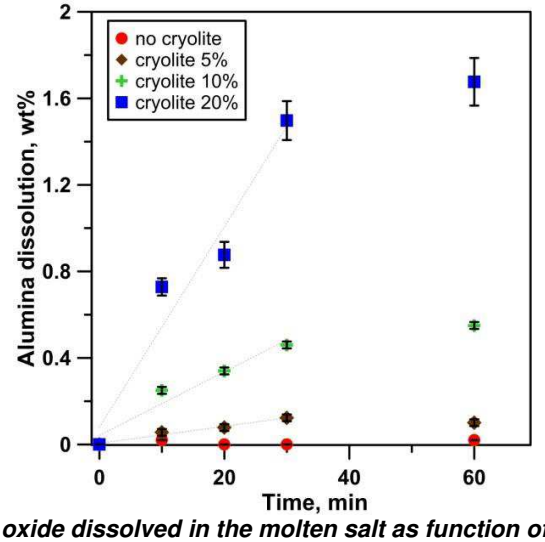

Fig. 7 - Fraction of Al oxide dissolved in the molten salt as function of the holding time and different addition of cryolite

The subsequent data analysis by means of ANOVA reveals a complete and more exhaustive evaluation of the relationship between the dissolution of the oxide and the independent variables, i.e. the fraction of cryolite and the holding time. In this case, the goodness coefficient R^2, indicating how properly the model fits the data, is equal to 0.78.

Table IV. Results of ANOVA for the influence of the fraction of cryolite in the flux and temperature on the fraction of Al oxide dissolved in the molten salt

Factor	Degrees of freedom	Sum of squares	Mean square	F-test	p-value
wt% cryolite	3	17.58	5.86	149.59	0.000
holding time	3	1.35	0.45	11.55	0.000
Error	30	2.86	0.04		
Total	35	21.79			

The main effects plot (Figure 8a) displays the mean values at each level of the experimental factors, i.e. the fraction of cryolite and the holding time. The more is the change across the levels, the higher is the magnitude of the factor. The cryolite content shows the main effect and its influence increasing at highest level. Nevertheless, the effect of holding time and their interaction cannot be neglected. Interaction is present when the response at a factor level depends upon the levels of other factors. Parallel lines in an interaction plot indicate no interaction. The greater the departure of the lines from the parallel state, the higher the degree of interaction. The interaction between the experimental variables is highlighted in Figure 8b; it is clear that increasing the quantity of cryolite, the effect of the holding time increases.

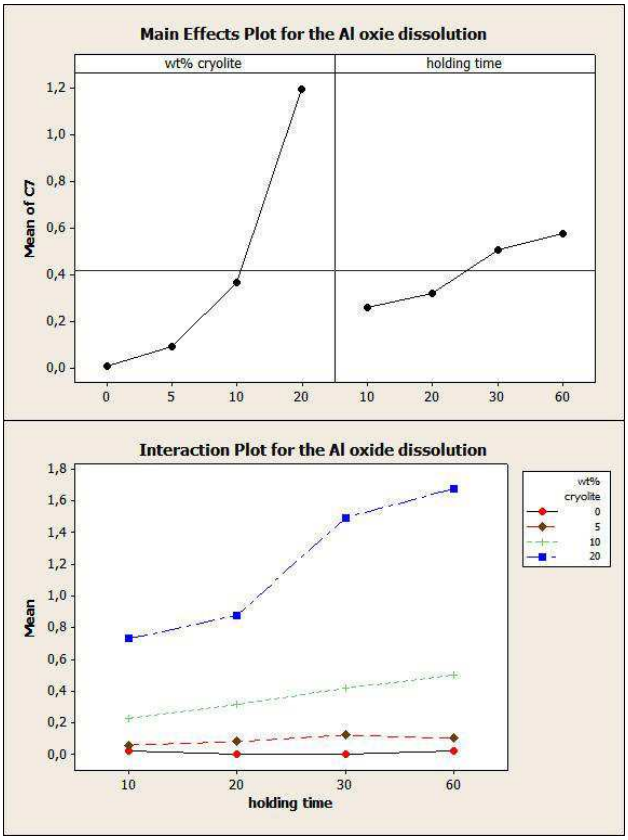

Fig. 8 - a) Main effects chart displaying the influence of the percentage of added cryolite and the holding time on the fraction of alumina dissolved and b) the interaction plot between these two variables

A regression analysis, with the time ranging from 0 minutes to 30 minutes, was performed for the addition of the 5%, the 10% and the 20% of cryolite in order to evaluate the dissolution rate. The achieved results are reported in Equation 7, 8 and 9, respectively.

$$\text{dissolution (\%)} = 0.004 * \text{t (min)} + 0.005 \qquad \text{Equation 7}$$

$$\text{dissolution (\%)} = 0.014 * \text{t (min)} + 0.042 \qquad \text{Equation 8}$$

$$\text{dissolution (\%)} = 0.046 * \text{t (min)} + 0.079 \qquad \text{Equation 9}$$

These equations suggest that the alumina weight decreases of the 0.014 for each minutes in a mixture of NaCl-KCl with the addition of the 10% of cryolite, while the reduction is equal to 0.046 per minute if the percentage of cryolite is doubled. These rates are valid up to 30 minutes and the goodness coefficient R^2 is 0.68, 0.72 and 0.69, respectively. The predicted R^2, used in regression analysis to indicate how accurately the model predicts responses for new observations, are also higher than 0.5, in particular 0.51, 0.52 and 0.59.

These trends are in agreement with those of Tenorio, et al. [18] whom investigated the alumina dissolution with addition of other fluorides, in particular NaF, CaF_2 and KF. The fluorides are here cited in order of effectiveness. Results are not easily comparable since different procedures were used but the alumina dissolution increases for all the additions of fluorides studied.

D. Salt dissolution

Figure 9 shows the effect of cryolite content on the salt dissolution in water. The efficiency of the water leaching is reduced increasing the cryolite content. More of the 90% of the salt sample was dissolved after two hours if no cryolite was added while the mass of the sample is reduced less than of 20% when the cryolite content is 20%. These results can be correlated to the different solubility in water between the NaCl and the Na_3AlF_6 salts, i.e. 358 g/l and 0.4g/l respectively.

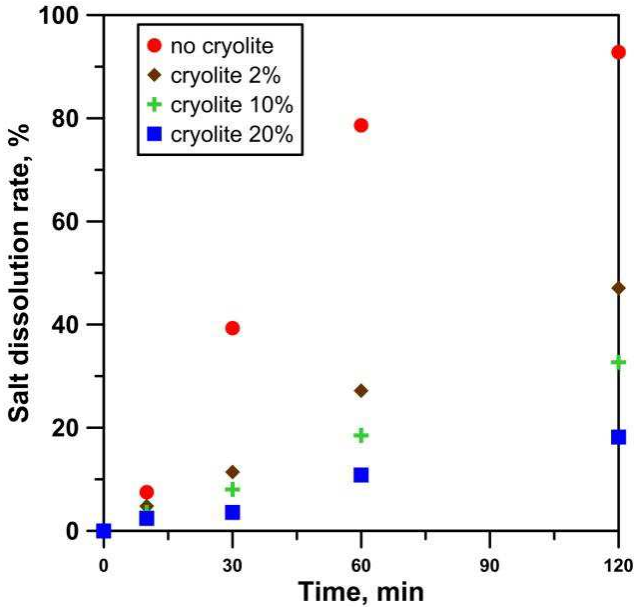

Fig. 9 - Fraction of salt dissolved in water as function of the holding time for different percentages of cryolite addition to the mixture of NaCl-KCl

Conclusions

The effects of cryolite on a mixture of 95%NaCl-5%KCl were investigated considering melting temperature, viscosity and ability in oxide reduction rate and salt dissolution in water. The following conclusions can be drawn.

- The addition of cryolite to the 95NaCl-5KCl flux causes a decrease in the melting temperature while the solidus temperature is the same for the various experimental fluxes.
- The cryolite addition produces an increment in the viscosity of the molten salt according to a polynomial trend, while increasing the temperature the viscosity weakly decreases.
- The effect of the cryolite addition on the flux viscosity is lower compared to the impact that the non metallic components have.
- A flux composed by NaCl and KCl is not able in dissolving the alumina, while adding the cryolite, a weight reduction of the alumina ball up to of 1.6% was achieved.
- The cryolite content evidences the main effects on the alumina dissolution, nevertheless, the effect of holding time and their interaction cannot be neglected.
- The dissolution rate of the alumina increases increasing the cryolite content in the flux from 0.004 to 0.038 wt%/min.
- The dissolution of the flux in water is slowed by the addition of cryolite that is in agreement with the different solubility in water between NaCl and Na_3AlF_6.

References

1. Klavdij Logozar, Gregor Radonjic and Majda Bastic, *Resour. Conserv. Recycl.* 2006, vol. 49, pp. 49-67.
2. J. Blomberg and P. Söderholm, *Resour. Conserv. Recycl.* 2009, vol. 53, pp. 455-463.
3. Eva Sevigné-Itoiza, Carles M. Gasola, Joan Rieradevalla and Xavier Gabarrella, *Resour. Conserv. Recycl.* 2014, vol. 89, pp. 94-103.
4. Peter Newman, *Mater. Sci. Forum* 2010, vol. 630, pp. 103-110.
5. B.E. Peter Whiteley, *Mater. Sci. Forum* 2011, vol. 693, pp. 73-79.
6. P.N. Crepeau, M.L. Fenyes and L.J. Jeanneret, *Mod. Cast.* 1992, vol. 82, pp. 28-30.
7. Yun Wang, Hu-Tian Li and Zhongyun Fan, *Trans. Indian Inst. Met.* 2012, vol. 65, pp. 653-661.
8. Petros E. Tsakiridis, *J. Hazard. Mater.* 2012, vol. 217-218, pp. 1-10.
9. Z. Wang and L. Brochu, Alcan 1993.
10. (a) Sandra Besson, Anne Pichat, Elodie Xolin, Patrice Chartrand and Bernd Friedrich, In *European metallurgical conference 2011*, (Dusseldorf, 2011), pp 1-16; (b) J. H. L. Van Linden and D. L. Stewart, In *Light Metals 1988*, ed. Paul G. Campell TMS: The Minerals, Metals & Materials Society: 1988, pp 173-181; (c) Ye-Sik Kim, Eui-Pak Yoon, Ki-Tae Kim, Woon-Jae Jung and Duk-Ho Jo, *J. Korea Foundry Soc.* 2000, vol. 20, pp. 39-45.
11. Raja R. Roy and Yogeshwar Sahai, *Mater. Trans.* 1997, vol. 38, pp. 995-1003.
12. K.J. Friesen, T.A. Utigard, C. Dupuis and L.P. Martin, In *Lights Metals 1997*, ed. Reidar Huglen TMS: The Minerals, Metals & Materials Society: 1997.

13. Ray D. Peterson, In *Second International symposium-Recycling of Metals and Engineered Materials*, ed. Jan H.L. van Linden, Donald L. Stewart Jr and Sahai Yogeshwar TMS: The Minerals, Metals & Materials Society: 1990, pp 69-84.
14. M. F. Jordan and D. R. Milner, *J. Inst. Metals* 1956, vol. 85, pp. 33-40.
15. E.I. Storchai and N.S. Baranov, *Chem. Petrol. Eng*+ 1976, vol. 12, pp. 252-255.
16. (a) Jian Ye and Yogeshwar Sahai, *Mater. Trans.* 1996, vol. 37, pp. 1479-1485. ; (b) Raja R. Roy and Torstein A. Utigard, *Metallurgical and materials transaction B* 1998, vol. 29B, pp. 821-827.
17. J. A. S. Tenorio and D. C. R. Espinosa, *J. Light Met.* 2002, vol. 2, pp. 89-93.
18. J. A. S. Tenorio, D. C. R. Espinosa and M.C. Carboni, *J. Light Met.* 2001, vol. 1, pp. 195-198.
19. Yanping Xiao, Markus A. Reuter and Udo. Boin, *J. Environ. Sci. Heal. A* 2005, vol. 40, pp. 1861-1875.
20. Antonio Gil and Sophia A. Korili, In *Environmental Management*, ed. Santosh Sarkar InTech: Rijeka, Croatia, 2010.
21. G.E. Leblanc, R.A. Secco and M. Kostic, In *The Measurement, Instrumentation, and Sensors: Handbook*, ed. John G. Webster Springer Science & Business Media: 1999, pp 30.1-30.23.
22. Leslie R. Bacon, *J. Frank. Inst.* 1936, vol. 221, pp. 251-273.
23. G.J. Janz, R.P.T. Tomkins, C.B. Allen, J.R. Downey Jr., J.L. Gardner, U. Krebs and S.K. Singer, *Journal of physical and chemical reference data* 1975, vol. 4, pp. 871-1178.
24. Ronald Aylmer Fisher, *Metron* 1921, vol. 1, pp. 3-32.
25. T.P: Madhavan, K. Matiasovsky and V. Danek, *Chemické Zvesti* 1970, vol. 25.
26. D.S. Coleman and P.D.A. Lacy, *Mat. Res. Bull.* 1967, vol. 2, pp. 935-938.
27. G. Ciccotti, G. Jacucci and I.R. McDonald, *Phys. rev. A* 1976, vol. 13.
28. George J. Janz and R.P.T. Tomkins, *Journal of physical and chemical reference data* 1983, vol. 12, pp. 591-813.
29. I. Votava and K. Matiasovsky, *Chemical papers* 1973, vol. 27, pp. 582-587.
30. Raja R. Roy, Jian Ye and Yogeshwar Sahai, *Mater. Trans.* 1997, vol. 38, pp. 566-570.
31. D.Dumas, B.Fjeld, K.Grjotheim and H.A. Øye, *Acta Chem. Scand.* 1973, vol. 27, pp. 319-328.

ARTICLE 4

INFLUENCE OF COATING AND DE-COATING ON THE COALESCENCE OF ALUMINIUM DROP

Stefano Capuzzi[1], Anne Kvithyld[2], Giulio Timelli[1], Arne Nordmark[2], Thorvald Abel Engh[3]

[1]Department. of Management and Engineering-DTG
University of Padua
36100 Vicenza
ITALY

[2]SINTEF
N-7465 Trondheim
NORWAY

[2]NTNU
N-7465 Trondheim
NORWAY

TMS2017, San Diego, 26th February – 2nd March 2017

Abstract

In a rotary furnace for aluminium recycling and dross treatment, a salt flux is added which protects against oxidation and captures non-metallic impurities. Furthermore, the salt has to promote the coalescence of the metal drops in the dross.

This work investigates the coalescence of molten aluminium for different types of scrap. One hundred discs were stamped from aluminium alloy sheets with and without coating. They were melted, covered in NaCl-KCl-Na_3AlF_6 molten salt, in an induction furnace at 790°C. The solidified aluminum droplets were extracted by leaching the salt with water.

The fraction of coalesced drops and the average diameter were determined to evaluate the coalescence efficiency. The effect of various de-coating temperatures was studied. The results show that the coalescence is negatively affected by coating. Long holding times has no effect. Complete coalescence off all discs are achieved with uncoated scrap. The drops coalesce if the temperature of the combustion reaction for the coating is attained.

Keywords: Aluminium recycling, Coalescence, De-coating

1. Introduction

During aluminium recycling, the surface of the scrap is a source of various impurities. An oxide layer always covers the surface of the aluminium scrap due to the high affinity of aluminium to oxygen. This oxide layer can be modified by anodization to increase the resistance to corrosion of the aluminium and for aesthetic reasons [1]. Coatings are applied for the same reasons [2] and the coats lead to more inclusions during the remelting of the aluminium scrap, lowering its quality. Also aluminium metal reacts with impurities, which increases the metal loss [3]. In industry, the charging sequence plays an important role in reducing the metal loss: it is important to rapidly submerge the scrap under the molten salt to prevent burn-off and high oxidation [4].

Pre-processes to reduce the presence of non-metallic coats on the scrap surface are therefore necessary. Various techniques are proposed to de-coat the Al scrap [5, 6]. However, the conventional thermal process in rotary kilns is the most frequently used strategy. The aim of the thermal de-coating process is to combust all the organic material without oxidizing the metal [7]. A significant portion of the combustion gas products is returned to the kiln, creating a recirculation loop. De-coating removes the organic fraction of the layers that cover the scrap, but oxides and other impurities remain and affect the scrap. Therefore, it is necessary to remove oxides and impurities present in the charged scrap and to protect the molten bath from oxidation. These two goals are achieved by the addition of salts, i.e. fluxing. An equimolar mixture of sodium and potassium chlorides is usually used due to the low cost and the low melting point [8]. The salt, however, entraps molten metal. The oxides collected in the salt increase its viscosity and density, slowing metal/salt separation. As a result, a non-negligible portion of metal is lost in the salt in form of aluminum drops. The ability of the salt to enhance the coalescence of these drops becomes a key factor in metal recovery.

Sodium and potassium chlorides do not promote the recovery of the metal drops, and in general chlorides, like $MgCl_2$ or $CaCl_2$, seem not to encourage coalescence [9]. The addition of fluorides is suggested to be the most effective. Various fluorides salts have been tested and classified in four categories regarding the coalescence ability: from poor, when no fluorides were added, to excellent in case of NaF, KF, LiF and Na_3AlF_6 addition [10, 11] The composition and the quality of the scrap are important issues. The presence of Mg negatively affects coalescence by forming a stronger oxide layer [12, 13], while non-metallic compounds (NMCs) slow the recovery due to a higher viscosity of the salt [14]

The aim of this paper is to study coalescence of the aluminium drops for different scrap surface conditions.

2. Experimental Procedure

The scrap was stamped out from AA3000 coil (Table 1) with and without coating in the form of discs with a radius equal to 4 mm and a height of 0.5 mm.

Table 1 Chemical composition of the experimental alloy (wt.%).

Alloy	Si	Fe	Cu	Mn	Mg	Cr	Ni	Pb	Zn	Ti
AA3000	0.53	0.58	0.20	0.68	0.34	0.02	0.01	0.01	0.23	0.02

The coated coils presented various protective layers. The coat was different on the front and the back side of the coils. The surfaces of the uncoated and coated discs, as well

as the thickness of the various coats, have been investigated by Scanning Electron Microscope (SEM).

The thermal de-coating treatments were performed in an electric resistance furnace at 400, 500 and 600 °C, with a heating rate 10 °C/min. The treatment at the highest temperature, i.e. 600°C, is the only one that reached the combustion temperature of the coat. The coils were placed obliquely. The slanting orientation of the coils is intended to avoid contact of the surfaces with the furnace walls. The back side was the upper side for all the treatments.

The coalescence tests were carried out at 790°C in an electric induction furnace.

A flux composed of an equimolar mixture of NaCl-KCl with the addition of 5% in weight of Na_3AlF_6 salts was used in all the tests. The amount of the salt was 2 times the amount of scrap. One hundred discs were charged to the molten flux. After the experiment, the crucible was cooled in air. The salt was leached with water, and the solidified drops were dried and sieved. A Matlab code was developed to evaluate the drop morphology in terms of roundness and aspect radio and to calculate the area and the equivalent diameter of the projection of the drops. A drop from a single disc has a diameter equal to 3.6 mm therefore only the particles whose equivalent diameter was greater than 3.6 mm, here called spherical drops, were considered for the coalescence efficiency. Two features were considered to evaluate the coalescence: the average diameter of the spherical drops and the ratio of the number of spherical drops to the number of all the drops. A coalescence factor (CF) was defined as follows:

$$CF = \underline{d} * \frac{N_b}{N_d} \qquad \text{Equation 1}$$

Here $\underline{d}$ is the average diameter of the spherical drops, N_b is the number of the spherical drops and N_d is the number of all the drops.

Each de-coating heating condition was studied for a holding time of 8 minutes and repeated three times. The influence of holding time was also considered, however only for the coated discs. In particular, tests were performed for 8, 15 and 60 minutes.

3. Results

3.1 Characterisation.

The surfaces of the coated and uncoated discs are completely different. Firstly, the thickness of the oxide layer on the coated discs (Figure 1a) is approximately 10 times greater than uncoated ones (Figure 1b), due to an anodization process applied before the coating.

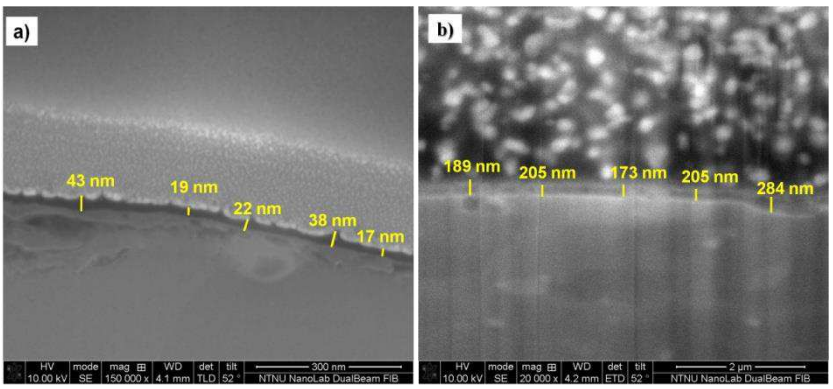

Fig. 1. Scanning Electron Microscope micrographs of the oxides that cover the (a) uncoated and the (b) coated discs. The thicknesses of the oxide layers are measured.

In addition, two different coatings cover the coated discs. The priming coating is the same for both sides; a thickness ranging from 4 to 5 µm was measured. The second layer differs depending on the side. The front size appears black and it is 5 µm thinner than the back side that is covered by a gray pigment. The total thicknesses of the layers are 20 µm and 25 µm, respectively (Figure 2).

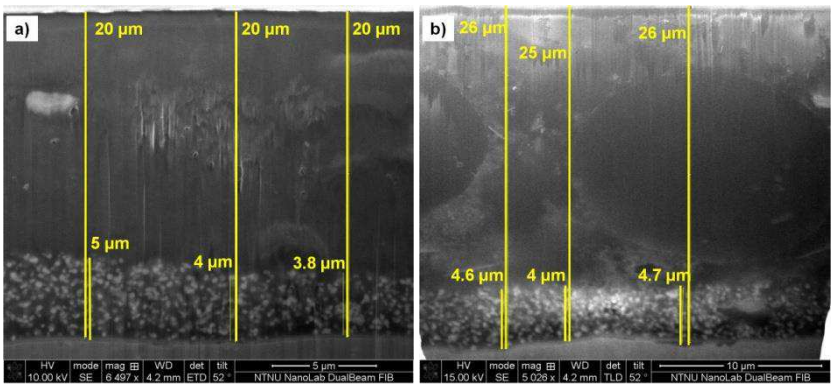

Fig. 2 Scanning Electron Microscope micrographs of and the coating layers on the (a) front side and on the (b) back side of the coated discs. The thicknesses of the coating layers are measured.

The evolution of the coating layers in response to the de-coating treatments is shown in Figure 3. In both cases, the thickness of the painted layers decreases even at the lowest temperature.

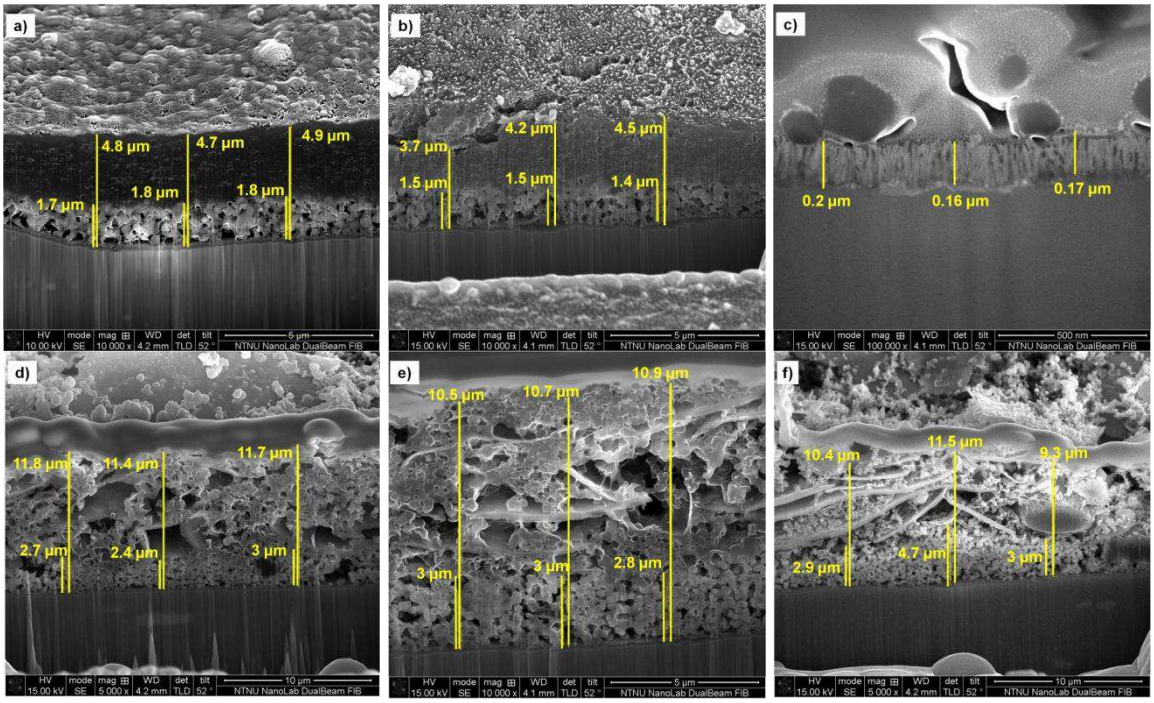

Fig. 3 Scanning Electron Microscope micrographs of the coating layers on the (top) front side and on the (bottom) back side after the different de-coating treatments: (a,d) 400°C, (b,e) 500°C and (c,f) 600°C. The thicknesses of the coating layers are measured

A greater effect was obtained on the front side. The thickness of the coat on this side decreased from 20 µm to less than 5 µm after a de-coating treatment at 400°C (Figure 3a). The reduction in thickness was more evident upon increasing the temperature

(Figure 3b) and at the highest temperature, i.e. 600°C, only the oxide layer is visible (Figure 3c).

On the front side, de-coating affects both painted layers, while the initial primary coating does not significantly change on the back side. Here, the thickness reduction of the coat is similar for all the de-coating temperatures (Figure 3 c,e,f) and a covering layer is still present even if the coil was heated at 600°C (Figure 3f). The thermal de-coating process can remove only the organic compounds present in the coats, so the different results for the two sides can be related to a different inorganic fraction in the paints.

Figure 4 summarizes the trends in thickness reduction of the coats for the two sides and the total coat, i.e. the sum of the two coats. The coat that covers the coil decreases with increasing thermal de-coating temperature. A layer of about 10 µm persists also at the highest temperature, but the carbon fraction is removed.

Furthermore, it must be taken in to account that layer present after the de-coting treatment was not firmly attached to the metal and a stamping process easily removes it decreasing even more the amount of impurities charged. A mechanical removal of the de-coated layer is likely to happen also during industrial processes in which scrap is treated in rotary kilns and then moved to storage.

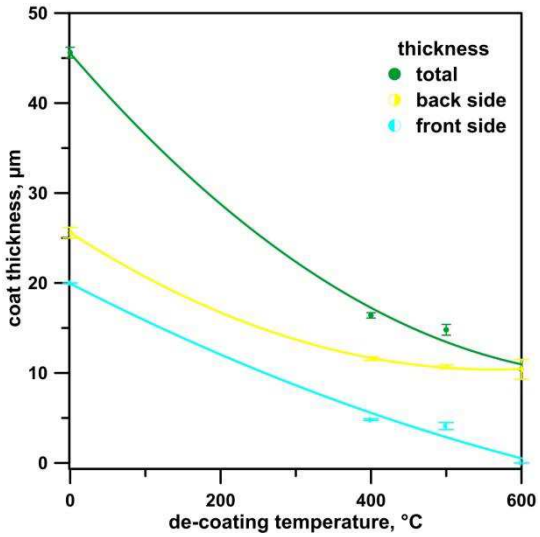

Fig. 4 Evolution of the coating thickness at different de-coating temperatures.

1.2 Effect of de-coating

The discs used for the experiments are reported in Figure 5 to show the initial conditions.

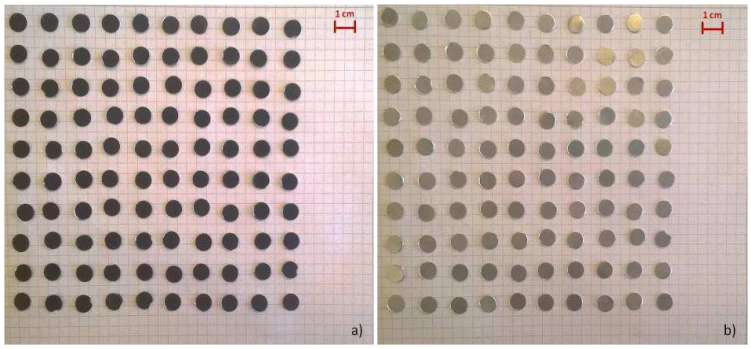

Fig. 5 Hundred discs before the experiment cut of the a) coated and b) uncoated coil

Figure 6 shows representative drops obtained from melting the coated discs not thermally treated as well as after the de-coating treatment. The results obtained from melting the untreated coated discs (Figure 6a) and those de-coated at 400°C (Figure 6b) are similar: at few drops coalescence and some oxidized discs are present. No disc is oxidized if they were de-coated at 500°C and most of them coalesced into bigger drops (Figure 6c). At the highest temperature, 600°C, all the drops coalesced forming a big drop (Figure 6d). This is also seen by the recovered drop of the uncoated discs. (6e)

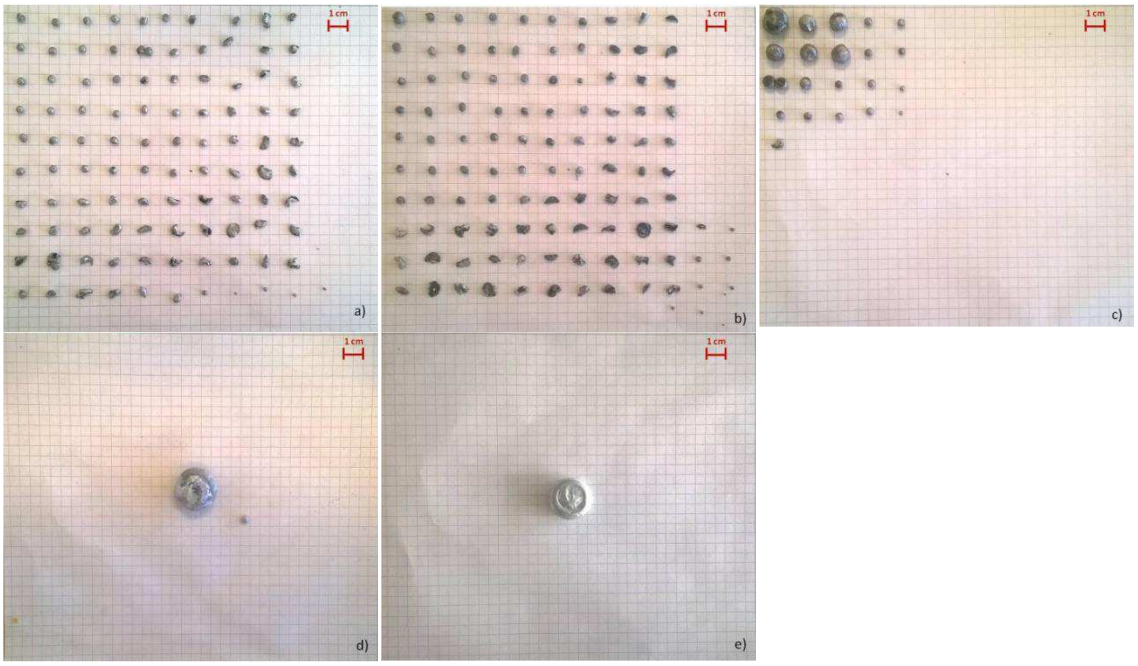

Fig. 6. Drops obtained melting the discs after different de-coating temperature: a) no treatment b) 400°C c) 500°C and d) 600°C and e) recovered drops of uncoated discs.

Figure 7 shows the percentage of spherical drops, average diameter, and CF obtained for all the tested conditions. The fraction of spherical drops is lower than 1 for the coated discs and those de-coated at 400°C, meaning that the scrap burn off took place. A fraction of spherical drops equal to 1 with a null standard deviation were achieved in the other experimental condition, i.e. discs de-coated at 500 and 600°C and uncoated discs. In fact, in all the tests no discs burned in these experimental conditions.

The low average diameter obtained with coated discs and those de-coated at 400°C highlights that the coat prevents drops coalescence. The uncoated discs reached the highest average diameter with no standard deviation as one big drop result in all the replicates. Only a fraction of the discs de-coated at 500°C and at 600°C coalesced. Therefore the average diameter is lower compared to uncoated discs. Better results were achieved with a de-coating at 600°C than at 500°C.

The CF is useful in ranking the response at the different surface condition of the scrap considering both the burn-off rate and the number of coalesced drops. As mentioned before, the uncoated discs reached the highest CF. The high efficiency of the de-coating at 500 and 600°C is evident.

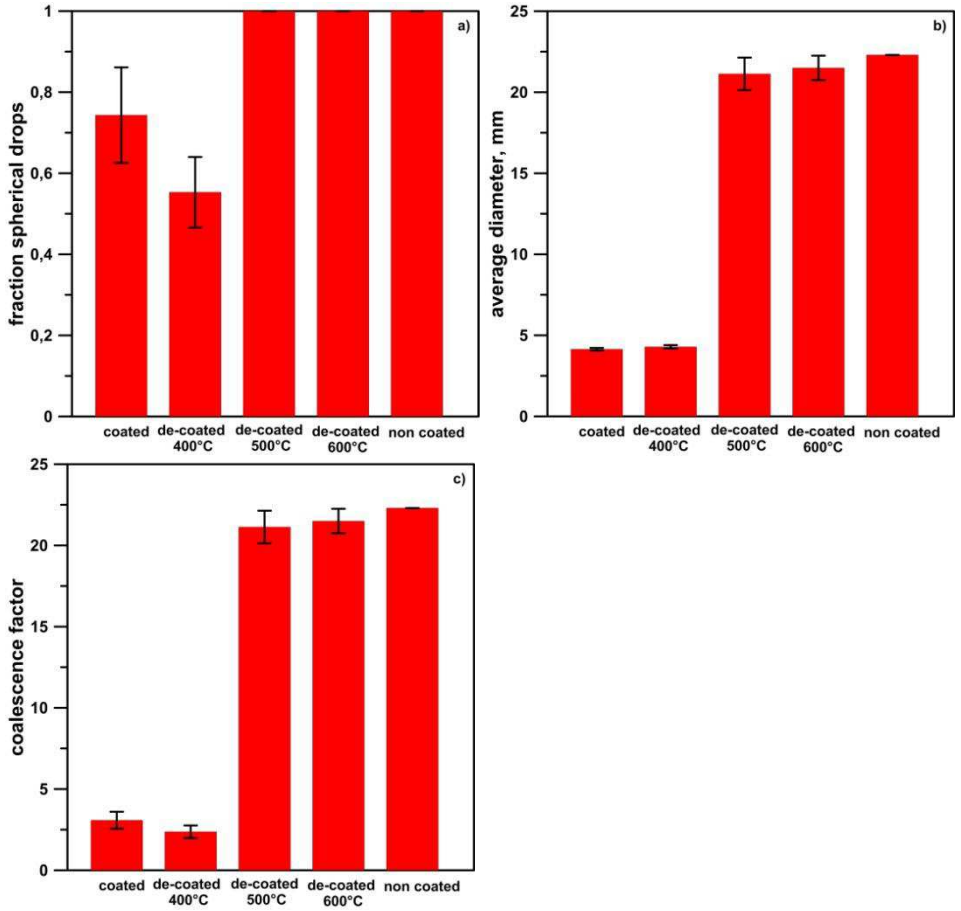

Fig. 7 Coalescence of the drops in terms of (a) fraction of spherical drops, (b) average diameter and (c) CF for the various types of scrap.

3.3 Effect of holding time

The influence of the holding time was tested at 8, 16 and 60 minutes (Figure 8) from melting the coated scrap with no de-coating treatments in the same experimental conditions.

No more coalescence of the drops is achieved by increasing the holding time. This suggests that coalescence takes place during the melting of the discs when they change morphology and break the oxide layer.

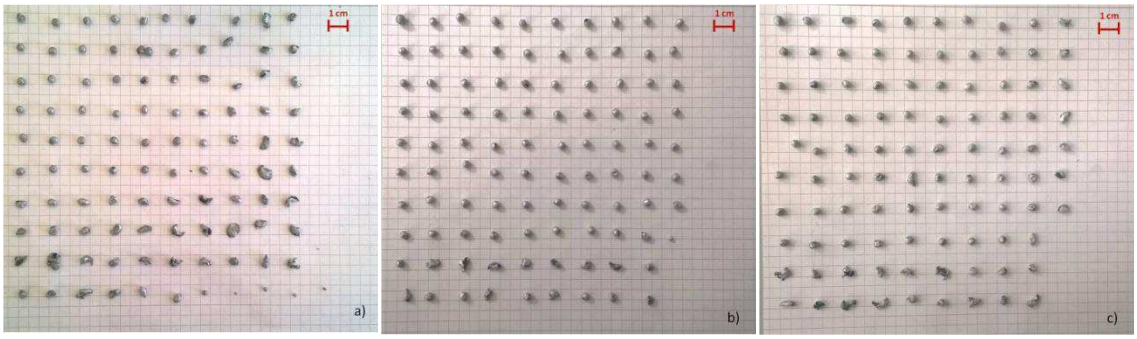

Fig. 8. No coalescence drops obtained melting and for non- treated coated discs at various holding times: a) 8 b) 16 and c) 60 minutes at 790ºC.

4. Conclusions

The effects of the surface coating and the de-coating treatment on aluminium drop coalescence in the salt during the re-melting of AA3000 scrap were investigated. Coalescence of Al drops in salt is measured. The following conclusions can be drawn.

- The coat that covers the scrap surface can hinder the coalescence of the aluminium drops in the molten salt, preventing their recovery.

- A temperature of de-coating equal to 400°C is too low and does not help the drops to coalesce.

- The drop coalescence increases if the combustion reaction temperature is reached in the de-coating treatment.

Acknowledgments

The authors acknowledge finical support from Erasmus, facilities of SFI Metal Production and Hydro Aluminium for providing materials. We would particularly like to thank Erik Vullum (SINTEF) for its support with the SEM micrographs and Eva Maria Gumbmann at Hydro for fruitful discussions.

References

1. I. Tsangaraki-Kaplanoglou, et al., "Effect of Alloy Types on the Electrolytic Coloring Process of Aluminum", *Surface & Coatings Technology,* 200 (2006), 3969-3979.
2. A. A. Tracton, *Coatings Technology Handbook* (6000 Broken Sound Parkway NW, Suite 300 Boca Raton, FL 33487-2742: CRC Press Taylor & Francis Group, 2006).
3. D. Dispinar, A. Kvithyld, and A. Nordmark, "Quality Assesment of Recycled Aluminium", *Light Metals 2011* (2011), 731-735.
4. G. Girard, et al., "Furnace Operation: “A Gold Mine in Your Casthouse”", *Materials Science Forum,* 630 (2010), 77-84.
5. M. A. Rabah, "Preparation of Aluminium–Magnesium Alloys and Some Valuable Salts from Used Beverage Cans", *Waste Managment,* 23 (2003), 173-182.
6. N. Li, and K. Qiu, "Study on Delacquer Used Beverage Cans by Vacuum Pyrolysis for Recycle", *Environmental Science & Technology,* 47 (2013), 11734-11738.
7. A. Kvithyld, et al., "Recycling Light Metals: Optimal Thermal De-Coating", *JOM,* 60 (2008), 47-51.
8. P. N. Crepeau, M. L. Fenyes, and L. J. Jeanneret, "Solid Fluxing Practices for Aluminum Melting (Part 1)", *Modern casting,* 82 (1992), 28-30.
9. R. D. Peterson, *Effect of Salt Flux Additives on Aluminum Droplets Coalescence*, *Second International Symposium-Recycling of Metals and Engineered Materials* (TMS: The Minerals, Metals & Materials Society, 1990), 69-84.
10. R. R. Roy, and Y. Sahai, "Coalescence Behaviour of Aluminum Alloy Drops in Molten Salts", *Materials Transactions,* 38 (1997), 995-1003.
11. A. Sydykov, B. Friedrich, and A. Arnold, 'Impact of Parameter Changes on the Aluminum Recovery in a Rotary Kiln', in *Light Metals 2002*, ed. by Wolfgang Schneider (TMS: The Minerals, Metals & Materials Society, 2002), 1045-1052.
12. Y.-S. Kim, et al., "Effects of Salt Flux and Alloying Elements on the Coalescence Behaviour of Aluminum Droplets", *Journal of Korea Foundry Society,* 20 (2000), 39-45.

13. S. Besson, et al., "Improving Coalescence in Al-Recycling by Salt Optimization" (Paper presented at the *European metallurgical conference 2011*,Dusseldorf, 2011), pp. 1-16.
14. M. Thoraval, and B. Friedrich, "Metal Entrapment in Slag During the Aluminium Recycling Process in Tilting Rotary Furnace" (Paper presented at the *European Metallurgical Conference 2015*,Dusseldorf, 2015), pp. 359-367.

ARTICLE 5

COALESCENCE OF CLEAN, COATED AND DE-COATED ALUMINIUM FOR VARIOUS SALTS AND SALT-SCRAP RATIOs

Stefano Capuzzi[1], Anne Kvithyld[2], Giulio Timelli[1], Arne Nordmark[2], Eva Gumbmann[3], Thorvald Abel Engh[4]

[1]Department. of Management and Engineering-DTG
University of Padua
36100 Vicenza
ITALY

[2]SINTEF
N-7465 Trondheim
NORWAY

[3]HYDRO
N-3080 Holmestrand
NORWAY

[3]NTNU
N-7465 Trondheim
NORWAY

Submitted for publication in: Journal of Sustainable Metallurgy

Abstract

In a rotary furnace for aluminium recycling and dross treatment, a salt flux covers the molten metal to prevent new oxidation and to capture oxides and impurities contained in the scrap. Furthermore, the salt has to promote the coalescence of the metal drops entrapped in the dross.

This work investigates the coalescence of aluminium droplets with different impurity contents in salt fluxes with various compositions, namely 1) Cryolite salt 2) Industrial salt and 3) Recycled salt.

The scrap was stamped out from AA3000 foil with and without coating in the form of discs. Thermal de-coating treatments at various temperatures, i.e. 400, 500 and 600 ºC were performed to reduce the amount of impurities on the scrap surface. CaF_2 was added to the Industrial and to the Recycled salt while Na_3AlF_6 was present in the Cryolite salt. The amounts of salt ranged from 0 to 4 times the amount of the scrap.

Hundred discs, covered by molten flux, were melted in a ceramic crucible placed in an induction furnace at 790°C. The fraction of coalesced drops and their average diameters were determined in order to evaluate coalescence efficiency. A coalescence factor was defined, ranging from zero (no coalescence) to more than 20 (all drops coalesce to one big drop).

The coalescence behaviour is negatively affected by the coating but a suitable de-coating treatment and fluxing can give the coalescence of the aluminium drops. The drops do not coalesce if coated scrap is melted in various CaF_2 salts while a complete coalescence is attained melting the clean discs cryolite containing salt, giving a coalescence factor of 21. The same result is obtained if coated discs are de-coated at a temperature higher than the combustion temperature of the coating, i.e. 600°C. Industrial salt gives a coalescence factor lower than 3, while Recycled salt gives a coalescence factor of 4. No positive effects are obtained adding CaF_2 amounts ranging between 2wt.% and 6wt.%.

Keywords: aluminum alloy scrap, salt flux, coalescence, de-coating, recycling

Graphical Abstract

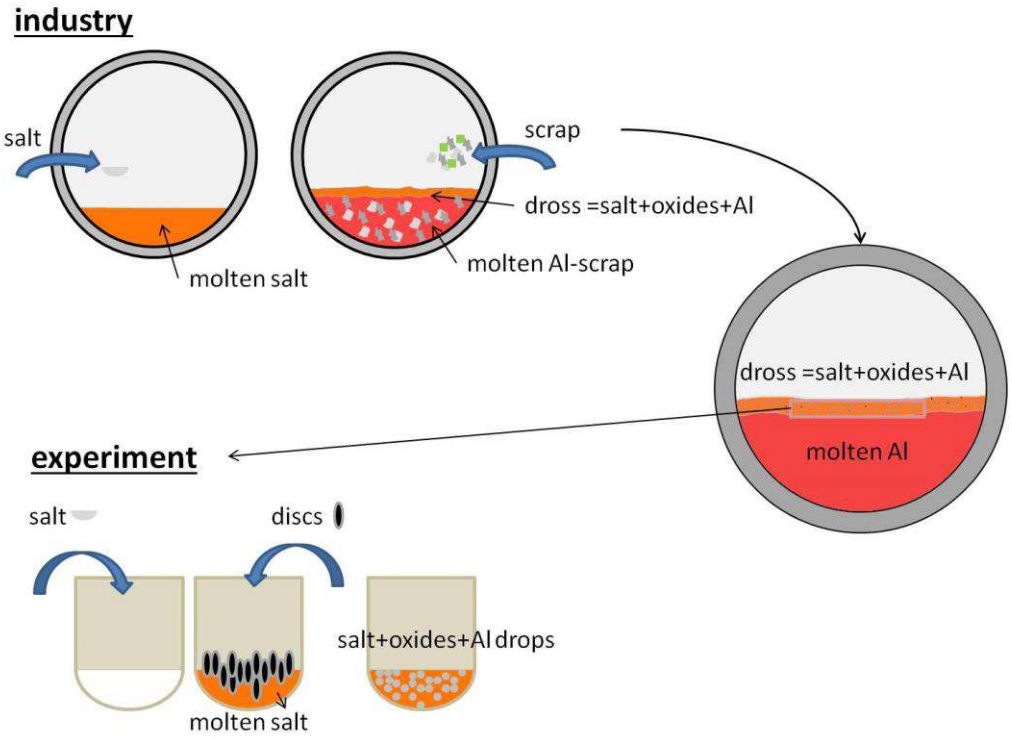

Introduction

Aluminium can be obtained from mined material, i.e. the bauxite ore is trated first into alumina (Bayer process) and then, through the Hall Héroult electrolytic process, into primary aluminium. As an alternative source of raw material, aluminium can be produced from metal scrap. The aluminium scrap destined for recycling can be divided into two categories: new scrap from in-plant working and handling of the aluminum, and old scrap, aluminum material from already produced aluminum goods, which have been used and discarded at the end of their useful life [1].

The old scrap comes from a great variety of goods, like used beverage cans (UBCs), automotive components or radiators and can be divided into various categories according to the standard EN 13920 [2]. Heterogeneity and presence of different impurities are the main characteristics of this type of scrap and the greatest challenge for the smelters.

The surface of the aluminium scrap is always covered by an oxide layer due to the high affinity between aluminium and oxygen. Various surface treatments can be performed to improve the quality of the aluminium goods. Anodizing is usually performed to increase the oxide layer, giving greater resistance to corrosion and aesthetic advantages [3, 4]. Paints have also been applied for the same reasons [5].

Coatings improve the properties and the value of the goods, nevertheless they are considered as surface contaminations during re-melting of the aluminium scrap, lowering its quality. The scrap quality affects the burn-off rate, defined as the percentage of metal content of the scrap which is converted inside the furnace into oxide [6].

The aluminium metal reacts with the surface layer and oxygen. Scrap burn-off, generates a large quantity of heat and increases the metal loss [7, 8]. Kvithyld, et al. [9] highlighted a significant decrease in the metal quality between remelting clean and coated aluminium in term of different bi-film contents.

Various techniques have been proposed to de-coat aluminium scrap. Rabah [10] and Wang, et al. [11] studied the efficiency of different chemical agents, while vacuum pyrolisis is proposed by Li and Qiu [12]. However, the conventional thermal process in rotary kilns is largely the most used. Hot gas flows through the kiln under controlled conditions of temperature and oxygen content. The kiln outflow gas is combusted an afterburner. A significant proportion of the combustion products recirculated to the kiln. The aim of the thermal de-coating process is to combust all the carbonized material without oxidizing the metal. Firstly, scission phase occurs during which the coating decomposes, releasing hydrocarbons and leaving pigment/fillers/carbon residues. Then, the residual carbon reacts with the oxygen, generating CO, CO_2 and heat and leaving on the surface inorganic pigment and filler particle [13].

De-coating removes the organic fraction of the layers that cover the scrap, but oxides and other impurities still affect the scrap quality. Therefore, especially when the scrap quality is low, fluxing is necessary. The flux is composed of salts; sodium and potassium chlorides are commonly used due to their low cost and their low melting point [14]. Sodium chloride is cheaper, while the addition of potassium chloride decreases the viscosity and the surface tension, increasing the fluidity. The mixture of salts protects the molten bath from oxidation and collects oxides and impurities present in the charged scrap, forming a slag. However, molten metal and oxides are entrapped in this slag, whose density and viscosity increase with increasing the amount of oxides. This may prevent salt/metal separation and as a result a non-negligible portion of metal remains in the salt in the form of aluminum drops.

The ability of the flux to enhance the coalescence of these drops becomes a key factor in metal recovery. The entrapped aluminium has to settle down to the molten bath to be recovered; the settling velocity of the drops increases if their size increases. Most of the studies on the aluminium drops coalescence in the molten flux focus on comparison of different additions in a NaCl-KCl mixture.

Fluorides are suggested as the most effective, while addition of other chlorides, like $MgCl_2$ or $CaCl_2$, does not seem to encourage coalescence [15]. Roy and Sahai [16] studied the coalescence of aluminium drops melting pure aluminium and used beverage containers (UBCs). They classified the fluxes into four coalescence categories of additions: from poor, when no fluorides were added, to excellent in case of NaF, KF, LiF and Na_3AlF_6 additions. The effectiveness of the fluorides on the coalescence was confirmed by Kim, et al. [17] and Besson, et al. [18], who also highlighted the negative effect of the presence of Mg in the scrap. Thoraval and Friedrich [19] studied the coalescence of aluminium drops in a salt flux with addition of non-metallic compounds (NMCs) to simulate the working condition in the presence of oxides and other impurities. The results show that impurities worsen drop coalescence.

In order to characterize the negative effect of the oxides, in the industrial process, the amount of salt required can be related to the quantity of the scrap charged by the salt factor, which is the ratio between the non-aluminum content in the scrap and the quantity of the salt required. A mass balance model for refiners in Europe fixes the main level of this factor to 1.3 [20]. In the development of aluminium recycling processes in fixed axis rotary furnaces, greater salt factors ranging from 1.5 to almost 2 are used, and a value of 1.8 is an often published value [21]. The amount of salt can be reduced with tilting rotary furnaces where the salt factor can be lower than 0.5.

The charging sequence plays another important role in reducing the metal loss. It is important to rapidly submerge the scrap under the molten salt to prevent oxidation of the scrap. Density, size and morphology of the scrap become very important. In an industrial furnace to minimize the aluminium oxidation, and consequently the melt loss, the scrap may be charged as high density bales, loosely packed bales, or as dry shredded scrap that is continuously fed from a conveyor [22].

The aim of this work is to describe the coalescence of the aluminium drops using different fluxes in various amounts for melting scrap for several levels of surface contaminants.

Experimental procedure

Material:

The scrap was cut out from AA3000 coil (Table 1) with and without coat in the form of discs with a radius equal to 4 mm and a height of 0.5 mm.

Table 1. Chemical composition of the experimental alloy (wt.%).

Alloy	Si	Fe	Cu	Mn	Mg	Cr	Ni	Pb	Zn	Ti
AA3xxx	0.53	0.58	0.20	0.68	0.34	0.02	0.01	0.01	0.23	0.02

The coated coils were anodized and covered by two painted layers. The initial priming coat, composed of a white polyester lacquer, was the same on both sides of the coils, while the second layer was different on the front and the back side. The front side was covered by a black polyurethane lacquer while the coating of the back side was polyester with a grey pigment. The surfaces of the clean and coated discs, as well as the

thickness of the different coatings, have been investigated by Scanning Electron Microscope (SEM).

The salts:

Three different salts were tested, namely Industrial, Recycled and Cryolite. The latter is used on laboratory scale while the other two are currently used industrially. The Recycled salt has been regenerated from a salt cake. The Industrial and Recycled salts were investigated with the addition of CaF_2 in 2 wt.% and 6wt.% while 2wt.% of Na_3AlF_6 was added in the Cryolite salt.

The three salts were mainly composed of a mixture of NaCl-KCl and the concentration of the other elements was studied by means of ICP-MS analysis. The composition of the Industrial and the Recycled salts were analysed before the CaF_2 addition while the Cryolite already contained Na_3AlF_6.

The amount of salt, under which the scrap was melted, was established by means of the salt-scrap ratio, i.e. the ratio between the quantity of salt and the quantity of scrap charged.

Thermal treatment and melting method:

Differential scanning calorimetry (DSC) analysis was performed to determine the scission and combustion temperatures of the coat. The two sides of the coat were studied individually. A plate 3x2 mm was cut off the coil and the coating of the non-investigated side was mechanically removed with a grinder pan. The tests were carried out in air atmosphere. The cell was heated up to 630°C at 10 °C/min-1 and then kept at this temperature for 5 min before cooling to room temperature at the same rate. An experiment with a plate completely mechanically de-coated was used as blank to reduce the influence of oxidation on the results.

The thermal treatments were performed in an electric resistance furnace; the temperatures tested were 400, 500 and 600 °C with a heating rate of 10 °C/min. The coils were placed obliquely. The slanting orientation of the coils is intended to avoid contact of the surfaces with the furnace. The back side was the upper side for all the treatments.

The coalescence tests were carried out at 790°C in an electric induction furnace. Hundred discs were charged after melting of the flux. After the experiment, the crucible was carefully taken out of the furnace and cooled in air. The solidified slag was leached in water and the solidified drops were dried and sieved.

Results analysis:

A Matlab code was employed to evaluate the morphology of the drops in terms of roundness and aspect radio and to calculate the area and the equivalent diameter of the projection of the drops.

The aspect radio denotes the ratio of the major axis to the minor axis and it is equal to 1 in the case of circles and squares. The roundness is equal to 1 only for the circles and it is defined as follows:

$$roundness = \frac{p^2}{4*\pi*A} \qquad \text{Equation 2}$$

Here p and A are the perimeter and the area of the projection of the drops.

A spherical drop obtained from a single disc has a diameter equal to 3.6 mm therefore only the drops whose equivalent diameter was greater than 3.6 mm were considered. Moreover, the drops were taken as spherical only if they had roundness greater than 0.85 and aspect ratio lower than 1.25.

Figure 1 shows the drops obtained melting the discs (Figure 1a) and the consequent image binarization (Figure 1b) to calculate the morphological and dimensional characteristics by means of Matlab code (Figure 1c). A spherical drop and a no spherical drop were indicated by a blue rectangle and a green ellipse, respectively.

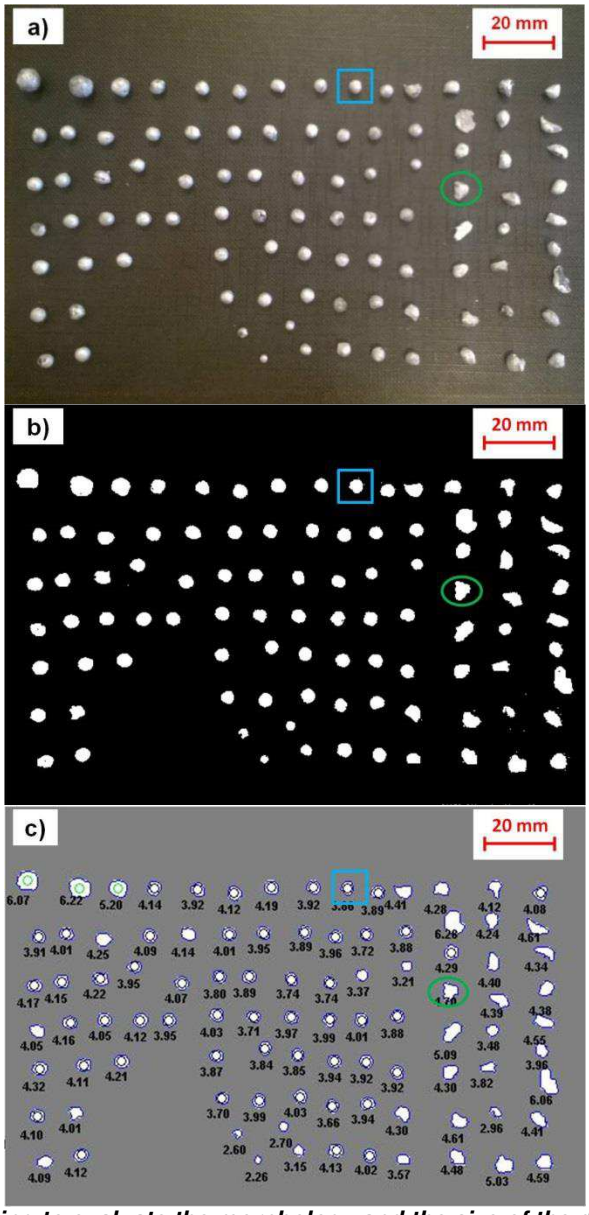

Figure 1: Image processing to evaluate the morphology and the size of the drops: (a) the initial image of the drops was (b) binarized and (c) the parameters were calculated through the Matlab code. In figure c the diameter is shown and a spherical drop and a no spherical drop are highlighted in blue and green respectively

One big sphere is the best obtainable result since it means that a complete coalescence of all the discs has occurred. Two features were considered to evaluate the coalescence: the average diameter of the spherical drops and the ratio between the number of spherical drops and the number of all the drops. A coalescence factor was defined as follows:

$$CF = \underline{d} * \frac{N_b}{N_d} \qquad \text{Equation 3}$$

Here $\underline{d}$ is the average diameter of the drops with spherical form, N_b is the number of the drops with spherical form, and N_d is the number of all the drops.

Experimental matrix:

The experimental procedure describe above was used to perform two designs of experiment (DoE). In the first DoE, the three experimental salts, melting coated and clean scrap with a salt-scrap ratio equal to 2, were compared in terms of favouring the drops coalescence. The Industrial and Recycled salts were also tested increasing the quantity of CaF_2 from 2% to 6% (Table 2).

Table 2. Factor investigated and relative levels in the DoE for salts comparison

Variable	Levels		
Salts	Industrial	Recycled	Industrial
CaF_2 amount (wt.%)	2	6	
Surface coating	Clean	Coated	

In the second DoE, the Cryolite salt was used to study the influence on the Al drops coalescence of the de-coating process temperature and salt-scrap ratio. The investigated levels of de-coating temperature and salt-scrap ratio are reported in Table 3

Table 3. Factors investigated in the DoE concerning the influence of de-coating and salt-scrap ratio

Variable	Levels				
Salts-scrap ratio	0	0.5	2	4	
Surface coating	Coated	De-coated at 400°C	De-coated at 500°C	De-coated at 600°C	Clean

Each condition was studied after a holding time of 8 minutes and repeated 3 times.

Statistical Analysis

The Kruskal-Wallis test was implemented to assess the influence of the de-coating temperature and the amount of salt on the Al drop coalescence. The same distribution was assumed for the results of each level, i.e. the different de-coating temperatures and the various salt scrap ratios. The homoscedasticity was verified with the Levine test. The Kruskal-Wallis test is the nonparametric equivalent of the Analysis of Variance (ANOVA), and it tests the null hypothesis that samples in two or more groups are drawn from populations with the same mean values.

The null hypothesis tested was that the results obtained with the various levels of de-coating temperature and salt-scrap ratio do not differ, i.e. the Al drops coalescence is not influenced by this two variables. The null hypothesis is rejected for a p-value less the α-level, assumed as usual equal to 0.5.

Results and discussion

Scrap characterisation, coating

The oxide layer that covered the clean discs had a thickness ranging from about 20 to 40 nm, while the thickness of the oxide on the coated discs was greater, up to 300nm, as highlighted in Figures 2a-b. This thickening of the oxide layer is due to an anodization process applied before the painting.

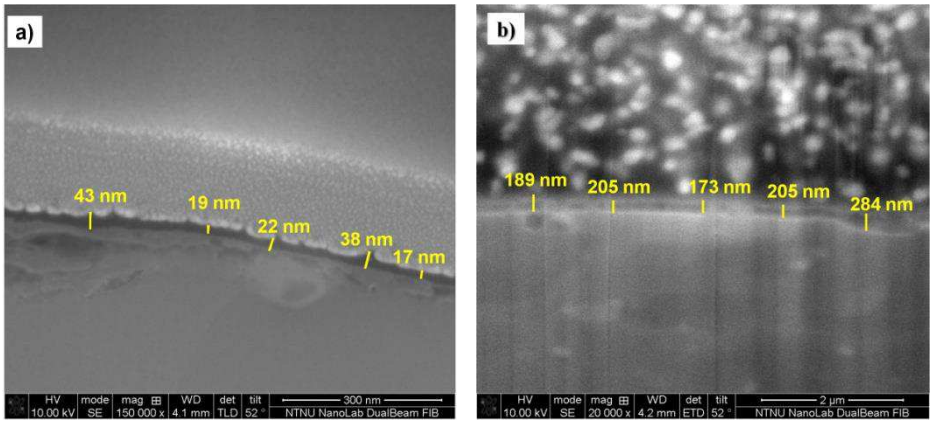

Figure 2: Scanning Electron microscope micrographs of the oxides that cover the (a) clean and (b) coated coils

The front and the back sides of the coated coils were covered by two different layers. The primer coat was the same for both sides and a thickness ranging from 4 to 5 µm was measured. The second coating was also due to painting but different paints were applied depending on the side. The black front side was 5 µm thinner than the back side that was covered by a gray pigment. The total thickness of the layers was 20 µm and 25 µm, respectively (Figure 3a-b). Figures 3c,d show the initial surface conditions for the front and back side, respectively.

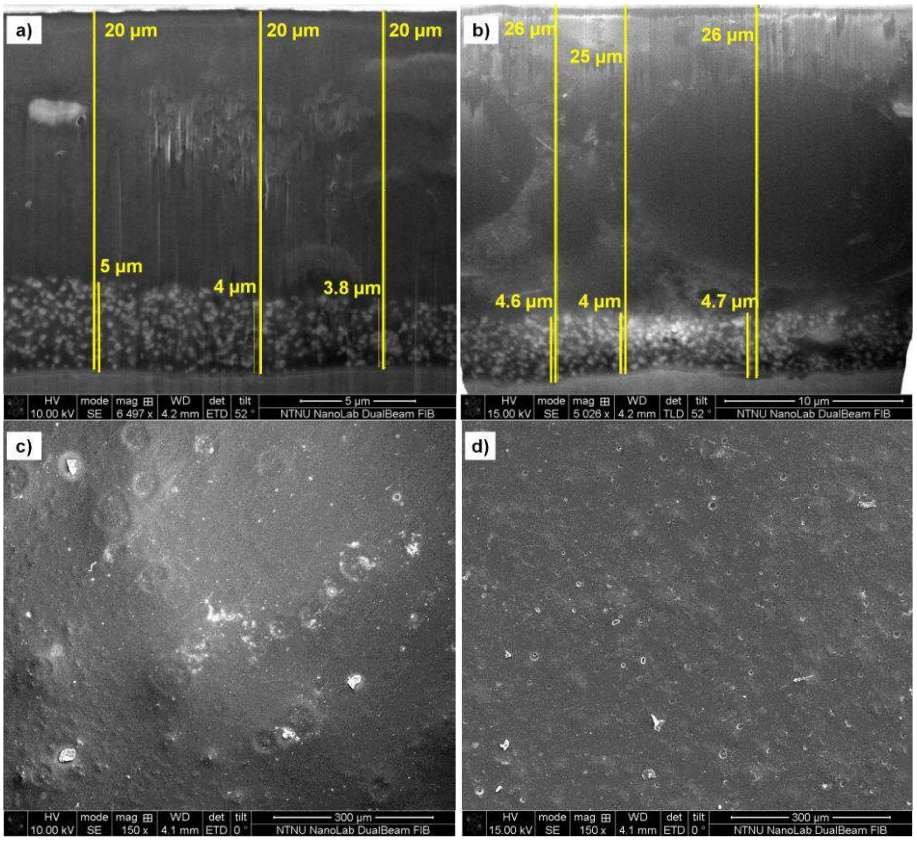

Figure 3. Scanning Electron microscope micrographs of the coating layers of the (a) front side and (b) back side of the coated samples The surface micrographs (c-d) for both sides are also reported.

Figure 4 shows the discs used in the experiments. The hundred discs are here arranged to form a 10x10 square. The drops obtained during the tests were placed in the same manner to facilitate the comparison.

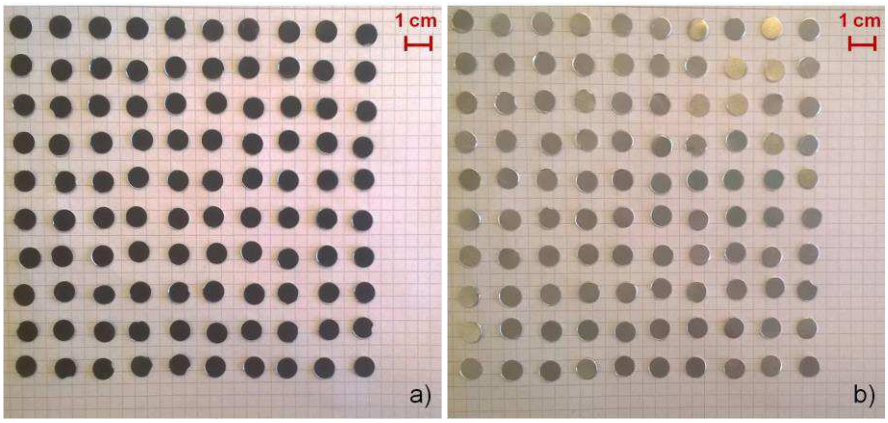

Figure 4. Hundred discs cut off from the a) coated and b) clean coil and used in the experiment

Salt characterisation

The concentrations of the main elements present in the experimental salts are reported in Table 4. The ICP-MS technique is not able to detect the Cl and the F, therefore these elements are not shown even though certainly present in the flux.

Table 4. Concentration of the main elements in the experimental salts measured by means of ICP-MS analysis

		Na	Mg	Al	Si	P	S	K	Ca
Industrial	µg/g	325525	794	14.3	3.8	0.6	4754	94281	922.4
	%	76.36	0.19	0	0	0	1.12	22.11	0.22
Recycled	µg/g	248056	249	5.176	1181	48.7	1182	203495	168.3
	%	53.98	0.05	1.13	0.26	0.01	0.26	44.27	0.04
Cryolite	µg/g	254798	47	576	9.5	0.6	67.1	184156	150.3
	%	57.93	0.01	0.13	0	0	0.02	41.87	0.03

The Recycled salt contained a larger amount of foreign elements than the other two salts. Si and P were detected only in this salt and also the quantity of Al was higher. This result was to be expected since the Recycled salt come from a production cycle where it treated scrap containing these elements. The Al fraction in the Cryolite salt is partly due to the presence of the cryolite, i.e. Na_3AlF_6, in the flux. The Industrial salt contained a larger amount of Mg and Ca; the latter can be associated to the presence of CaF_2 in the mixture.

The fraction of S in the Industrial salt is 4 times higher than found in the Recycled salt while in Cryolite salt only traces of this element were detected.

It is assumed that the Cl is present only in the form of NaCl and KCl. An equal molar concentration between Cl and the elements in the salt is assumed. The concentration of Cl in µg/g was obtained as product between its calculated molar concentration and its molar mass. The calculated mass ratios between NaCl and KCl were are 82-18, 62-38, 65-35 for the Industrial, the Recycled and the Cryolite salts respectively.

Influence of the charging sequence

Preliminary tests were performed to investigate if the charging sequence would have affected the coalescence results. The discs were charged with the salt in the first charging sequence while the salt was melted before charging the discs in the second one.

One big spherical drop was obtained melting the clean discs in both cases as shown in Figure 5. The tests were stopped after 8 minutes, even though complete coalescence was obtained for shorter times. Four minutes instead two minutes, were necessary to melt the salt with the scrap; probably this difference was related to the melting of the salt.

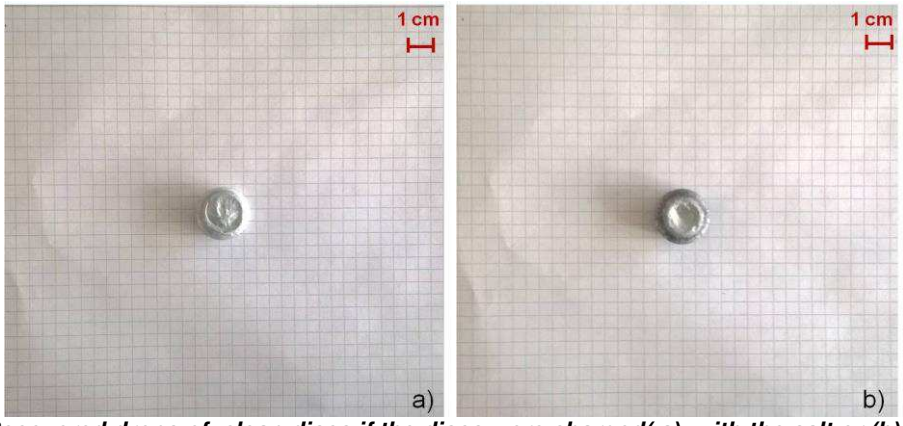

Figure 5. Recovered drops of clean discs if the discs were charged(a) with the salt or (b) in the molten salt

Less favourable results were obtained for the coated scrap if charged when the salt was not already molten (Figure 6a). The coated discs did not coalesce in any case, but they partly formed spherical drops melting inside the molten flux (Figure 6b).

The coat burned before the melting of the scrap and locally generated an increase of the temperature that gave a higher oxidation of the.

The results obtained for the different charging sequences support the industrial importance of submerging the scrap in the molten salt. Salt cannot prevent oxidation of the coated scrap if they are charged together.

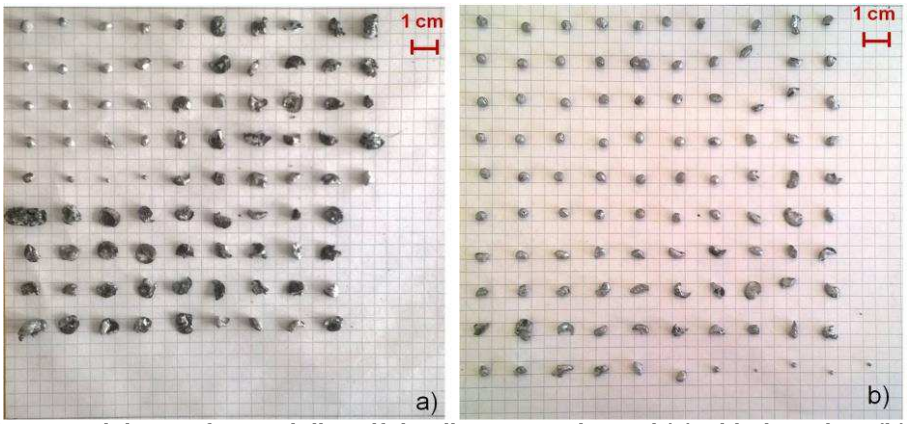

Figure 6. ***Recovered drops of coated discs if the discs were charged (a) with the salt or (b) in the molten salt***

Coalescence of clean discs with various salts

The drops obtained melting the clean discs under the different salts are compared in Figure 8. The scrap was covered only by the natural oxide layer, but coalescence did not take place when Industrial and Recycled salts with the 2 wt.% of CaF_2 were used. However, Cryolite salt allowed complete coalescence of the discs to one big sphere. The holding time in the molten flux was 8 minutes for all the experiments. Coalescence with Cryolite salt took place during the first 4 minutes

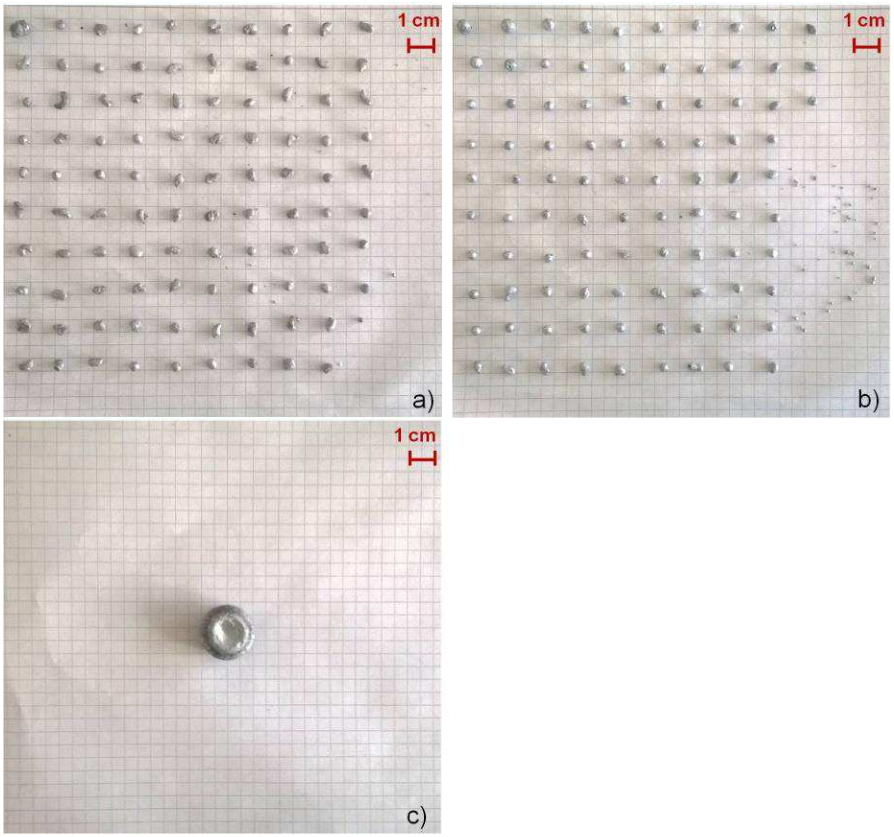

Figure 7: Recovered drops of clean discs when melted under different flux: (a) Industrial, (b) Recycled and (c) Cryolite

The results achieved with the Industrial and Recycled salts increasing the quantity of CaF_2 up to 6 wt.% are shown in Figure 8. No coalescence of the aluminium drops was measuered.

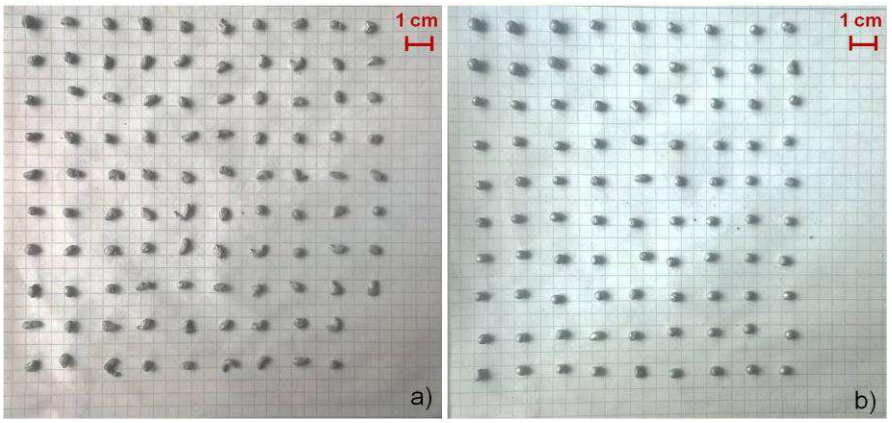

Figure 8: Effects of the 6 wt.% addition of CaF_2 on the drops coalescence from melting the clean discs under the (a) Industrial and the (b) Recycled salts.

The coat affected the coalescence of the Al drops using all the experimental fluxes (Figure 9). Coalescence was completely prevented using Industrial and Recycled salts but also the coalescence the Cryolite salt was strongly reduced.

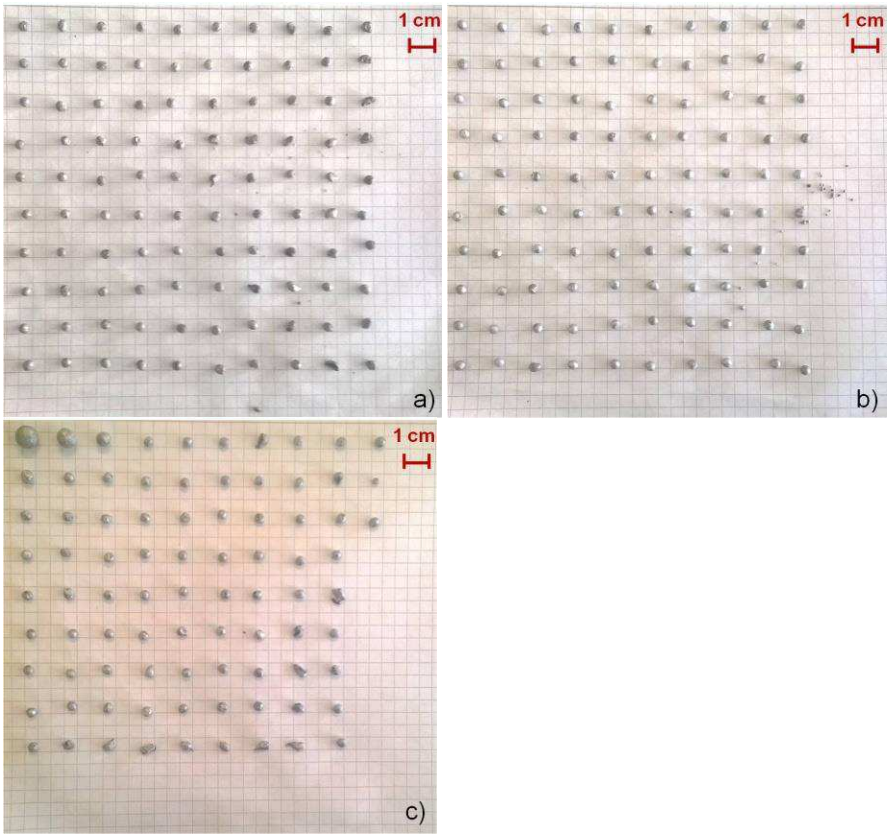

Figure 9: Recovered drops of coated discs when melted under different flux: (a) Industrial, (b) Recycled and (c) Cryolite

Figure 10 highlights that the addition of more CaF_2 in the Industrial and Recycled salts had no effect on the results as observed for the clean discs.

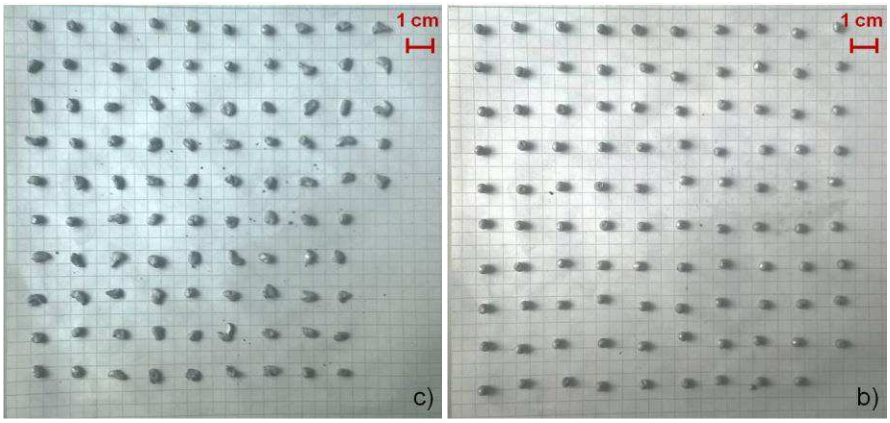

Figure 10: Effects of the 6 wt.% addition of CaF_2 on the drops coalescence from melting the coated discs under the (a) Industrial and the (b) Recycled salts.

Effect of the amount of salt

The effect of the amount of salt was investigated melting the coated and the clean discs under the Cryolite flux with various salt-scrap ratios.

The discs, both coated and clean, completely oxidized if no salt was used (Figure 10a-b) that is in agreement with the results obtained charging the salt together with the scrap. A molten flux is necessary when the scrap is melted in an oxygen rich atmosphere.

For the lower amount of salt studied, i.e. an amount of salt equal to half the amount of the scrap, a complete coalescence of the clean discs was achieved (Figure 11c) while a

fraction of the coated discs oxidized (Figure 11d). Increasing the salt-scrap ratio up to 2, the clean discs coalesced in one big drop as seen before (Figure 11e) and spherical or semi-spherical drops were obtained from the coated discs but none of them coalesced in a big single drop (Figure 11f).

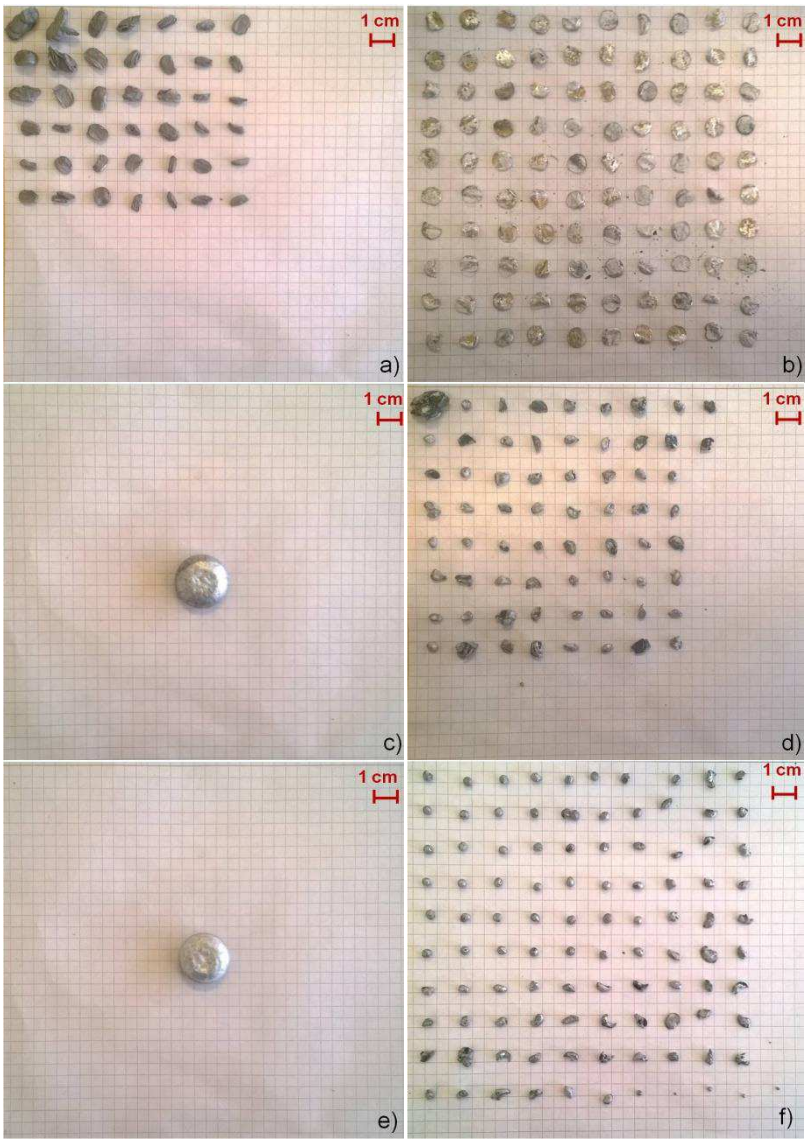

Figure 11: Recovered drops of (left)clean and (right)coated discs melted under Cryolite flux with different salt-scrap ratio: (a,b) 0, (c,d) 0.5 and (e,f) 2

Effects of the de-coating on the discs surface and on their coalescence

The temperature intervals of the reactions that occur during the de-coating treatment were measured by means of DSC analysis (Figure 12). Two peaks were revealed corresponding to the endothermic reaction due to the decomposition of the coating and to the exothermic reaction due to the combustion of the carbon residuals. This latter reaction, in particular, with an heating rate equal to 10 K/min started at 398°C and ended at 552°C, while the peak temperature was at 441°C.

The experimental de-coating temperatures for the coalescence test, i.e. 400, 500 and 600°C , are at the beginning, in the middle and at the end of the combustion reaction, respectively.

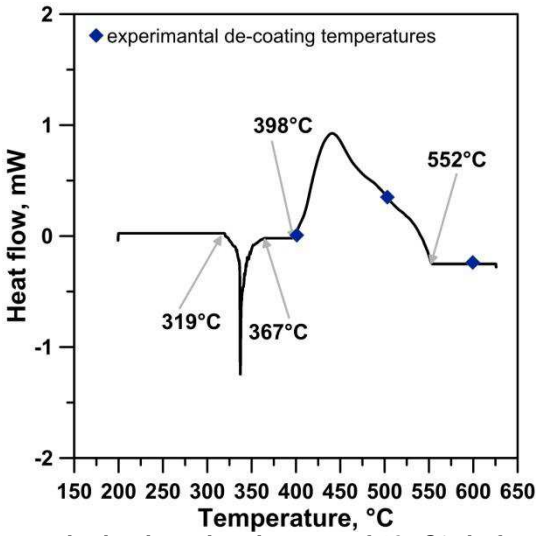

Figure 12: DSC curve obtained at a heating rate of 10 °C/min for the coated coil. The blue diamonds highlight the experimental de-coating temperatures.

The coating found layers in response for the various de-coating treatments is shown in Figure 13. On both sides, the thickness of the painted layers already decreased at the lowest temperature, i.e. 400°C, and a greater effect was obtained on the front side.

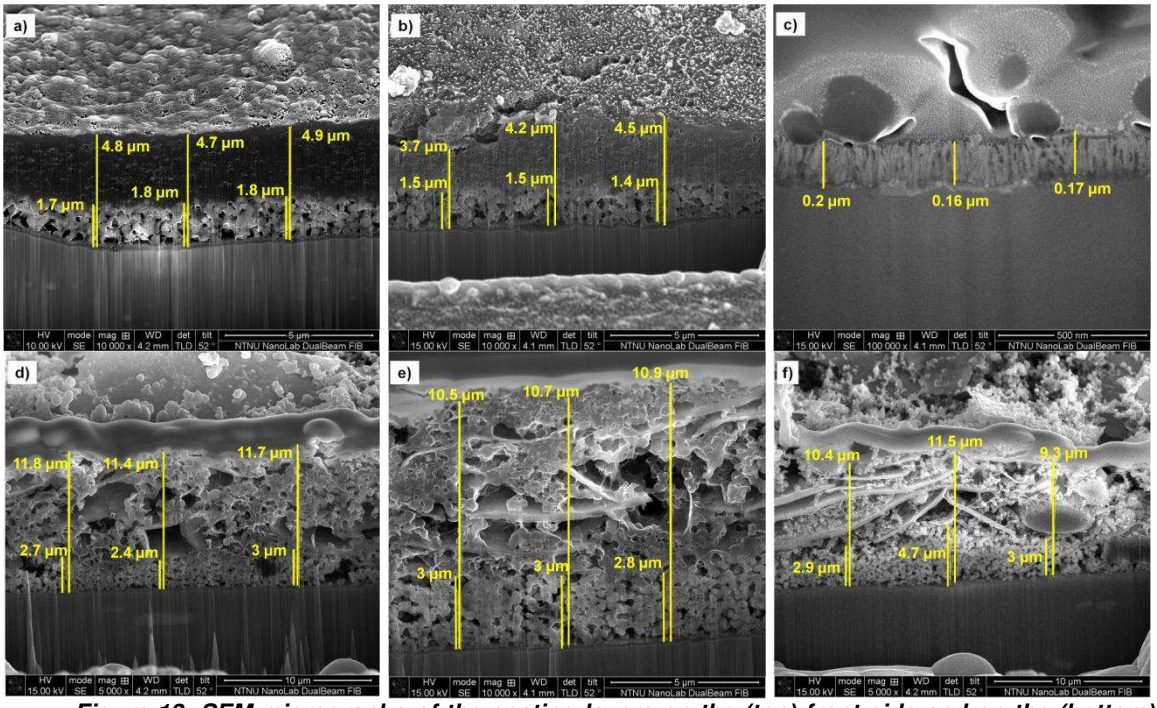

Figure 13: SEM micrographs of the coating layers on the (top) front side and on the (bottom) back side after the different de-coating treatments: (a,d) 400°C, (b,e) 500°C and (c,f) 600°C

The thickness of the coat on the front side decreased from 20 µm to less than 5 µm, but both layers appeared to be compact (Figure 13a). The thickness reduction was more evident increasing the temperature (Figure 13b) and at the highest temperature only the oxide layer remained (Figure 13c). These results are in accordance with the reaction temperature obtained by the DSC analysis whereby it is necessary to reach 552°C to remove the organic fraction. On the front side, de-coating affected both painted layers, while the initial primary coating did not significantly change on the back side. Here also the reduction of the thickness of the coat was similar for the de-coating temperatures

(Figure 13 d,e), and a covering layer was still present even if the coil was heated at 600°C (Figure 13f). The thermal de-coating process could remove only the organic compounds present in the coats, so the different results relate to the different inorganic fractions in the paints.

Figure 14 shows different responses of the two sides to the de-coating treatments, considering the surfaces of the coats. As previously seen, the coat degradation is more evident on the front side. Carbon compounds are visible on the surface at the lowest temperature (Figure 14a) while they were removed at temperature of 500°C (Figure 14b). The aluminum surface with the milling marks (rolling stripes) can be seen when de-coated at the highest temperature (Figure 14c). No clear variation in the surface of the grey side can be noticed comparing the experimental conditions (Figures 14 d-f).

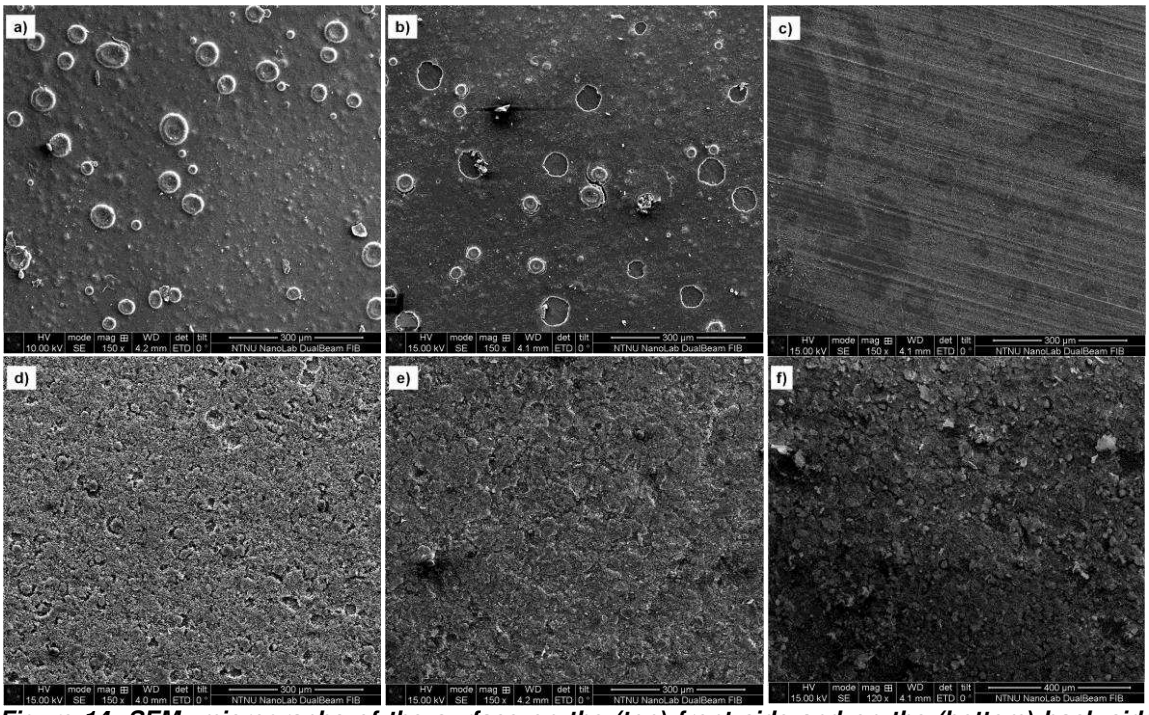

Figure 14: SEM micrographs of the surface on the (top) front side and on the (bottom) back side after the different de-coating treatments: (a,d) 400°C, (b,e) 500°C and (c,f) 600°C

A high temperature de-coating gives increased coalescence. The effectiveness of the de-coating treatment in increasing the coalescence behaviour of the Al drops strongly depends on the de-coating temperature as shown in Figure 15. The experiment performed melting the discs de-coated at 400°C resulted in drops similar to those obtained with coated discs for all the salt-scrap ratios tested. According to the DSC results, at 400°C the decomposition takes place but combustion does not. The organic fraction of the coat is partially removed when the discs are de-coated at 500°C and a greater coalescence was reached in particular using the highest salt-scrap ratios. A lower amount of salt is sufficient to favour the drops coalescence for the de-coating performed at 600°C. This last temperature is the only one higher the measured temperature necessary to complete the combustion reaction, i.e. 552°C.

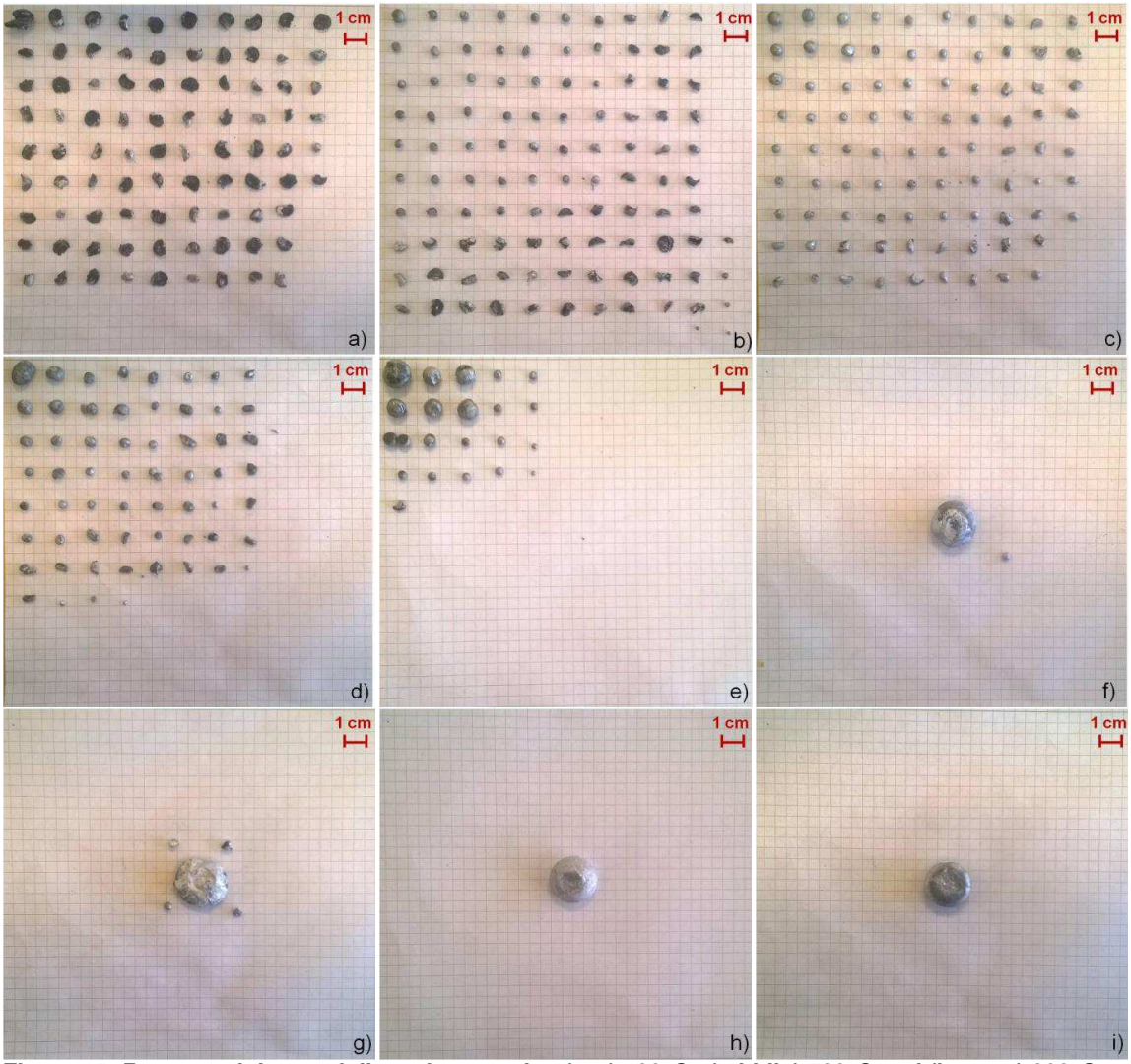

Figure 15: Recovered drops of discs de-coated at (top) 400°C, (middle) 500°C and (bottom) 600°C melted under the Cryolite flux with different salt-scrap ratio: (a,d,g) 0.5, (b,e,h) 2 and (c,f,i) 4

Discussion

The spherical shape minimizes the surface-volume ratio; thus when a disc melts it tends to become spherical. The oxide layer is an obstacle to this. The surface-volume ratio is higher for two drops than for a bigger drop with the same volume. In Table 5 the surface-volume ratio is calculated in the case of 1 disc, a drop obtained from 1 disc and one obtained from 100 discs to a single big drop resulting from 100 discs

Table 5. Surface, volume and their ratio for one disc, a drop obtained melting 1 disc and a drop obtained melting 100 discs.

Element	Surface (S), mm^2	Volume (V), mm^3	S/V ratio
1 disc	113	25	4.52
drop from 1 disc	40	25	1.6
drop from 100 discs	890	2500	0.36

The aluminium drops can coalesce only if the flux can release the metal from the oxide layer. Figure 16 shows the ranking of the various fluxes in terms of CF from melting coated and clean discs. Cryolite is the most effective salt when clean discs are

melted as it allows the coalescence of the discs into one big drop. However, Recycled salt has the best ranking with coated discs obtaining a higher fraction of spherical drops than the other salts. The coating reduces the ability of the Cryolite salt in releasing the Al from the oxide while it does not affect the Recycled salt. The Industrial salt is the worst for both clean and coated scrap.

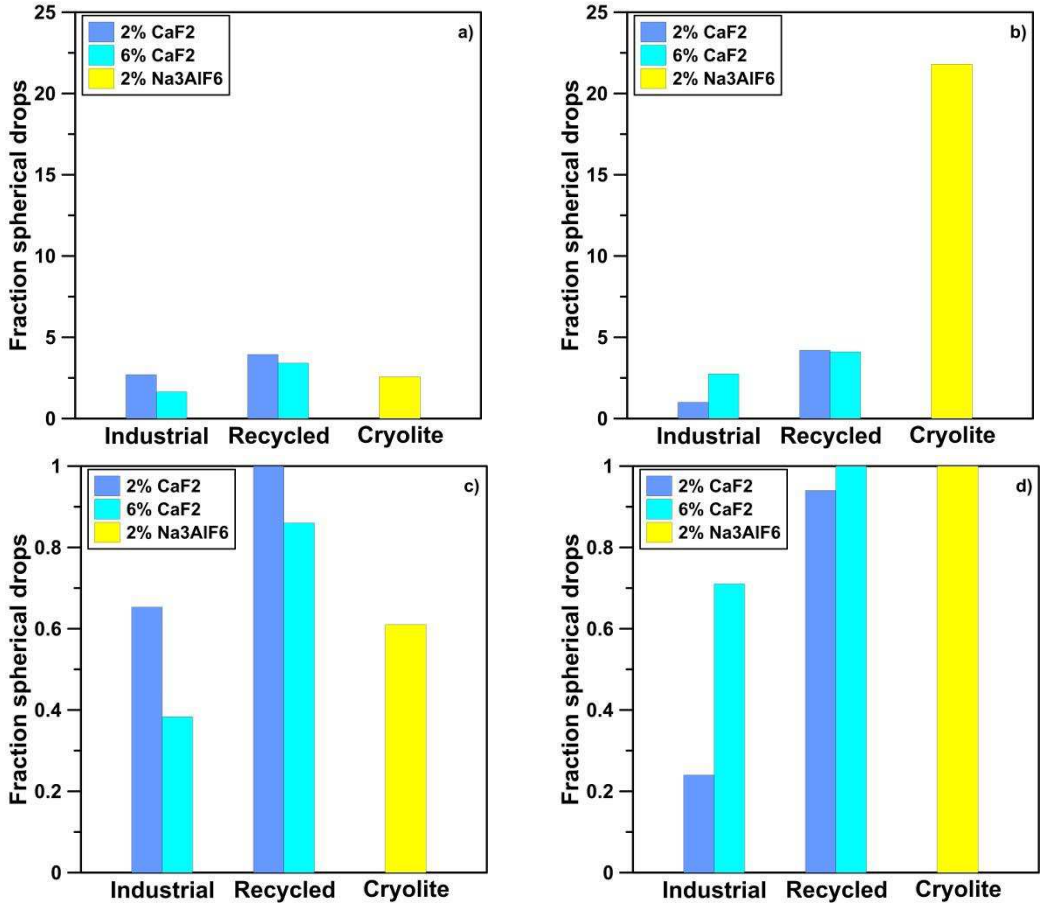

Figure 16: Coalescence in terms of (top) coalescence factor and (bottom) fraction of spherical drops from melting (a,c) coated and (b-d) clean discs

The main difference between the Cryolite salt and the Industrial and Recycled salts is the type of fluoride added. The best results were achieved using the Na_3AlF_6 instead of the CaF_2. Adding the same quantity of fluoride the amount of F added is a little bit higher for cryolite, i.e. in 100gr of Na_3AlF_6 and CaF_2 there are 54gr and 49gr of F respectively.

The experimental fluxes containing the greatest quantity of F are the Industrial and the Recycled salts with the addition of 6% of CaF_2 but they do not give the best coalescence. According to Sydykov, et al. [23] dissolving CaF_2 and Na_3AlF_6 in a 70NaCl-30KCl mixture a different concentration of active fluoride is obtained due to different dissolution rates. They calculated a concentration of fluorides ions equal to 0.5wt.% and 1wt.% for a concentration of 2wt.% of CaF_2 and Na_3AlF_6 respectively. The concentration of F^- did not increase for greater concentration of CaF_2.

Moreover, the effect of the CaF_2 addition in the Industrial and Recycled salt can be lowered by the concentration of S. The S reacts with the F forming SF_6, reducing the concentration of active F. The Industrial salt shows the worst ranking and the highest concentration of S.

The NaCl-KCl ratio in the Industrial salt is higher than the other salts. According to Bolivar and Friedrich [24] a decrease in the KCl concentration does not the metal recovery effectiveness.

The influence of the surface contaminations and the salt quantity on aluminium drops coalescence is plotted in Figure 17. The discs oxidised completely if no salt was added, while different results achieved melting the discs under the flux depend on the coating.

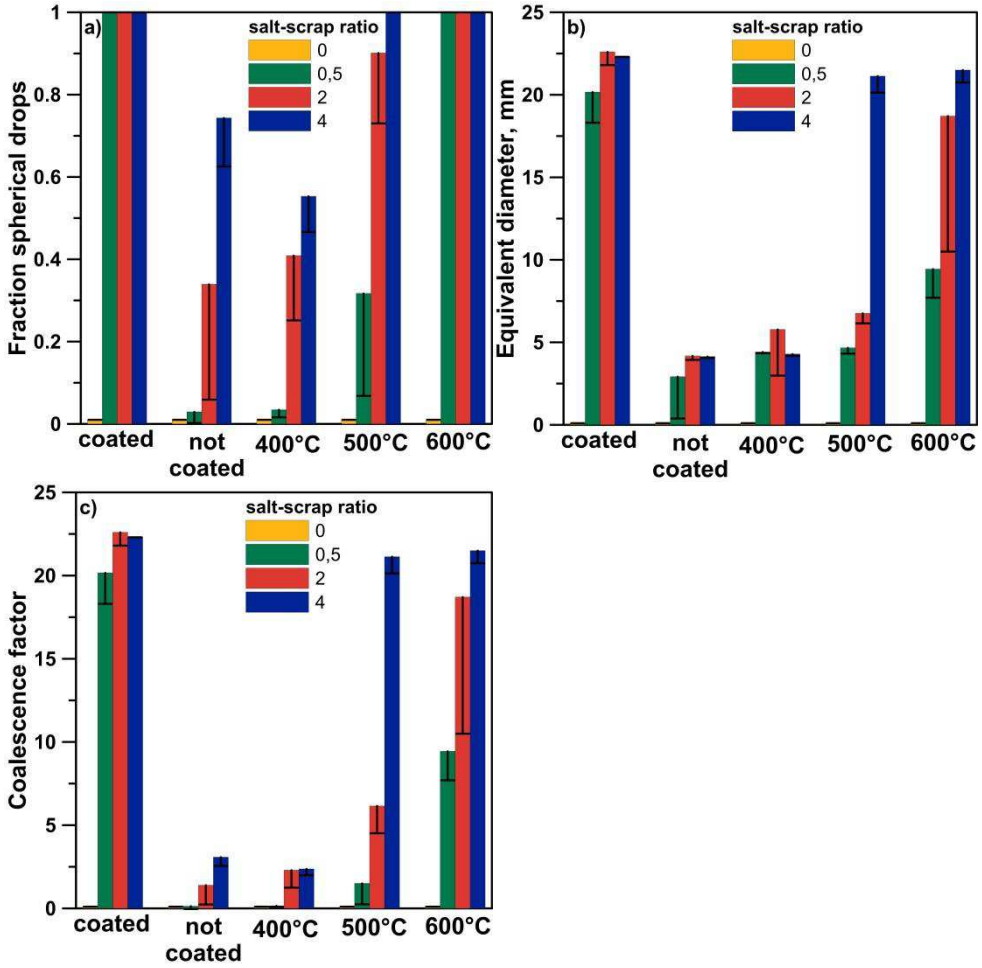

Figure 17: Coalescence in terms of (a) fraction of spherical drops, (b) average diameter and (c) CF for scrap studied at different salt-scrap ratios.

The greater CF values were obtained with the clean discs. In all the experiments, from melting the clean scrap the fraction of spherical drops was equal to 1, meaning that none of the discs oxidized and were released from the oxide. The same conclusion can be drawn from the discs de-coated at 600°C. The salt completely protected the molten metal from the atmosphere and no exothermal reaction took place in the salt.

A de-coating temperature lower than 600°C, does not allow a complete removal of the organic compounds present in the coat. Similar results were achieved melting the coated discs and the ones de-coated at 400°C, while greater CF values were reached with the discs de-coated at 500°C using the two highest levels of salt-scrap ratio. Probably a decrease of the CF is related to higher thicknesses of the coating.

The organic fraction present in the coat burned locally increased the temperature and oxidised the disc surface and decreased the efficiency of the salt to release the metal from the oxide.

The main effect plot in Figure 18a displays the mean values of CF of the various levels of the de-coat temperature and the salt-scrap ratio. The amount of salt positively affects the results, while the de-coating temperature highlights effects only at the highest levels. The greatest difference is between coated and clean scrap. Nevertheless, the effect of their interaction cannot be neglected. The interaction between the experimental variables is highlighted in Figure 18b. Parallel lines in an interaction plot indicate no interaction. The greater the departure of the lines from the parallel state, the higher the degree of interaction. It is clear that the effect of the amount of salts varies when the coating conditions change.

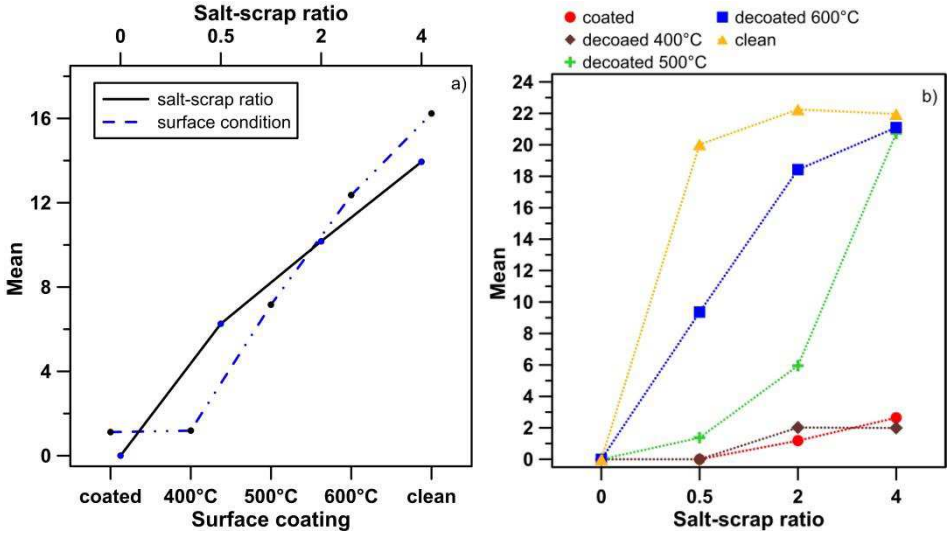

Figure 18. a) Main effects chart displaying the influence of the de-coat temperature and the salt-scrap ratio on the coalescence factor and b) the interaction plot between these two variables

The results for the Kruskal-Wallis test are reported in Table 6. The results obtained confirm that both the de-coating process and the amount of salt influence the coalescence of aluminum droplets.

Table 6. Results of Kruskal-Wallis test for oxide dissolution

Factor	Levene test	p-value
salt-scrap ratio	0.709	0.011
de-coat temperature		0.000

The salt-scrap ratio and in particular the tested levels are not applicable on industrial scale where lower amount of salt are used relative to the amount of scrap.

In a rotary furnace the salt is correlated to the whole amount of scrap but only a little fraction of the molten metal is entrapped in the flux. The experiments were developed in order to study the slag when higher salt-scrap ratios are used also in a rotary furnace. It is difficult to predict the amount of metal during crap melting but an indication of it can be drawn from the ratio between the amounts of the Al metal and the soluble salts in the salt cake generated during the scrap melting.

Tsakiridis [25] in a review of the salt slag characterization reports that dross typically contains 10–20% of Al metal and 40–55% salt-flux mixture. According to Lopez, et al. [26], the salt slag contains about 25% of Al, but with only 7.25% in the form of Al metal, while Pereira, et al. [27] studying Portuguese salt cake found 50-60% of soluble salts. Moreover, Hwang, et al. [28] investigated several salt cakes from different

smelters with a mean ratio between salts and Al metal of 44:13 while Gil [29] investigating Spanish smelters industry found a ratio of 48:8.

Conclusion

The ability of various fluxes to promote the aluminium drops coalescence was investigated by melting clean and coated scrap. Moreover, the effects of the amount of salt and the de-coating treatment were considered. The following conclusions can be drawn.

- The coating scrap surface can hinder the coalescence of the aluminium drops in the molten salt, preventing their recovery.
- A temperature of de-coating equal to 400°C is too low and does not help the drops to coalesce.
- Drop coalescence increases if the combustion reaction temperature is reached in de-coating treatment.
- The results obtained with a complete combustion reaction, i.e. de-coating at 600°C, are equal to those achieved with clean scrap.
- Different results are achieved when clean scrap is melted depending on the salt
- Complete coalescence melting clean scrap is obtained only with salt containing cryolite.
- Drops melted in Recycled flux are more rounded than those melted in Industrial and Cryolite fluxes and part of them are coalesced

Acknowledge

The authors acknowledge finical support from Erasmus, facilities of SFI Metal Production and Hydro Aluminium for providing materials. We would particularly like to thank Erik Vullum (SINTEF) for its support with the SEM micrographs and Syverin Lierhagen for its assistance with the ICP-MS analysis.

References

1. CEN, Aluminum and aluminum alloys. European Committee for Standardization: 2012; Vol. EN 12258.
2. 13920, Aluminium and Aluminium Alloys-Scrap. European Committee for Standardization (CEN): Bruxelles, 2003; Vol. EN 13920.
3. Tsangaraki-Kaplanoglou, I.; Theohari, S.; Dimogerontakis, T.; Kallithrakas-Kontos, N.; Wang, Y.-M.; Kuo, H.-H. H.; Kia, S., Effect of alloy types on the electrolytic coloring process of aluminum. *Surf. Coat. Tech.* **2006,** 200, 3969-3979.
4. Shi, Z.; Song, G.; Atrens, A., Influence of the b phase on the corrosion performance of anodised coatings on magnesium–aluminium alloys. *Corros. Sci.* **2005,** 47, 2760-2777.
5. Tracton, A. A., *Coatings technology handbook*. third ed.; CRC Press Taylor & Francis Group: 6000 Broken Sound Parkway NW, Suite 300 Boca Raton, FL 33487-2742, 2006.
6. Boin, U.; Reuter, M. A.; Probst, T., Measuring – Modelling: Understanding the Al Scrap Melting Processes Inside a Rotary Furnace. *World of Metallurgy* **2004**.

7. Zhou, B.; Yang, Y.; Reuter, M. A.; Boin, U. M. J., Modelling of aluminium scrap melting in a rotary furnace. *Mineral. Eng.* **2006,** 19, 299-308.
8. Dispinar, D.; Kvithyld, A.; Nordmark, A., Quality assesment of recycled aluminium. *Light Metals 2011* **2011**, 731-735.
9. Kvithyld, A.; Nordmark, A.; Dispinar, D.; Ghaderi, S.; Lapointe, H., *Quality comparison between molten metal from remelted sheets, mill finish and coated*. TMS: The Minerals, Metals & Materials Society: 2012; p 1031-1035.
10. Rabah, M. A., Preparation of aluminium–magnesium alloys and some valuable salts from used beverage cans. *Waste Manag.* **2003,** 23, 173-182.
11. Wang, M.; Woo, K.-D.; Kim, D.-K.; Ma, L., Study on de-coating used beverage cans with thick sulfuric acid for recycle. *Ener. Convers. Manage.* **2007,** 48, 819-825.
12. Li, N.; Qiu, K., Study on Delacquer Used Beverage Cans by Vacuum Pyrolysis for Recycle. *Environ. Sci. Technol.* **2013,** 47, 11734-11738.
13. Kvithyld, A.; Meskers, C. E. M.; Gaal, S.; Reuter, M.; Engh, T. A., Recycling light metals: optimal thermal de-coating. *JOM* **2008,** 60, (8), 47-51.
14. Crepeau, P. N.; Fenyes, M. L.; Jeanneret, L. J., Solid fluxing practices for aluminum melting (part 1). *Mod. Cast.* **1992**, 28-30.
15. Peterson, R. D., *Effect of salt flux additives on aluminum droplets coalescence*. TMS: The Minerals, Metals & Materials Society: 1990; p 69-84.
16. Roy, R. R.; Sahai, Y., Coalescence behaviour of aluminum alloy drops in molten salts. *Mater. Trans.* **1997,** 38, (11), 995-1003.
17. Kim, Y.-S.; Yoon, E.-P.; Kim, K.-T.; Jung, W.-J.; Jo, D.-H., Effects of Salt Flux and Alloying Elements on the Coalescence Behaviour of Aluminum Droplets. *J. Korea Foundry Soc.* **2000,** 20, (1), 39-45.
18. Besson, S.; Pichat, A.; Xolin, E.; Chartrand, P.; Friedrich, B., Improving coalescence in Al-Recycling by salt optimization. In *European metallurgical conference 2011*, Dusseldorf, 2011; pp 1-16.
19. Thoraval, M.; Friedrich, B., Metal entrapment in slag during the aluminium recycling process in tilting rotary furnace. In *European Metallurgical Conference 2015*, Dusseldorf, 2015; pp 359-367.
20. Boin, U. M. J.; Bertram, M., Melting Standardized Aluminum Scrap: A Mass Balance Model for Europe. *JOM* **2005,** 57, (8), 26-33.
21. Moloodi, A.; Amini, H.; Karimi, E. Z. V.; Golestanipour, M., On the Role of Both Salt Flux and Cold Pressing on Physical and Mechanical Properties of Aluminum Alloy Scraps. *Mater. Manuf. Process.* **2011,** 26, 1206-1012.
22. Girard, G.; Barresi, J.; Dupuis, C.; Riverin, G., Furnace Operation: “A Gold Mine in your Casthouse”. *Mater. Sci. Forum* **2010,** 630, 77-84.
23. Sydykov, A.; Friedrich, B.; Arnold, A., Impact of parameter changes on the aluminum recovery in a rotary kiln. *Light Metals* **2002**, 1045-1052.
24. Bolivar, R.; Friedrich, B., The influence of increased NaCl:KCl ratios on Metal Yield in salt bath smelting processes for aluminium recycling. *World of Metallurgy* **2009,** 62, (6), 1-10.
25. Tsakiridis, P. E., Aluminium salt slag characterization and utilization – A review. *J. Hazard. Mater.* **2012,** 217-218, 1-10.
26. Lopez, F. A.; Sainz, E.; Formoso, A.; Alfaro, I., The recovery of alumina from salt slags in aluminium remelting. *Can. Metall. Quart.* **1994,** 33, 29-33.
27. Pereira, D. A.; Aguiar, B. d.; Castro, F.; Almeida, M. F.; Labrincha, J. A., Mechanical behaviour of Portland cement mortars with incorporation of Al-

containing salt slagsags in aluminium remelting. *Cement and Concrete Research* **2000,** 30, 1131-1138.
28. Hwang, J. Y.; Huang, X.; Xu, Z., Recovery of Metals from Aluminum Dross and Saltcake. *J. Miner.Mater. Charact. Eng.* **2006,** 5, (1), 47-62.
29. Gil, A., Management of the Salt Cake from Secondary Aluminum Fusion Processes. *Ind. Eng. Chem. Res.* **2005,** 44, 8852-8857.

APPENDIX

APPENDIX A

Matlab code for the morphological and dimensional analysis of the metal drops

```
% read the binarised image
E=imread('B 2% 2x c B.png');

% remove all object containing fewer than 30 pixels
E = bwareaopen(E,20);

% fill any holes in the drops
E= imfill(E,'holes');

% creo matrice L con etichetta per e diverse gocce e coordinate dei
contorni in B
[B,L] = bwboundaries(E,'noholes');

% Display the label matrix and draw each boundary
imshow(label2rgb(L,@white, [.5 .5 .5]));
hold on

% draw each boundary
for k = 1:length(B)
  boundary = B(k);
  plot(boundary(:,2), boundary(:,1), 'b', 'LineWidth', 0.5);
end

% measure area, centroid, perimeter and axis per each element in L
stats =
regionprops(L,'Area','Centroid','Perimeter','MinorAxislength','MajorAxis
Length');

% fix thr threshold values
thresholdR = 0.85; % roundness
thresholdMR = 1.25; % aspect ratio
thresholdD = 3.5; % diameter

%  measure the size of the currency used as a reference and define the
actual size in mm2
areamonreal = 314; % inserisco valore reale
q =length(B);     areamon = stats(q).Area;

% define null the counters
n=0;    % number of drops
m=0;    % number of spherical drops from more than 1 disc
l = 0; % number of spherical drops

for k = 1:length(B)

  % obtain (X,Y) boundary coordinates corresponding to label 'k'
  boundary = B(k);

  % obtain the perimeter calculation corresponding to label 'k'
  perimeter = stats(k).Perimeter;

  % obtain the area calculation corresponding to label 'k'
  area = stats(k).Area;
  areareal = area*areamonreal/areamon;

  % compute the equivalent diameter
  diametro = 2*(areareal/3.14)^(1/2);

  % compute the roundness
```

```
  metric = 4*pi*area/perimeter^2*(1.05);
  if metric>1
    metric = 1;
  end

   % compute the aspect ratio
  min = stats(k).MinorAxisLength;
  max = stats(k).MajorAxisLength;
  aspectratio = max/min;

  % associo i valori calcolati a delle stringhe
  metric_string = sprintf('%2.2f',metric);
  area_string = sprintf('%2.2f',areareal);
  ratio_string = sprintf('%2.2f',aspectratio);
  diametro_string = sprintf('%2.2f',diametro);


  % measure the spherical drops
  if (aspectratio < thresholdMR)&&(metric > thresholdR) && (diametro >
  thresholdD) && (diametro < (thresholdD*1.3))
    centroid = stats(k).Centroid;
    plot(centroid(1),centroid(2),'ko');
    n = n+1;
    l =l+1;
    aream(l)=areareal;
    diametrom(l)=diametro;
    roundnessm(l)=metric;
    aspectratiom(l)=aspectratio;

  % measure the spherical drops from more than 1 disc

  elseif (aspectratio < thresholdMR)&&(metric > thresholdR) && diametro
  > (thresholdD*1.35)
    centroid = stats(k).Centroid;
    plot(centroid(1),centroid(2),'go');
    m =m+1;
    l = l+1;
    aream(l)=areareal;
    diametrom(l)=diametro;
    roundnessm(l)=metric;
    aspectratiom(l)=aspectratio;
  end
  % put the counter at 0
  for j=l:length(B)
  j = j+1;
  aream(j)=0;
  diametrom(j)=0;
  roundnessm(j)=0;
  end

  % display the diameter
  text(boundary(1,2)-20, boundary(1,1)+20, diametro_string,
  'Color',[0,0,0], ...'FontSize',8,'FontWeight','bold');
end

% measure the numer of drops
K=length(B);

% create an array  with the counters
num = [n,m,l,k];
```

```
% export results in Excel
xlswrite('ris',num);
xlswrite('diameter',diametrom);
xlswrite('roundness',roundnessm);
xlswrite('area',aream);

% title
title('Al drops roundness and dimensions');
```